12-2000

Leaf Area, Stemwood Volume Growth, and Stand Structure in a Mixed-Species, Multi-Aged Northern Conifer Forest

Laura Kenefic

LEAF AREA, STEMWOOD VOLUME GROWTH, AND STAND STRUCTURE IN A MIXED-SPECIES, MULTI-AGED NORTHERN CONIFER FOREST

BY

Laura Susan Kenefic

B.A. State University of New York at Binghamton, 1992

M.S. State University of New York College of Environmental Science and Forestry, 1995

A THESIS

Submitted in Partial Fulfillment of the

Requirements for the Degree of

Doctor of Philosophy

(in Forest Resources)

The Graduate School

The University of Maine

December, 2000

Advisory Committee:

Robert Seymour, Curtis Hutchins Professor of Forest Resources, Advisor

John Brissette, Project Leader and Research Forester, U.S.D.A. Forest Service

Malcolm Hunter, Libra Professor of Conservation Biology

Ralph Nyland, Distinguished Service Professor of Silviculture, S.U.N.Y C.E.S.F.

Alan White, Associate Professor of Forest Resources

LEAF AREA, STEMWOOD VOLUME GROWTH, AND STAND STRUCTURE IN A MIXED-SPECIES, MULTI-AGED NORTHERN CONIFER FOREST

By Laura Susan Kenefic

Thesis Advisor: Dr. Robert Seymour

An Abstract of the Thesis Presented
in Partial Fulfillment of the Requirements for the
Degree of Doctor of Philosophy
(in Forest Resources)
December, 2000

Tree- and stand-level leaf area (LA) - stemwood volume growth relationships were explored in mixed-species, multi-aged northern conifer stands dominated by *Tsuga canadensis* (L.) Carr. (eastern hemlock), *Abies balsamea* (L.) Mill. (balsam fir), and *Piceu rubens* Sarg. (red spruce). A *T. cunudensis* LA model was developed to supplement published equations for *A. balsamea* and *P. rubens.* Sapwood area was an effective *T. cunudensis* LA surrogate, though nonsapwood-based models using stem cross-sectional area and modified live crown ratio produced results comparable to sapwood-based models.

Equations for predicting tree-level stemwood volume increment (AVINC) were derived, and implied growth efficiencies (GE) were used to assess magnitude and pattern of GE change between strata and species. AVINC was effectively modeled using LA alone, and the slightly peaking GE - LA relationships approximated those previously

conceptualized for shade-tolerant species. *A. balsamea* and trees in upper strata were most efficient. *T. canadensis* maximum GE occurred at a higher LA than *A. balsamea* or *P. rubens*, and *A. balsamea* maximum GE was less than that previously observed in even-aged stands. Age was not a significant predictor of tree-level GE or stemwood increment.

Multi-aged, stand-level stemwood volume increment - leaf area index (LAI) relationships were assessed on 0.02-ha plots dominated by *T. cunudensis, A. balsamea*, and *P. rubens*. Structures conceptually associated with even-, two-, and multi-aged stands were documented. Inter-plot structural variability was attributed to incomplete stand-level conversion to a balanced condition, and a hybrid single-tree and group selection regeneration method.

Plot-level stemwood volume increment (PAVINC) was modeled for all plots combined using LAI and proportion of midstory leaf area (LAC). Two clusters of plots with different basal area, LAI, LAC, and PAVINC were identified. Average diameter distributions within each cluster were typical of multi-aged stands. Within-cluster analysis indicated that quantified structural variables did not improve estimation of PAVINC from LAI, though additional study is warranted due to small sample size. LAI - relative density relationships suggested that plot-level stocking and PAVINC could be increased.

This study extends physiologically based silviculture research to mixed-species, multi-aged stands of shade-tolerant species, and confirms the usefulness of LA - growth relationships for describing and evaluating stand dynamics.

Dedicated to my sons

Liam Foster Kenefic and Evan Lukas Kenefic

ACKNOWLEDGMENTS

Financial support for this research was provided by the U.S.D.A. Forest Service Northeastern Research Station; The University of Maine College of Natural Sciences, Forestry, and Agriculture, Department of Forest Ecosystem Science; and the Maine Agriculture and Forest Experiment Station, Orono.

I am indebted to Bob Seymour for his understanding, support, and tireless dedication to my silvicultural education. I am honored that he has taken the time to share his knowledge with me. I thank John Brissette for helping to bring me to the University of Maine through a cooperative education agreement, and for guiding me in my U.S.D.A. Forest Service endeavors. I am grateful to my mentor, Ralph Nyland, for believing in me before I knew what silviculture was, and for being a dedicated friend and supporter. I thank my committee members, Mac Hunter and Al White, who have exhibited an unprecedented level of patience and support.

I thank my colleagues, past and present, at he U.S.D.A. Forest Service, especially Tom Skratt (retired), Tim Stone, Rick Dionne, Al Meister, Paul Sendak, Steve Stedman, Alison Dibble, David Robinson, Susan Stout, Gerry Walton (retired), Harry Valentine, and Bill Leak. I acknowledge Bob Frank (retired), who maintained the Penobscot Experimental Forest experiment for 30 years and introduced me to the woods in Maine.

My field and laboratory assistants were invaluable - Dan Scott, Jon Rivers, Scott Robinson, Mark Fogarty, Steve Bacon, Jason Renchy, Mike Charnick, Andrew Lyman, Matt Smith, Joe McBreen, Bill Burman, and Mike Maines. Their tireless efforts are

greatly appreciated. Also, I am thankful to Norman Kalloch, Natural Resources Conservation Service, for both advising me and visiting me in the field.

I have benefitted from interactions with fellow graduate students, especially Unna Chokkalingam, Dave Ray, Jim Baker, Mike Day, Audrey Barker Plotkin, Dan McConville, Shawn Fraver, Martha Schumann, Duncan Wilson, Yuhui Qian, and Mary-Madelyn Ferraro. Numerous faculty at this and other universities have made themselves available to me - particularly Doug Maguire, Oregon State University, who was on my committee until 1996 and continues to provide statistical advice; Chris Nowak and Russ Briggs, State University of New York College of Environmental Science and Forestry; Dan Gilmore, University of Minnesota; Kevin O'Hara, University of California, Berkley; and Bill Livingston, Bill Halteman, Al Kimball, Barry Goodell, Dick Jagels, Mike Greenwood, Kathy Carter, and Bob Wagner, The University of Maine.

I thank my friends, who have supported and encouraged me - Pat Cody; Greg, Teddy, and Elizabeth Markowsky; Ann Dieffenbacher-Krall; Laurie Baker; Suzanne Mapes; Jeanne Taylor; Carol Redelsheimer; Ellen Vollmers; KaDonna Randolph; Alice and Mitchell Bruce; and the late L. Rex Pyles. I appreciate the love and support of my family - my parents John and Susan Wolslegel; my sister Kristen Wolslegel; my aunts Ellen Zappala and Sharon Rothman; and my grandmother Genevieve Wolslegel. Most of all, I thank my husband, Richard Kenefic, for being beside me every day and always believing in me.

Lastly, I give thanks to God, for being with me in the good times, helping me to find the strength to get through the bad times, and giving me my children, who are healthy, smart, and beautiful.

TABLE OF CONTENTS

LIST OF TABLES

LIST OF FIGURES

LIST OF ABBREVIATIONS

CHAPTER 1

LEAF AREA PREDICTION MODELS FOR *TSUGA CANADENSZS* IN MAINE

CHAPTER ABSTRACT

Tsuga canadensis (L.) Carr. (eastern hemlock) is a common species throughout the Acadian Forest. Studies of leaf area and growth efficiency in this forest type have been limited by the lack of equations to predict leaf area of this species. We found that sapwood area was an effective leaf area surrogate in ***T.*** *canadensis*, though adding crown length to the sapwood equations improved model performance. Prediction bias was observed at the upper end of our data for the best sapwood equation. Sapwood area at crown base did not predict leaf area as well as sapwood area at breast height. Equations using crown length or crown volume alone were the least effective of all models tested. Models using stem cross-sectional area inside the bark or tree basal area with a modified live crown ratio produced results comparable with those of the best sapwood-based model and were unbiased across the range of our data. These findings verify the value of nonsapwood-based approaches to ***T.*** *canadensis* leaf area prediction.

INTRODUCTION

The ecophysiological basis of production silviculture is greatly enhanced when stand density and structure are described directly in terms of leaf area (LA) rather than traditional empirical measures based on numbers and sizes of stems (O'Hara 1996, 1998). The use of LA in structural control requires accurate and efficient means of estimating the

amount of foliage on standing trees. Equations that predict LA from diameter or basal area have a long history, but are often inaccurate (Marshall and Waring 1986, Bormann 1990). Sapwood area has become the preferred predictor based on the close biological relationship between the conducting xylem and the foliage it supports.

Tsuga canadensis (L.) Carr. (eastern hemlock) is a common species in the Lake States and New England, including the southern part of the Acadian Forest. Although LA equations have been developed for other conifers in this forest type (Marchand 1984, Coyea and Margolis 1992, Gilmore et al. 1996, Maguire et al. 1998, A.A. Barker Plotkin and R.S. Seymour unpublished), no equations exist for *T. canadensis.* This deficiency has been an impediment to research on LA and growth efficiency (stem volume growth per unit LA) in northeastern forests. The research reported here explores allometric leaf area equations for *T. canadensis* and compares these models to equations published for other species in this and other regions.

STUDY AREA

The stand sampled in this study is part of a long-term silvicultural experiment on the 1540-ha Penobscot Experimental Forest (PEF) in east-central Maine, located at approximately 44°52'N, 68°38'W. The PEF was purchased in 1950 by a number of industrial landholders and leased to the U.S.D.A. Forest Service to allow that agency to begin experiments to study uneven- and even-aged silvicultural systems. Ongoing treatments and remeasurements follow a long-term study plan that ensures consistency in

management over time. The 6.6-ha study stand is one of two replicates of selection cutting on a 5-year cycle, with eight selection cuttings prior to our study. The structural goal was defined using the BD*q* (basal area, maximum diameter, q-factor) method with a q-factor of 1.96 on 5-cm classes, a residual maximum diameter goal of 48 cm, and a target residual basal area (BA) of 26 m^2/ha (Seymour and Kenefic 1998).

Within-stand species composition is highly variable because of differences in soil drainage and stand structural condition. The dominant species on the study site are *T. canadensis*, *Picea rubens* Sarg. (red spruce), and *Abies balsamea* (L.) Mill. (balsam fir). Other species include *Thuju occidentalis* L. (northern white-cedar), *Acer rubrum* L. (red maple), *Betula papyrifera* Marsh. (paper birch), *Piceu glauca* (Moench.) Voss (white spruce), and other hardwoods (Kenefic and Seymour 1997). The species composition of this stand typifies much of the Acadian region, a transitional zone between the eastern hardwood and boreal forests.

METHODS

A 25-m systematic grid was established in the study stand in 1995. A random sample of 50 *T. canadensis*, stratified by 5-cm diameter at breast height (dbh, 1.3 m) classes, was taken from 12.5-m radius plots centered on the grid points. The sample included trees at least 1.3 m in height, up to 50.0 cm dbh. Sampling was restricted to somewhat poorly, moderately well, and well drained soils, and excluded areas encompassed by the U.S.D.A. Forest Service continuous forest inventory plots. A

subsample of 20 trees representing a range of heights and canopy positions was chosen for the leaf area study in May 1996 from the initial 50-tree sample (Table 1.1).

Tree height, dbh, bark thickness, crown class, crown radii in four cardinal directions, height to the lowest branch, and height to the lowest cluster of branches were measured on each sample tree prior to felling. The lowest cluster of branches (analogous to a true whorl) was defined as the first group of three or more closely space branches, unless a lower branch made up 40% or more of the crown projection area (CPA, m') at that height. Cross-sectional area inside the bark at breast height (bh) was calculated for each tree (ABH, $cm^2 = \pi [(dbh/2) - \text{bark thickness}]^*$).

Each sample tree was felled and a random branch removed from the lower, middle, and upper third of the crown (Table 1.2). Foliage samples were removed from all needle age classes in approximate proportion to their occurrence and immediately frozen in a portable cooler for subsequent specific leaf area (SLA) determination. Remaining foliage and biomass components of each branch were stored in paper bags. Diameter above basal swelling and height of all live branches were measured for calculation of branch cross-sectional area and position within the crown. Diameter at crown base (DCB, cm) was measured and cross-sectional disks approximately 1 - 2 cm thick were removed at stump height (0.1 m), breast height, lowest live branch, and at 2-m intervals from the lowest live branch to the tip. The sapwood-heartwood boundary was tentatively identified in the field by holding each disk to the sunlight, and tracing the apparent boundary between the translucent (water conducting) and non-translucent zones with a fine-tipped permanent marker. Other translucent wetwood zones separated from the apparent sapwood by continuous opaque bands of growth rings were ignored.

Table 1.1. Characteristics of twenty trees sampled in 1996 to develop *Tsuga canadensis* leaf area prediction models.

	Minimum	Maximum	Mean ± SE
Diameter at 1.3 m (cm)	6.8	48.4	28.2 ± 2.8
Height (m)	5.61	20.95	14.71 ± 1.11
Crown length (m)	3.63	16.94	11.36 ± 0.85
Live crown ratio	0.62	0.95	0.78 ± 0.02
Crown projection area[a] (m^2)	7.41	73.55	33.80 ± 4.39
Sapwood area at 1.3 m (cm^2)	24.72	663.69	303.4 ± 45.4
Sapwood area at crown base (cm^2)	17.94	547.45	245.1 ± 35.2
Projected leaf area (m^2)	10.54	267.58	118.58 ± 17.21

[a] Crown projection area = $\sum(\pi * r_i^2)/4$, where the r_i are the four individual radius measurements (Gregoire and Valentine 1995).

Table 1.2. Characteristics of sixty-nine branches sampled in 1996 and 1998 to develop *Tsuga canadensis* branch-level leaf area (BLA, m^2) prediction models.

	Minimum	Maximum	Mean ± SE
Branch diameter (cm)	0.2	8.2	3.4 ± 0.3
Height from ground (m)	1.89	19.79	9.11 ± 0.54
Depth into crown (m)	0.31	15.76	6.06 ± 0.48
Relative depth into crown	0.03	1.00	0.52 ± 0.04
Leaf mass (g)	0.939	1632.015	344.426 ± 46.887
Projected leaf area (m^2)	0.006	10.546	1.950 ± 0.276
Specific leaf area (cm'lg)	41.95	79.35	58.43 ± 1.15

Nine additional branches larger than 6 cm in diameter were sampled in June 1998 to supplement small sample size in this range. Trees larger than 29 cm dbh (the minimum dbh of trees in the 1996 sample with branches larger than 6 cm) were selected from the remaining trees in the initial 50-tree sample as sources of new branches. Updated height and crown measurements were taken. An arborist climbed to the top of each tree, measuring and numbering all branches above the threshold size. One branch was selected at random from each tree and lowered with cables to prevent breakage. Needle subsampling and drying procedures followed those described above.

Prior to drying, projected leaf area was determined for each branch based on two loo-needle subsamples taken from the bag of foliage frozen from that branch. Subsamples were limited to 100 needles because of the restricted field of vision associated with the Ag-Image optical analysis system (Decagon Devices, Inc.), which was used to obtain measurements in 1996. The 1996 projected leaf area values were consistently higher than those obtained in 1998 with the WinNEEDLE system (Regent Instruments, Inc.). Microscope analysis of needle cross-sections using a calibrated stage micrometer revealed that the Ag-Image system overestimated needle width at the recommended grayscale threshold settings (M. Day unpublished data). This was attributed to shadow effects, which are exacerbated by large pixel size. The WinNEEDLE system provides more accurate estimates of needle size due to its balanced-by-directional lighting system and higher resolution. Measurements from the two systems were compared, and a ratio correction factor of 0.8 1 was calculated from branches of similar size and crown position and applied to all branches measured in 1996 to obtain a corrected leaf area.

Each loo-needle subsample was dried in a convection oven at 65" C for 48 hours and weighed to the nearest 0.0001 g. The area of each subsample was divided by its weight to determine SLA (cm^2/g). A single SLA was calculated for each branch by averaging the values obtained form the two subsamples. Whole-branch samples and the remaining frozen needles were dried in a drying room at 46" C for at least 72 hours. Foliage and woody materials from each branch were hand separated and weighed to the nearest 0.0001 g. Branch-level projected leaf area (BLA, m^2) was calculated by multiplying dry foliage weight by a branch-specific SLA.

It is difficult to consistently identify the *T. canadensis* sapwood-heartwood boundary, in part because of the potential for areas of translucent wetwood caused by bacterial infection in the heartwood. A 0.1 M solution of ferrous ammonium sulfate ($Fe(NH_4)_2(SO_4)_2.6H_2O$) was applied to seasoned disks to identify the sapwood colorimetrically (Eades 1958). The field-marked sapwood boundary was either confirmed or adjusted in favor of the dye. The mechanism for this reaction is believed to be differences in the forms of tannins in the sapwood and heartwood (B. Goode11 pers. commun.). This was tested by applying a 0.01 M solution of anhydrous ferric chloride ($FeCl_3$) and a 0.25 mM solution of Ferrozine iron reagent, monohydrate ($C_{20}H_{13}N_4NaO_6S_2.H_20$) (Hach Company) to a subsample of seasoned cross-sectional disks. Each disk was polished and width of the sapwood measured along the average stem radius with a Velmex measuring system (Velmex, Inc.). Sapwood area was determined for each disk as a function of stem diameter and sapwood radius at that location, and bark thickness at breast height.

Analysis

Branch-level Equation

We compared linear and nonlinear equations of the form $y_i = f(\beta | x_i) + \varepsilon_i$, where $\varepsilon_i \overset{iid}{\sim} N(0, x_i^n \sigma^2)$, to identify an equation suitable for predicting BLA from branch cross-sectional area (XSECT, cm^2) and branch position (iid, independently and identically distributed). Equations were weighted by x_i^n with n = 0, -1, -2, and -3 in order to identify the optimal weighting factor to correct for heteroskedasticity. Generalized R^2 (Kvålseth 1985) was calculated on the original scale using the corrected sum of squares (1-[cssresid/$\sum(y_i-y_m)^2$]), where cssresid is the corrected residual sums of squares, the y_i are the individual sample values, and y_m is the sample mean. Collinearity statistics were used to detect the presence and severity of multicollinearity between predictor variables. The condition index, or square root of the ratio of the largest to smallest eigenvalues in the correlation matrix for the independent variables, was calculated (Huang and Titus 1995). This value was compared to the proposed critical value for moderate multicollinearity (Belsley et al. 1980) to determine the degree of multicollinearity. Values less than 30 indicate that collinearity is not a serious problem. Furnival's (1961) index of fit (FI), a modified maximum likelihood criterion that allows concurrent evaluation of root mean square error (RTMSE), normality, and homoskedasticity, was used to identify optimal model form. Index of fit has the advantage of simultaneously allowing comparison both across model forms and within models across weighting factors. The lower the FI value, the better the fit based on the criteria listed above.

Tree-level Eauation

Tree-level projected leaf area (PLA, m^2) was calculated for each sample tree by applying the branch-level model to each branch and summing the predicted BLA values. A number of linear and nonlinear, published and unpublished model forms were tested, and analysis was done as above to identify which of those was optimal. Both sapwood and nonsapwood-based models were explored.

Only equations with significant parameters (a = 0.05) were considered, and plots of standardized residuals against predicted variables were used to verify homogeneous variance. Reasonable biologic behavior was taken into consideration, and evaluated using scatter plots of the sample data against the predictor equations.

RESULTS

Branch-level Projected Leaf Area

The average SLA was 58.43 cm^2/g, but varied with branch position: SLA values were generally higher for branches lower in the crown. BLA was best expressed as a function of XSECT and relative depth into the crown (RDINC = (tree height - branch height)/(tree height - height to lowest live branch)). The significance of these predictor variables, but not the model form, is consistent with the findings of Maguire et al. (1998) for ***P.*** *rubens*. A comparison of a number of model forms and transformations showed that a linear model with a cube-root transformation was optimal (Figure 1.1). This model behaved well over the range of data available in this study but was not tested outside this

Figure 1.1. Observed and predicted branch projected leaf area (BLA) relative to branch cross-sectional area (XSECT), as a function of XSECT and relative depth into the crown (RDINC). BLA = (-0.1589 + 0.4375 x XSECT"' + 0.4544 x RDINC"')'.

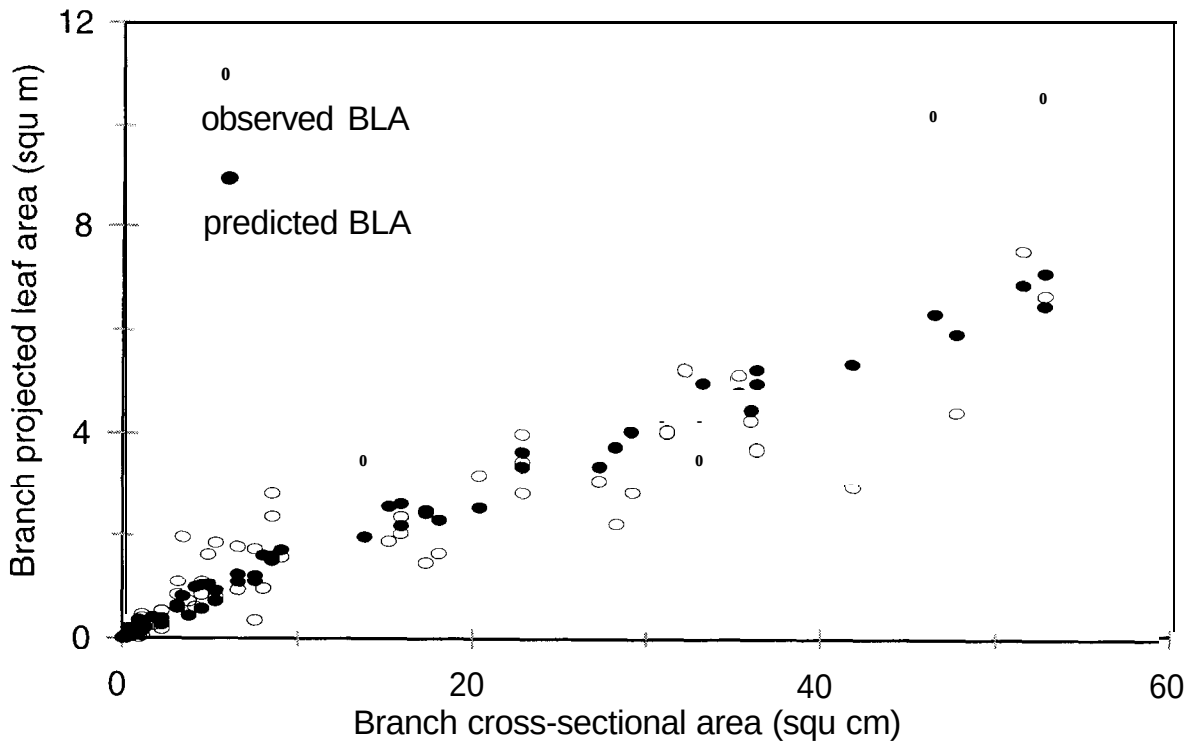

range. Bias correction was deemed unnecessary because the average predicted BLA transformed back to the original scale was only 3 % less than the average observed BLA> The R^2 for this equation was 0.92. The intercept term was marginally non-significant (p=0.057), but removing it from the model biased the residuals for small branches. The condition index was 12.3, indicating that multicollinearity is not a serious problem.

Tree-level Projected Leaf Area

Thirteen models were tested for the tree-level equation (Tables 1.3 and 1.4). PLA was best estimated as a function of sapwood area at breast height (SA_{bh}, cm^2) and crown length (CL = tree height - height to the lowest live branch, m). Model 4, weighted by SA_{bh}^{-2} to correct for increasing variance in the residual plots, had the lowest FI of those tested. The condition index was 12.9, indicating an acceptable level of multicollinearity between the predictor variables. Using the lowest significant whorl to identify crown base and calculate crown length (Gilmore et al. 1996) diminished model performance. Using SA_{bh} as the sole predictor variable (linear model 2, weighted by SA_{bh}^{-1}) worked fairly well relative to the other sapwood-based models and requires easier and less expensive data collection. However, nonsapwood-based models 10, 12, and 13 were superior to all but models 4 and 6 (additive linear and multiplicative nonlinear models using SA_{bh} and CL). Model 10 uses area inside the bark at crown base (ACB, cm*), while 12 and 13 use ABH or $BA_{,,}$ (stem cross-sectional area at bh) with a modified live crown ratio (mLCR = CL/(tree height - 1.3)) (Valentine et al. 1994). These equations produced results comparable to those of sapwood-based models 4 and 6 and have the advantage of not requiring coring or measurement of sapwood area.

Table 1.3. Model forms, weighting factors, and fit statistics for linear and nonlinear, sapwood- and nonsapwood-based models screened for prediction of *Tsuga canadensis* projected leaf area (PLA). Abbreviations used in models are PLA, projected leaf area (m^2); SA_{cb}, sapwood area at crown base (cm^2); SA_{bh}, sapwood area at 1.3 m (cm^2); CL, crown length (m), CV, crown volume (0.33(CL x crown projection area)) (m^3); BA_{bh}, basal area (cm^2); ACB, cross-sectional area inside the bark at crown base (cm^2); ABH, cross-sectional area inside the bark at 1.3 m (cm^2); mLCR, modified live crown ratio (CL/(tree height- 1.3)) (Valentine et al. 1994).

Model	Model form	Weight	R^2 [a]	RtMSE	FI [b]	Source [c]
1	$PLA = b_0 + b_1 SA_{cb}$	SA_{cb}^{-2}	0.93	0.09527	17.261	Marchand 1984, Coyea and Margolis 1992
2	$PLA = b_0 + b_1 SA_{bh}$	SA_{bh}^{-1}	0.95	1.09079	15.878	Marchand 1984, Coyea and Margolis 1992
3	$\ln(PLA) = b_1 \ln(SA_{bh})$	n/a	0.93	0.18887	16.735	Espinosa Bancalari et al. 1987
4	$PLA = b_0 + b_1 SA_{bh} + b_2 CL$	SA_{bh}^{-2}	0.94	0.05376	11.392	Coyea and Margolis 1992
5	$\ln(PLA) = b_1 \ln(SA_{bh}) + b_2 \ln(CL)$	n/a	0.92	0.16171	14.329	Gilmore et al. 1996
6	$PLA = b_1 SA_{bh}^{b2} CL^{b3}$	SA_{bh}^{-2}	0.93	0.06137	13.004	Gilmore et al. 1996
7	$\ln(PLA) = b_1 \ln(CL)$	n/a	0.77	0.30796	27.287	Gilmore et al. 1996
8	$PLA = b_1 CV^{b2}$	CV^{-1}	0.93	1.79515	17.847	Maguire pers. commun. 1998
9	$PLA = b_0 + b_1 BA_{bh}$	BA_{bh}^{-1}	0.96	0.61937	13.576	
10	$PLA = b_1 ACB + b_2 ACB^2$	none needed	0.97	12.74561	12.746	-
11	$PLA = b_1 ABH + b_2 ABH^2$	none needed	0.97	14.74640	14.746	
12	$PLA = b_0 + b_1 (ABH \times mLCR)$	ABH“	0.95	0.67798	13.005	Valentine et al. 1994
13	$PLA = b_0 + b_1 (BA_{bh} \times mLCR)$	BA_{bh}^{-1}	0.95	0.58927	12.916	

[a] Kvålseth's (1985) generalized R^2.
[b] Furnival's (1961) index of fit.
[c] Model forms, but not weighting factors, are attributed to the cited sources.

Table 1.4. Parameter estimates, SEs (in parentheses), and log bias correction factors (Baskerville 1972) for *Tsuga canadensis* projected leaf area (PLA) models.

Model	Parameters
1	b_0 = 3.6541 (1.5968), b_1 = 0.4783 (0.02701)
2	b_0 = 7.5432 (3.3681), b, = 0.3659 (0.01787)
3	b, = 0.8378 (0.007752)
	log bias correction factor = 1 .018
4	b_0 = -9.9148 (2.7889), b_1 = 0.2688 (0.02401), b_2 = 3.8895 (0.6440)
5	b_1 = 0.60 13(0.08428), b_2 = 0.5406 (0.1921)
	log bias correction factor = 1 .013
6	b_1 = 0.7587 (0.1285), b_2 = 0.5558 (0.07075), b_3 = 0.7586 (0.1771)
7	b_1 = 1.9071 (0.02881)
	log bias correction factor = 1.049
8	b_1 = 2.2 109 (0.6068), b_2 = 0.8093 (0.05347)
9	b_0 = 10.8264 (2.3662), b, = 0.1454 (0.006001)
10	b_1 = 0.2862 (0.01615) b_2 = -0.00005680 (0.000018 19)
11	b_1 = 0.247 1 (0.01615), b_2 = -0.00005089 (0.00001472)
12	b_0 = 9.9455 (2.2715), b, = 0.2264 (0.009060)
13	b_0 = 8.9221 (2.3341), b, = 0.1789 (0.007060)

Model 4, though best in terms of FI, does exhibit slight bias at the upper end of the data (Figure 1.2). Model 2, the linear model with SA_{bh} as sole predictor, had a higher (less desirable) FI, but less bias at the upper end of the data (Figure 1.3). Model 10, the best nonsapwood-based equation, yielded only a slightly higher FI than model 4 and does not exhibit any prediction bias (Figure 1.4). However, this model predicts PLA from ACB and thus requires data which are more difficult to collect. Model 13, which is based on BA,, and mLCR, proved to be an excellent alternative. It does not require difficult data collection, has a comparable FI, and predicts PLA without bias across the range of the data (Figure I.5).

Crown parameters alone were not precise predictors. Crown length only, for example, resulted in FI values twice those of both the best sapwood- and nonsapwood-based models. This sharply contrasts results from Gilmore et al. (1996), who recommend crown length as a SA_{bh} surrogate in A. *balsamea*. Lastly, sapwood taper below the live crown (Maguire and Hann 1987, Maguire and Batista 1996) has led some authors to recommend using the distance from bh to the center of the crown (D) as a predictor variable (Dean and Long 1986, Dean et al. 1988, Long and Smith 1989). This variable failed to contribute significantly to any of the models tested in this study, including the power function $PLA = b_1(SA_{bh}^{b2})(D^{b3})$ originally suggested by Dean and Long (1986).

Figure I .2. Observed and predicted tree projected leaf area (PLA) relative to sapwood area at 1.3 m (SA_{bh}), as a function of SA_{bh} and crown length (CL). Predicted PLA values obtained from model 4, PLA = -9.9148 + 0.2688 x SA_{bh} + 3.8895 x CL.

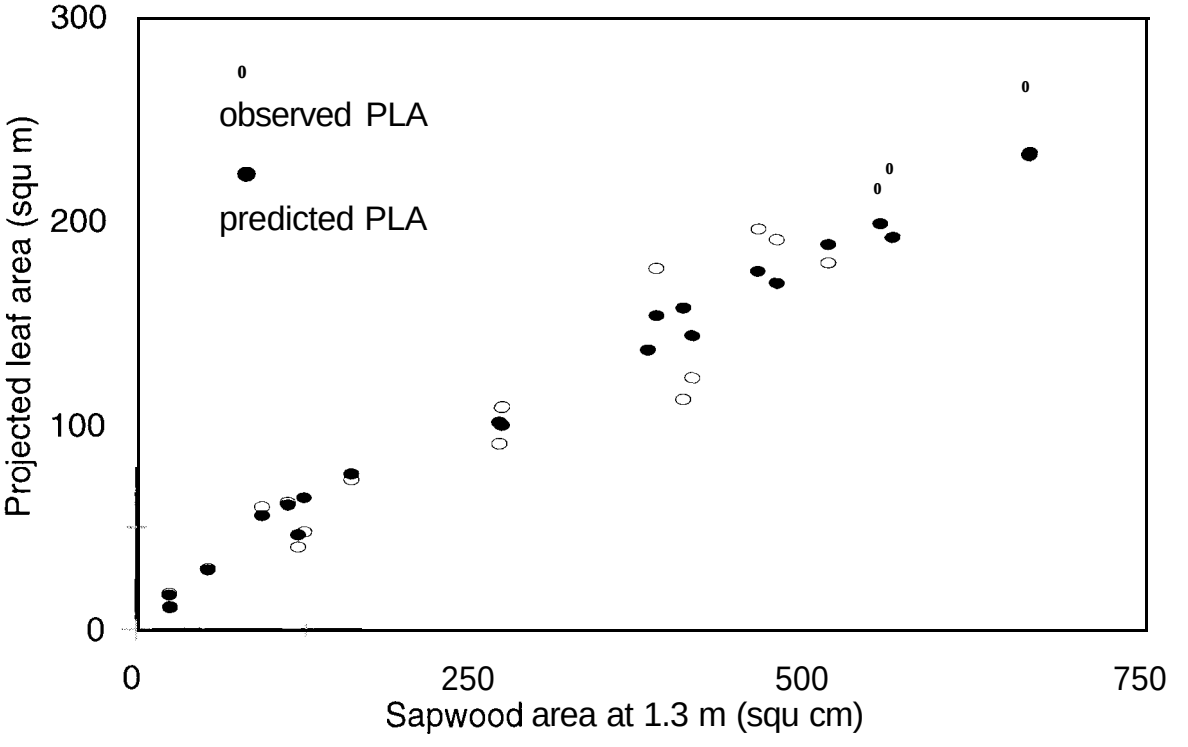

Figure 1.3. Observed and predicted tree projected leaf area (PLA) relative to sapwood area at 1.3 m (SA_{bh}), as a function of SA_{bh}. Predicted PLA values obtained from model 2, PLA = 7.5432 + 0.3659 x SA_{bh}.

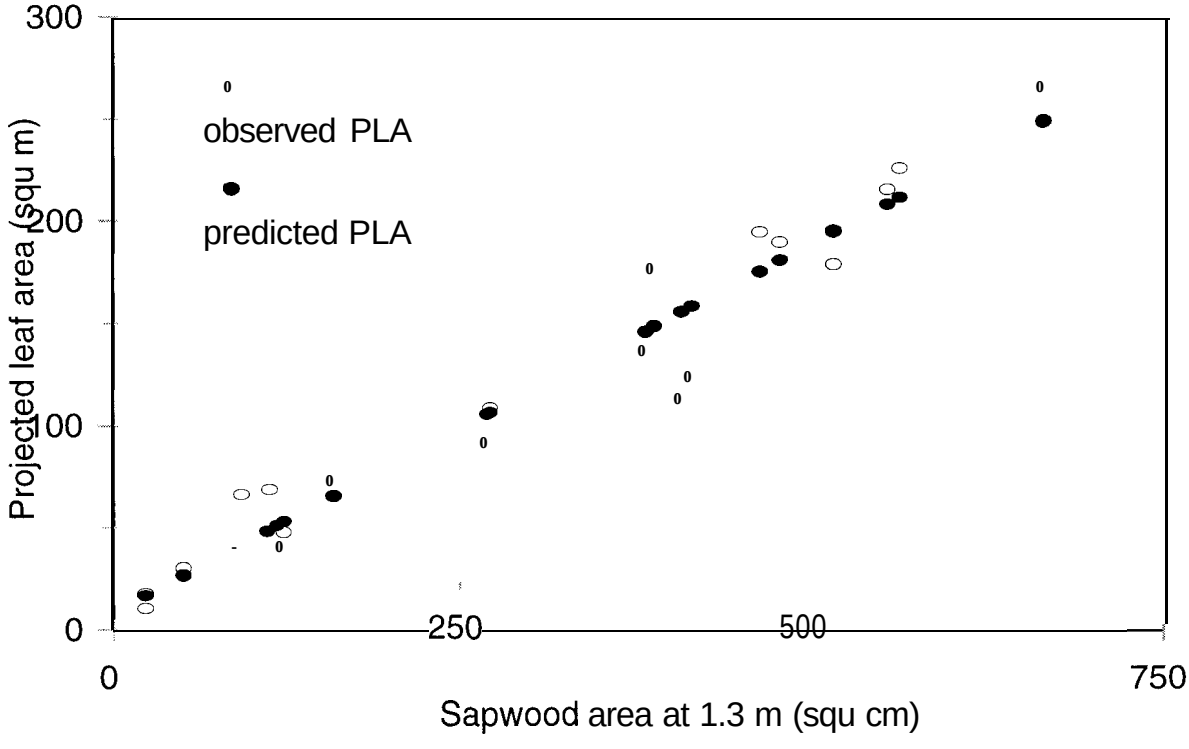

Figure 1.4. Observed and predicted tree projected leaf area (PLA) relative to cross-sectional area inside the bark at crown base (ACB), as a function of ACB. Predicted PLA values obtained from model 10, PLA = 0.2862 x ACB - 0.00005089 x ACB^2.

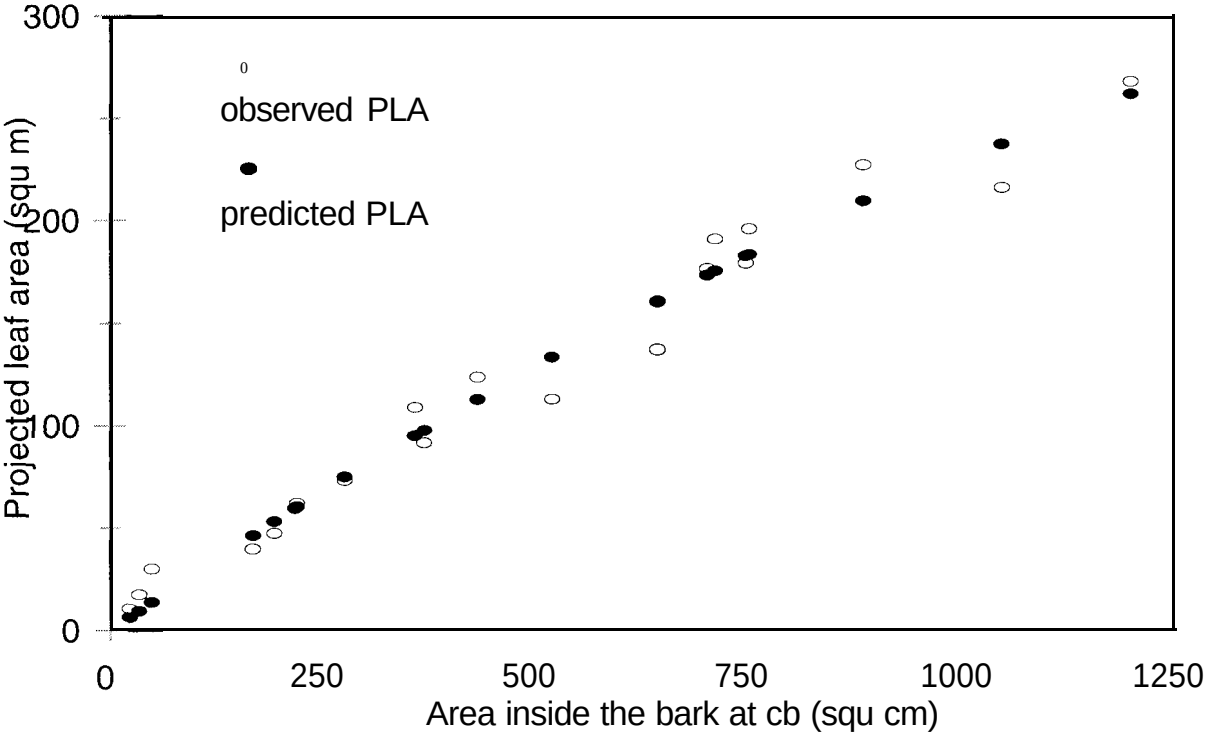

Figure 1.5. Observed and predicted tree projected leaf area (PLA) relative to basal area at 1.3 m ($BA_{,,}$), as a function of $BA_{,,}$ and a modified live crown ratio (mLCR). Predicted PLA values obtained from model 13, PLA = 8.9222 + 0.1789 x ($BA_{,,}$ x mLCR).

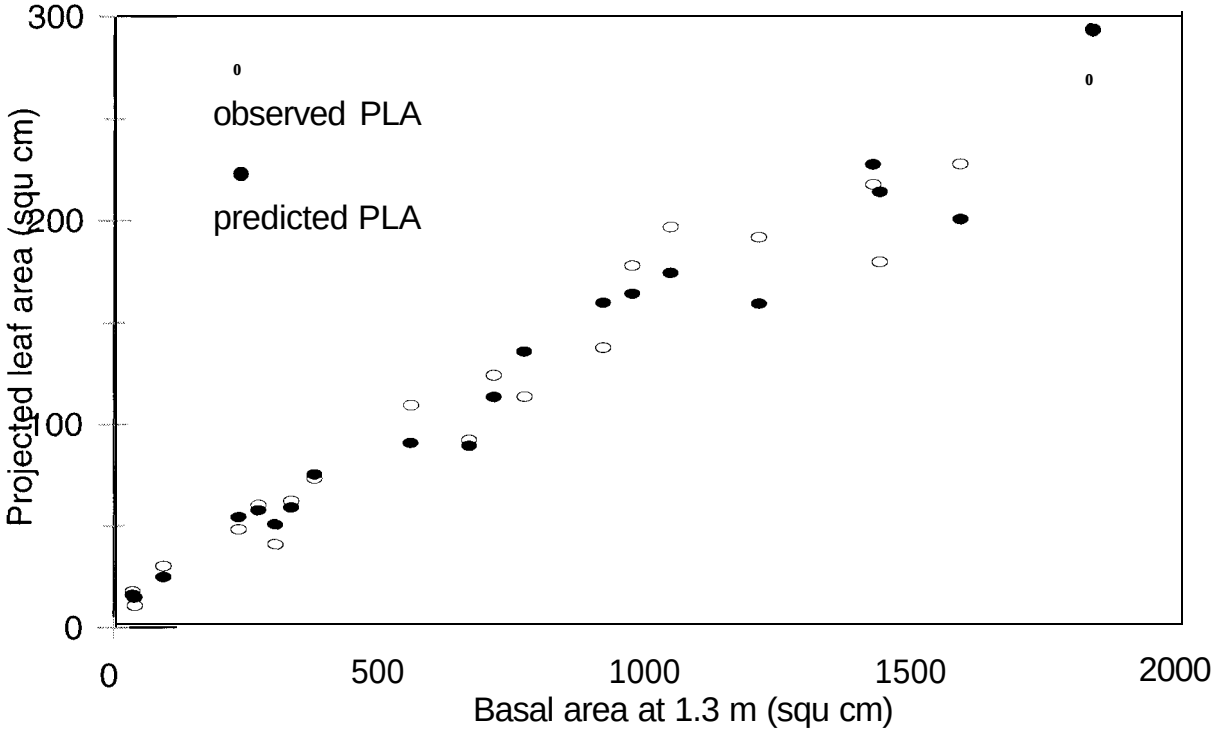

DISCUSSION

Our findings demonstrate the variability in performance of a number of similar and commonly used PLA models when applied to *T. canadensis*. This result is hardly surprising, since these models were developed for different species in different geographic areas, and optimal model form has been found to vary even within species across geographic regions (O'Hara and Valappil 1995, Gilmore et al. 1996). This variation underscores the importance of developing species- and region-specific equations.

One of the reasons for the lack of previous research on *T. canudensis* LA relationships is the difficulty in identifying the sapwood. Unlike other softwood species in the Northeast, the *T. cunudensis* sapwood-heartwood boundary cannot be consistently distinguished with the "light transmittance" test (transparent sapwood, opaque heartwood), especially in increment cores. Eades (1958) noted this problem in *Tsuga heterophylla* (Raf.) Sarg. (western hemlock) and recommended iron salts as a means of colorimetrically differentiating the sapwood. Eades validated this method by applying the chemical to *Pseudotsugu menziesii* (Mirb.) Franco (Douglas-fir), which has a sapwood-heartwood boundary that is easily distinguished with the naked eye by a change in translucence.

T. cunudensis sapwood radii determined in the field and with iron salts did not differ significantly at $a = 0.05$ (paired t-test for means, 39 df, $p = 0.75$). Both methods thus provide independent confirmation of the sapwood-heartwood boundary. Areas of wetwood did not react with the dye. The ferric sulfate reaction is a traditional test for

tannins (Jensen 1962), and apparently highlights differences in the form of tannins between the heartwood and sapwood. Because iron salts are unspecific phenolic reagents, potentially causing a positive result due to reaction with other plant constituents (Swain 1965), we felt it necessary to confirm the validity of this test by identifying the causal mechanism. Some forms of tannins are able to reduce Fe^{3++} to Fe'". Our application of anhydrous ferric chloride (Fe^{3++}) and a Fe^{2++} reagent (Ferrozine) indicated the presence of Fe^{2++} in the sapwood, but not in the heartwood. This confirmed that $Fe^{3++} \rightarrow Fe^{2++}$ reducing tannins are not present in the heartwood, and provided evidence that a difference in the forms of tannins is the mechanism for the ferric sulphate reaction.

Our results confirm the value of SA as a LA surrogate, as is suggested by the functional relationship between conducting xylem and foliage. This supports the findings of Waring et al. (1982), who recommended linear models with SA_{bh} or SA_{bh} for *T. heterophylla* and *Tsuga mertensiana* (Bong.) Sarg. (mountain hemlock). However, Waring et al. (1982) did not test other predictor variables. Our findings indicate that models with SA alone are not optimal for *T. canadensis*. The significance of CL as a second predictor variable may be attributed to the fact that it reflects tree height, the arrangement of foliage in space, or light environment. Unlike Gilmore et al. (1996), we found that crown parameters alone (either CL or conic crown volume) did not perform well as PLA predictors. This may be due to the fact that *A. balsamea*'s growth pattern results in a consistent, geometric crown shape, while *T. canadensis* crowns are more irregular. Additionally, model 4, with SA_{bh} and CL as predictor variables, performed well across most of the range of the data but underestimated PLA of our largest trees. This model could lead to overestimation of growth efficiency for large trees, and should not be

applied to trees at the upper range of our data. Model 2 based on SA_{bh} alone is a less biased alternative.

The equation with sapwood area at crown base SA_{bh} (model 1, weighted by SA_{cb}^{-1}) did not perform as well as the model using SA_{bh}. This is surprising since SA_{bh} is theoretically better related to leaf area, given the taper in sapwood from breast height to crown base (Waring et al. 1982, Maguire and Hann 1987). Gilmore et al. (1996) also found SA_{bh} to be a better predictor than SA_{bh} for *A.balsamea* PLA, but the magnitude of difference in model performance was much greater in their study. Their results may be explained for by the fact that SA_{bh} was measured at the lowest significant whorl in their study, excluding isolated branches below this height.

Perhaps the most interesting result was the performance of models 10, 12, and 13 based on stem cross-sectional area at crown base and breast height with and without mLCR. There is no evidence that the superior performance of these nonsapwood-based models was due to the difficulty of identifying the sapwood in this species (i.e. errors in sapwood identification). The agreement between optical and colorimetric identification of the sapwood - heartwood boundary in this study suggests that the sapwood radius was correctly identified. Model 10, using ACB alone, had the highest R^2, a FI value comparable to that of the best sapwood-based model, and no prediction bias. The superior performance of this model relative to models based on breast height measurements was not surprising, since sapwood taper below the base of the live crown weakens the correlation between stem cross-sectional area and sapwood area (Maguire and Bennett 1996). Despite the superior performance of this model, practical application is limited by the difficulty of measuring area inside the bark at crown base.

Models 12 and 13, nonsapwood-based approaches to PLA estimation suggested by Valentine et al. (1994), produced results comparable to those of the best sapwood-based equations and were free of bias. It has been proposed that mLCR is a surrogate for a taper model (Maguire and Bennett 1996). The approach suggested by Valentine et al. (1994) is thus effective because it approximates estimating LA from cross-sectional area at crown base. There was no detectable advantage to using ABH, which requires bark thickness, instead of the easy-to-measure BA_{bh}, presumably because the two are highly correlated. The ability to substitute BA,, for inside-bark cross-sectional area at breast height means that standard nondestructive measurements of dbh, tree height, and crown length can be used when coring is undesirable. Additionally, these findings suggest that recent theoretical advances made in the understanding of growth dynamics through assessment of leaf area can be implemented via manipulation of trees based on their size and crown ratio. Application of nonsapwood-based models, such as the one proposed by Valentine et al. (1994), may prove valuable for bridging the gap between theoretical and actual manipulations of stand structure based on leaf area distribution.

CHAPTER 2

LEAF AREA AND STEMWOOD VOLUME GROWTH RELATIONSHIPS FOR *TSUGA CANADENSZS, ABZES BALSAMEA,* AND *PZCEA RUBENS* IN MIXED-SPECIES, MULTI-AGED NORTHERN CONIFER STANDS

CHAPTER ABSTRACT

This study explores relationships between tree-level mean annual stemwood volume increment (AVINC) and projected leaf area (PLA) for *Tsuga canadensis* (L.) Carr. (eastern hemlock), *Abies balsamea* (L.) Mill (balsam fir), and *Piceu rubens* Sarg. (red spruce) in mixed-species, multi-aged stands. Equations for prediction of AVINC were derived for these species, and compared to published ones for *A. balsamea* and *P. rubens*. The growth efficiencies (GE = AVINC/PLA) implied by the chosen models were used to discern the magnitude and pattern of change of GE within and between species. AVINC was effectively modeled for each species using nonlinear functions of PLA. Other variables, including age, did not contribute significantly to model performance in the presence of PLA. GE - PLA patterns for all three species approximated the peaking relationships previously conceptualized for shade-tolerant species. Trees in upper canopy strata were more efficient stemwood producers than lower stratum trees, and *A. balsamea* was more efficient than the other two species. *A. balsamea* and *P. rubens* had similarly shaped GE - PLA relationships; magnitudes and ranges differed, however, consistent with the divergent growth rates and longevities of these species. Maximum GE and the subsequent decline over increasing PLA occurred at a higher PLA for *T. canadensis* than for *A. bulsumeu* or *P. rubens*, and maximum GE for *A. bulsumeu* was less than that previously observed in even-aged stands. Results confirm the previously recognized biological relationship between AVINC and PLA, and clarify patterns of tree growth in mixed-species, multi-aged stands.

INTRODUCTION

Research reported here explores relationships between tree-level projected leaf area (PLA), mean annual stemwood volume increment (AVINC), and growth efficiency (GE) in mixed-species, multi-aged northern conifer stands in the Acadian Forest of northeastern North America. This is an ecotone forest between the northern hardwood and boreal forests, with significant components of *Tsuga canadensis* (L.) Carr. (eastern hemlock), *Abies balsamea* (L.) Mill (balsam fir), and *Picea rubens* Sarg. (red spruce). Though previous research has explored leaf area relationships for ***A.*** *balsamea* in even-aged stands (Gilmore and Seymour 1996), and for ***P.*** *rubens* in uneven-aged stands (Maguire et al. 1998), understanding of growth dynamics in complex stands remains incomplete. This study was undertaken to advance knowledge of the relationships between leaf area and tree growth in structurally and compositionally diverse stands.

Hypotheses are as follows:

Hypothesis 1. AVINC = f(PLA)

The biological link between leaf area and stem volume growth has been established in numerous studies (Waring et al. 1981, Vose and Allen 1988, O'Hara 1988, 1989 and 1996, Aplet et al. 1989, Smith and Long 1989 and 1992, Long and Smith 1990 and 1992, Jack and Long 199 1 and 1992, Roberts and Long 1992, Roberts et al. 1993, Gilmore and Seymour 1996, Maguire et al. 1998, Brunner and Nigh 2000). The changes in leaf area allocation that occur in response to silvicultural treatment are determinants of

stemwood growth, and advances in the understanding of leaf area relationships are key to improving our understanding of silviculture.

Previous research has provided models for prediction of *P. rubens* (Maguire et al. 1998) and *A. balsamea* (Gilmore and Seymour 1996) volume increment from PLA. These model forms will be evaluated for application to our data, and an AVINC model for *T. canadensis* will be proposed.

Hvpothesis 2. GE = f(PLA)

It has long been recognized that GE, the amount of stem volume growth per unit leaf area (or leaf area surrogate), varies in response to a number of stand and individual tree factors. Assmann (1970), and later Roberts and Long (1992) and Roberts et al. (1993), proposed that GE of shade-tolerant trees in even-aged stands increases then declines as PLA increases (Figure 2.1). Gilmore and Seymour (1996), however, found that the GE - PLA relationship for even-aged *A. balsamea* varied as a function of the chosen AVINC model form and GE surrogates. They were unable to identify a specific pattern of change in GE with increasing PLA, but did conclude that suppressed trees were less efficient than those of other crown classes. This supported previous research on *Pseudotsugu menziesii* (Mirb.) Franco (Douglas-fir) that documented lower GE values for suppressed trees in even-aged stands (Waring et al. 1980, O'Hara 1988). The peaking GE - PLA pattern has not been documented for shade-intolerant species, which exhibit declining GE with increasing PLA in even-aged stands (Figure 2.1, O'Hara 1988, Long and Smith 1990 and 1992, Jack and Long 199 1 and 1992, Smith and Long 1992, Roberts et al. 1993).

Figure 2.1. Conceptual patterns of stemwood growth efficiency over leaf or crown area for trees in (A) even-aged stands of shade-tolerant species (Assmann 1970, Roberts and Long 1992), (B) even-aged stands of intolerant species (O'Hara 1988, Jack and Long 1991 and 1992, Long and Smith 1990 and 1992, Smith and Long 1992, Roberts et al. 1993), (C) multi-aged stands of intolerant species (O'Hara 1996), and (D) multi-aged stands of tolerant species (Assmann 1970).

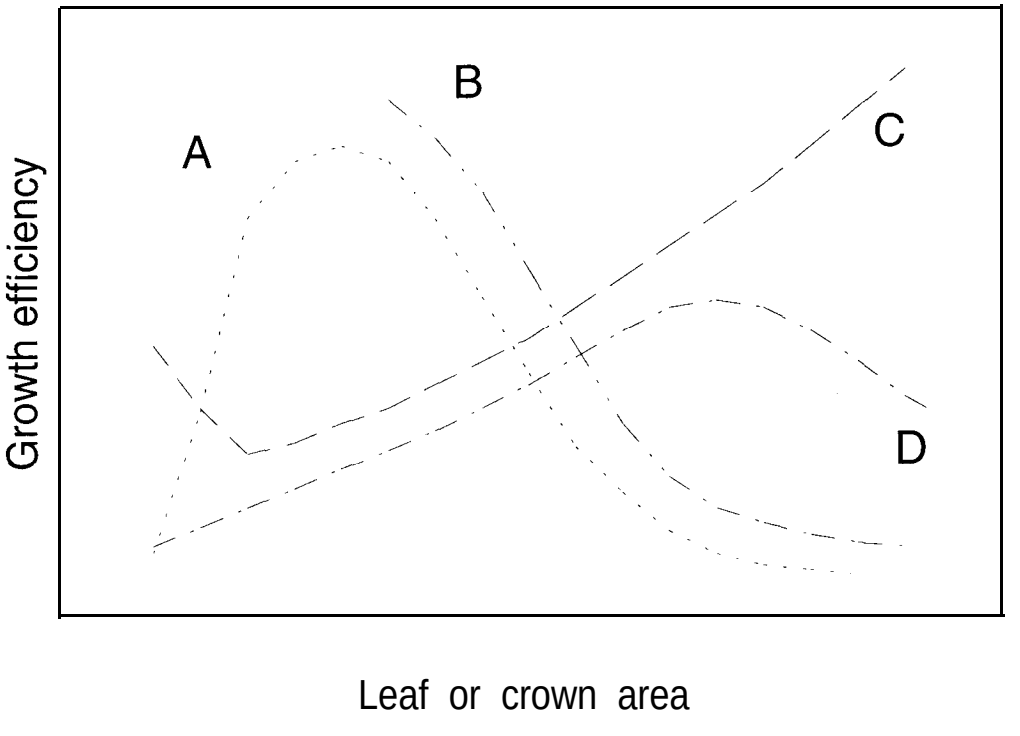

Assmann (1970) suggested a peaking relationship for GE of shade-tolerant species in multi-aged stands, though the attainment of maximum GE is postponed until trees reach upper canopy positions (Figure 2.1). A different pattern, indicating increasing GE with increasing PLA, was suggested by O'Hara (1996) for the shade-intolerant *Pinus ponderosa* Dougl. Ex Laws. (ponderosa pine) in multi-aged arrangements (Figure 2.1). Neither pattern agrees with a study of *P. rubens* in multi-aged stands, which found that *P. rubens* GE decreased with increasing PLA (Maguire et al. 1998).

The study reported here revisits *P. rubens* GE relationships, expands the *A. balsamea* leaf area research to multi-aged structural arrangements, and addresses patterns in *T. canadensis* - a common species in the Acadian Forest and the largest component of stand basal area (BA) in the study stands.

Hvpothesis 3. GE = f (PLA, canopy stratum)

Research in even-aged stands for *A. balsamea* (Gilmore and Seymour 1996) and in multi-aged stands for *P. rubens* (Maguire et al. 1998) suggests that while PLA relationships are complex and a multitude of variables affect GE, there is generally a benefit resulting from improved light environment with regard to AVINC per unit PLA. Assmann (1970) discussed this phenomenon with regard to canopy structure, and presented data supporting a positive relationship between GE and canopy position for *Picea abies* (L.) Karst (Norway spruce) and *Abies alba* Mill. (silver fir) in multi-aged stands. Canopy position, expressed as canopy stratum (Oliver and Larson 1996, Smith et al. 1997), is used as a surrogate for light environment in this study. The influence of canopy position on GE is modeled for each species.

Hypothesis 4. GE = f(PLA, species)

The research reported here has provided, for the first time, data to compare GE - PLA relationships among *A. balsamea*, *P. rubens*, and *T. canadensis*. These species are among the most common shade-tolerant conifers in the Acadian Forest, and are also important components of many forest types in the eastern United States and Canada. Species differences in GE magnitude and GE - PLA relationships will be examined.

STUDY AREA

The two stands sampled in this study, C9 and C16, are part of a long-term silvicultural experiment on the 1540-ha Penobscot Experimental Forest (PEF) in east-central Maine, located at approximately 44°52'N, 68°38'W. The PEF was purchased in 1950 by a number of industrial landholders and leased to the U.S.D.A. Forest Service, which initiated an experiment to study even- and multi-aged silvicultural systems. Treatments and remeasurements have continued to the present and follow a long-term study plan which ensures consistency in management over time. The two stands used for this research are replicates of selection cutting on a 5-year cycle, with nine (C9) and eight (C 16) selection cuttings prior to our research. C9 (11 .O ha) and C 16 (6.6 ha) both have a structural goal defined using the BD*q* method (Guldin 199 1), with a q-factor of 1.96 on 5-cm classes, a residual maximum diameter goal of 48 cm, and a target residual BA of 26 m^2/ha. Both stands have irregular diameter and age distributions (Figures 2.2 and 2.3,

Figure 2.2. Diameter distributions of multi-aged stands C9 and Cl6 on the Penobscot Experimental Forest in Maine.

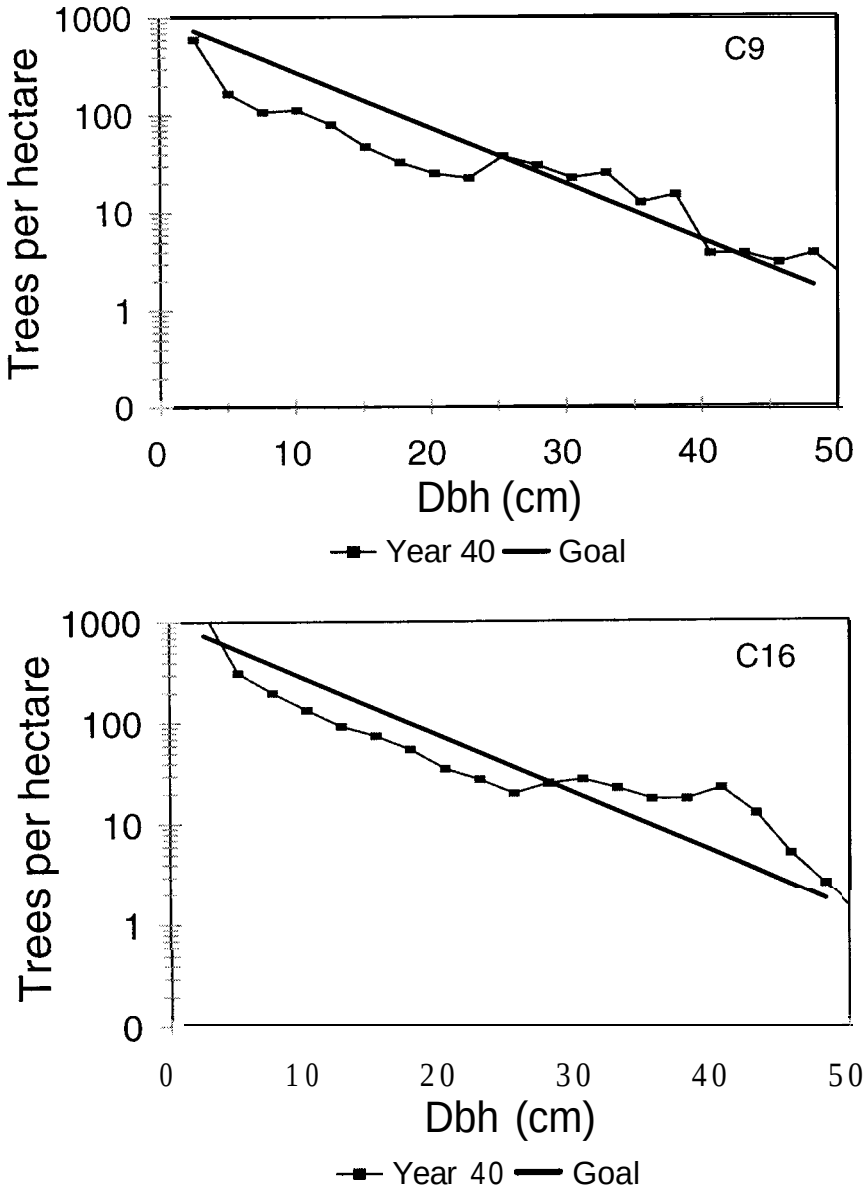

Figure 2.3. Age structures for *Tsuga* ***canadensis, Abies balsamea,*** and *Picea rubens* in two multi-aged northern conifer stands on the PEF.

C9

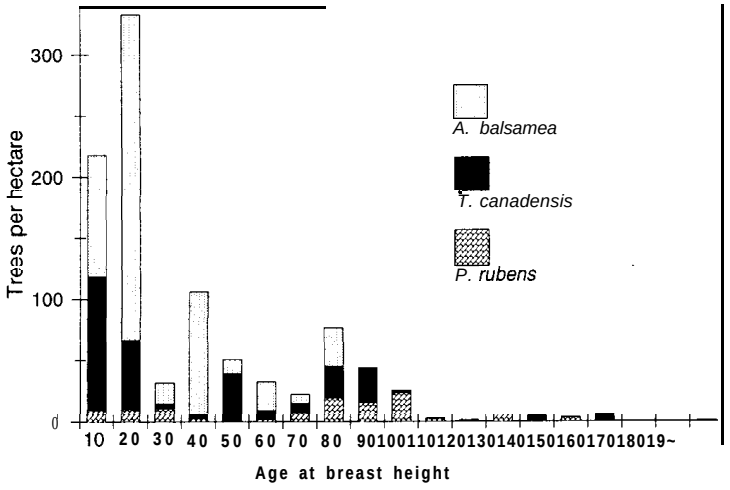

Cl6

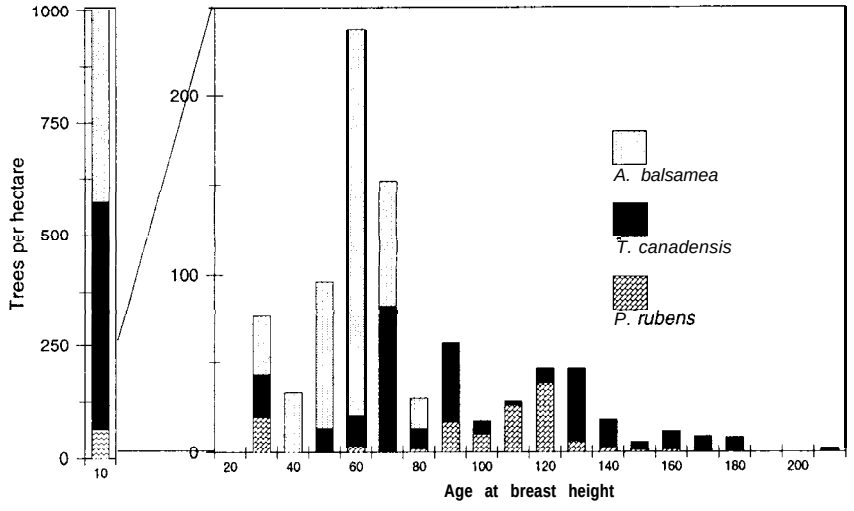

Kenefic and Seymour 1997 and 2000, Seymour and Kenefic 1998). Relative density (RD, Wilson et al. 1999) in the study stands is low; data from recent pre-cut inventories indicate RD = 0.30 in C9 (1998) and RD = 0.3 1 in C 16 (1996).

Within- and between-stand species compositions are highly variable due to small-scale differences in soil drainage and stand structural condition. The dominant species are *T. canadensis, P. rubens*, and *A. balsamea.* Other species include *Pinus strobus* L. (eastern white pine), *Thuja occidentalis* L. (northern white-cedar), *Acer rubrum* L. (red maple), *Betula papyrifera* Marsh. (paper birch), *Picea glauca* (Moench.) Voss (white spruce), and other hardwoods (Kenefic and Seymour 1997, Kenefic 2000). Species composition goals based on species' relative desirability are used to prioritize removals (Table 2.1). Treatments to date have emphasized removal of *T. canadensis* and *A. balsamea,* and retention and release of *P. rubens*.

METHODS

A 25-m systematic grid was established in the study stands in 1995. A random sample of 100 *T. canadensis,* 100 *P. rubens*, and *50 A. balsamea,* stratified by 5-cm diameter at breast height (dbh, 1.3 m) classes, was taken from 12.5-m radius plots centered on the grid points in July and August of 1995 (C 16) and 1997 (C9). The sample included trees at least 1.3 m in height, up to a maximum of 50.0 cm dbh *(T. canadensis* and *P. rubens*) or 25.0 cm dbh *(A. balsamea).* Sampling was restricted to somewhat poorly, moderately well, and well drained soils, and excluded the U.S.D.A. Forest Service

Table 2.1. Species compositions of multi-aged stands C9 and C 16 on the Penobscot Experimental Forest and the U.S.D.A. Forest Service goal, expressed as percent of basal area (BA) of trees >1.27 cm dbh. Species are listed in order of desirability, per the U.S.D.A. Forest Service study plan (R.M. Frank unpublished).

Species	c 9	**Cl6**	**Goal** [1]
Picea spp.	25.0	21.8	35 - 55 %
Abies balsamea	12.7	15.5	15 - 25 %
Pinus strobus	12.0	0.5	5 - 10 %
Betula papyrifera	3.8	1.8	5 - 10 %
Tsuga canadensis	32.1	51.0	15 - 25 %
Thuja occidentalis	3.5	4.4	5 - 10%
Acer rubrum [2]	8.6	5.0	5 - 10 %
	100	100	

[1] R.M. Frank, unpublished.

[2] Goal is for *Acer rubrum* and other hardwoods combined.

continuous forest inventory plots. Diameter at breast height, bark thickness, total height (HT, m), height to live crown, crown radii in four cardinal directions, and canopy stratum (Table 2.2, Oliver and Larson 1996, Smith et al. 1997) were recorded for each sample tree. In order to be consistent with measurements taken for development of published nonsapwood-based PLA prediction equations, height to live crown was defined as height to lowest branch for *T.* canadensis (Chapter 1, Kenefic and Seymour 1999) and *P. rubens* (Maguire et al. 1998), and height to the lowest whorl consisting of at least three live branches for *A. balsamea* (Gilmore et al. 1996). A lo-basal area factor (BAF) prism tally, centered on the sample tree, was made to determine stand BA at that location (an index of competition). Two increment cores were removed at breast height for determination of tree age, annual radial increment, and sapwood radius. Ages at breast height of trees smaller than 5.0 cm were determined by counting internodes on the main stem. Height and dbh were remeasured in July 2000.

Sapwood-heartwood boundaries were identified in the field by holding each increment core to the sunlight, and marking the apparent boundary between the translucent (water conducting) and non-translucent zones. Translucent wetwood zones in *T.* canadensis cores, separated from the sapwood by opaque bands of growth rings, were assumed to be bacterial infection of the heartwood and were ignored. A 0.1 M solution of ferrous ammonium sulfate ($Fe(NH_4)_2(SO_4)_2.6H_2O$) was applied to *T. canadensis* cores in the laboratory to identify the sapwood colorimetrically (Eades 1958, Kenefic and Seymour 1999). Field-marked sapwood boundaries were either confirmed or adjusted in favor of the dye for this species.

Table 2.2. Canopy strata in 5-year selection stands on the PEF, described by *Tsuga canadensis, Abies balsamea,* and *Picea rubens* mean ages at bh, tree heights, crown lengths, and crown projection areas (SEs in parentheses).

Species	Stratum	Age at bh (years)	Height (m)	Crown length (m)	Crown projection area (m^2)
T. canadensis n= 100	B	118.6 (5.4)	18.66 (0.38)	14.52 (0.44)	41.55 (2.85)
	c	77.3 (5.8)	12.42 (0.36)	9.66 (0.47)	34.80 (7.4)
	D	52.8 (8.1)	6.85 (0.56)	4.75 (0.44)	9.78 (1.42)
	E	14.4 (8.1)	2.61 (0.56)	1.95 (0.33)	2.35 (0.94)
A. balsamea n = 50	B	65.6 (3.8)	16.89 (0.63)	12.07 (0.67)	13.24 (1.55)
	C	56.3 (4.8)	10.84 (0.8 1)	7.86 (0.68)	10.56 (1.45)
	D	38.6 (4.6)	6.33 (0.65)	3.95 (0.5 1)	8.01 (1.26)
	E	9.1 (3.2)	2.5 l (0.40)	1.86 (0.39)	3.51 (1.06)
P. rubens n= 100	B	107.6 (2.5)	19.30 (0.35)	11.36 (0.41)	32.31 (2.18)
	C	83.4 (5.7)	11.73 (0.50)	6.69 (0.55)	7.96 (0.85)
	D	76.5 (11.4)	6.78 (0.72)	3.68 (0.25)	6.10 (1.20)
	E	8.9 (2.1)	2.31 (0.18)	1.72 (0.15)	1.62 (0.14)

Each increment core was hand polished with fine grit sandpaper and radial increments and width of the sapwood were measured to 0.01 mm with a Velmex measuring system (Velmex, Inc.). Sapwood area at breast height (SA_{bh}) was determined for each tree as a function of diameter, average sapwood radius, and average bark thickness at breast height. Ring-width series were crossdated using COFECHA (Holmes 1983), and missing rings accounted for when possible. Ages at breast height of trees with incomplete cores (28 trees (25 %) in C9, 42 trees (38 %) in C16) were estimated using pith locators, i.e. transparencies with concentric circles equal in width and curvature to the last measured increment (Applequist 1958).

Calculations

Projected Leaf Area

Projected leaf area was determined for each sample tree using published equations for prediction of PLA (Gilmore et al. 1996, Maguire et al. 1998, Kenefic and Seymour 1999), or leaf biomass (Young et al. 1980) multiplied by specific leaf area (SLA, cm^2/g). Saplings < 2.5 cm dbh were excluded from analysis because there are no published PLA or biomass equations for trees of this size, thus reducing sample size of *T. canadensis* by 8, *A. balsamea* by 5, and *P. rubens* by 6.

Projected leaf area was predicted for *T. canadensis* with dbh > 6.8 cm (the smallest dbh used for PLA model development) using the equation $PLA = b_0 + b_1 (BA_{cs} \times mLCR)$ (Valentine et al. 1994), where $b_0 = 8.9221$, $b_1 = 0.1789$, and $R^2 = 0.95$ (Kenefic and Seymour 1999). BA_{cs} is stem cross-sectional area at breast height (cm^2) and mLCR (modified live crown ratio) = CL/(HT- 1.3), where CL is crown length (m) and HT is tree

height (m). Four trees had stem and/or crown parameters slightly exceeding those used for PLA nonsapwood-based model development, but sapwood areas fell within the range used for development of the sapwood-based model (Kenefic and Seymour 1999). Projected leaf area of these trees was predicted with the equation PLA = b_0 + b_1 SA_{bh}, where b_0 = 7.5432 and b_1 = 0.3659. Leaf biomass equations (R^2 = 0.88, Young et al. 1980) were used to predict dry leaf weight of trees 2.5 - 6.8 cm dbh, which was then multiplied by mean SLA (58.43 cm^2/g, Kenefic and Seymour 1999) to determine PLA.

The equation PLA = b_1 SA_{bh}^{b2}, where b_1 = 0.595009, b_2 = 0.987084, and R^2 = 0.89 (Maguire et al. 1998) was applied to ***P. rubens*** with dbh > I 1 .O cm (the smallest tree used for model development in that study). The data used for Maguire's et al. (1998) research were collected on the PEF, allowing PLA estimation without concern for regional variation in model form **and** parameter estimates (O'Hara and Valappil 1995). The PLA values of trees 2.5 - 11 .0 cm dbh were determined using a ***P. rubens*** leaf biomass equation (R' = 0.86, Young et al. 1980) and mean SLA for this species (43.51 cm^2/g, Maguire et al. 1998).

Tree-level PLA was predicted for ***A. balsamea*** using the equation PLA = $b_1 SA_{bh}^{b2} CL^{b3}$ (Long and Smith 1989), where b_1 = 0.422, b_2 = 0.288, b_3 = 1.665, and R^2 = 0.94 (Gilmore et al. 1996). Data for their study were collected on the PEF and nearby University of Maine Dwight D. Demeritt Forest. Projected leaf area values of trees which were too small to core were predicted using the nonsapwood-based equation ln(PLA) = b_0 + b_1 ln(CL) (Gilmore et al. 1996), where b_0 = 0.250, b_1 = 1.707, R^2 = 0.88 and the log bias correction factor (Baskerville 1972) = 1.173.

Mean Annual Volume Increment

Total stem volume (V) was determined in ft^3 for each sample tree at the initial sampling date *t* (1995 in C 16 and 1997 in C9) using Honer's (1967) volume equations, and converted to m^3 using the conversion factor 0.02832. Mean annual radial increment (ARINC, cm) for the 5-year period prior to sampling was determined for each tree using the average of radial increments from the two breast height cores. Radial increments from the two cores were averaged to determine a mean value for each year, then ARINC was calculated by averaging mean annual values across the 5-year period. Radial increments of trees too small to core, and mean annual height increments (AHINC, m) of all trees, were determined by remeasuring dbh and height in 2000, subtracting the earlier (1995 or 1997) measurement and dividing by the number of intervening years. Trees that were cut or damaged were excluded from analysis (T. *canadensis* n = 16, *A. balsamea* n = 8, and P. *rubens* n = 18), with the exception of 15 *T. canadensis* for which height increment had been measured after felling for the PLA study (Chapter 1, Kenefic and Seymour 1999).

AVINC was calculated by subtracting ARINC x 2 and AHINC from dbh at time *t* and HT at time *t*, respectively. The new dbh and HT (at time t-l, 1994 in Cl6 and 1996 in C9) were entered into Honer's (1967) stem volume equations to calculate volume at t-l (V_{t-1}). Finally, AVINC = $V_t - V_{t-1}$. Note that we are assuming that AHINC and ARINC are constant over a short (< 5 year) period.

Analysis

Regression Modeling

We compared nonlinear equations (Table 2.3) of the form $y_i = f(\beta | x_i) + \varepsilon_i$, where $\varepsilon_i \overset{iid}{\sim} N(0, x_i^n \sigma^2)$, to identify equations suitable for predicting AVINC from PLA (SAS 1990, PROC NLIN). Only equations with significant parameters (a = 0.05) were considered, and plots of standardized residuals against predicted variables were used to verify homogeneous variance. Equations were weighted by x_i^n with n = 0, -1, -2 in order to identify the optimal weighting factor to correct for heteroskedasticity. Reasonable biological behavior was taken into consideration, and evaluated using scatter plots of the sample data against the predictor equations.

Generalized R^2 (Kvålseth 1985) was calculated for weighted equations using the corrected sum of squares $(1 - (\text{cssresid}/\sum(y_i - y_m)^2))$, where the y_i's are the individual sample values and y_m is the sample mean. Graphs of the residuals from the AVINC - PLA models were used to determine if predictions were biased relative to other potential predictor variables (dbh, HT, and age at breast height). Furnival's (1961) index of fit (FI), a modified maximum likelihood criterion that allows concurrent evaluation of root mean square error, normality, and homoskedasticity, was used to identify optimal model forms. FI has the advantage of simultaneously allowing comparison both across model forms and within models across weighting factors. The lower the FI value, the better the fit based on the criteria listed above.

Table 2.3. Nonlinear equations tested for prediction of *Tsuga canadensis*, *Abies balsamea*, and *Picea rubens* AVINC from PLA.

	Model	Reference
1	$AVINC = b_1 PLA^{b2}$	Long and Smith (1990, 1992), Gilmore and Seymour (1996), Brunner and Nigh (2000)
2	$AVINC = b_1 (\exp(b_2/(PLA + b_3)))$	Ratkowsky (1990)
3	$AVINC = b_1 (1-\exp(-b_2 PLA))^{b3}$	Yang et al. (1978), Gilmore and Seymour (1996), Shvets and Zeide (1996)
4	$AVINC = b_1 (PLA^{b3-1} \exp(-(b_2 PLA)^{b3}))$	Maguire et al. (1998)
5[a]	$AVINC = \exp(b_1 + b_2 \ln(PLA)) - (3.78 \cdot 10^{-3})$	

[a] variation of model 1 tested for *P. rubens* only

Analysis of Variance

Growth efficiency, defined as AVINC (m") / PLA (m^2), was calculated for each sample tree. Analysis of variance (ANOVA, SAS 1990, PROC GLM) was applied to test the effects of canopy position and species on mean GE and PLA (a = 0.05). Bonferroni pairwise comparisons, which control experimentwise Type I error rate but are conservative (i.e., higher Type II error rate for pairwise comparisons) (Schlotzhauer and Littel 1997), were used to explore the differences in mean GE by species and stratum (a = 0.05). ANOVA assumptions of normality and equal variance were assessed using the Wilk-Shapiro test (SAS 1990, PROC UNIVARIATE) and Levene's test (SAS 1990, PROC ANOVA).

RESULTS

AVINC - PLA Relationshim

All models tested for prediction of *T. canadensis* AVINC yielded similar R^2 values (range 0.78 - 0.80, Table 2.4). Model 3 (Yang et al. 1978, Gilmore and Seymour 1996, Shvets and Zeide 1996) proved to be the best, in terms of FI, of the four equations tested for estimation of *T. canadensis* AVINC from PLA (Table 2.4, Figure 2.4). Model 4 yielded comparable FI and R^2 values, and is also a reasonable equation for prediction of *T. canadensis* PLA. Model 1 overestimated AVINC of *T. canadensis* with PLA < 25 m^2, while model 2 underestimated AVINC of trees at the upper range of the data.

Table 2.4. Parameter estimates, weighting factors and fit statistics for nonlinear models tested for prediction of ***Tsuga*** *canadensis*, *Abies balsamea*, and *Picea rubens* AVINC from PLA, SEs in parentheses.

	Model	Parameter estimates	$R^{2\,a}$	FI [b]	Weight
T. canadensis					
	1	b_1 = 0.00005191 (0.00001111), b_2 = 1.1810 (0.04517)	0.775	0.00298	LA^{-2}
	2	*b_1 = 0.05302* (0.007071), b_2 = -172.433 1 (23.9412), b_3 = *27.3797 (4.7665)*	0.788	0.00299	LA^{-2}
	3 [d]	*b_1 = 0.05328* (0.01970) b_2 = *0.004589* (0.002121), b_3 = 1.4158 (0.134756)	0.795	0.00289	LA-'
	4	*b_1 = 0.00003544* (0.00001072), b_2 = 0.002615 (0.0005869), b_3 = *2.2905 (0.07284)*	0.797	0.0029 1	LA^{-2}
A. balsamea					
	1	*b_1 = 0.00005564* (0.00001291), b_2 = 1.2645 (0.06621)	0.878	0.00086	LA^{-2}
	2 [d]	*b_1 = 0.03368* (0.008717), b_2 = -92.4196 (19.7341), b_3 = 15.4520 (3.4121)	0.887	0.00083	LA^{-2}
	3	b_1 and b_2 are not significant			
	4	b_2 is not significant			
P. rubens: D and E strata					
	1 [d]	*b_1 = 0.0002446 (0.00008* 114), b_2 = *0.5384 (0.1361)*	0.694	0.00033	LA-'
	2	b_2 and b_3 are not significant			
	3 - 4	failed to converge			
P. *rubens*: B and C strata					
	1	b_1 is not significant			
	2	*b_1 = 0.038* 11 (0.005486), b_2 = - 13 1.68 12 (26.7536), b_3 = 18.3719 (7.843 1)	0.773	0.0034 1	LA^{-2}
	3	*b_1 = 0.02890 (0.005* 179), b_2 = *0.009* 174 (0.009 175), b_3 = 1.6875 (1.6875)	0.779	0.00344	LA^{-2}
	4	*b_1 = 0.00004077* (0.000016 19), b_2 = *0.002648 (0.0005* 127), b_3 = *2.2386 (0.09100)*	0.775	0.00357	LA^{-2}
	5 [d]	b_1 = -7.3433 (0.1745), b_2 = 0.6868 (0.03689), log bias correction[c] = 1.02912	0.846	0.00345	none

[a] Kvålseth (I 985), [b] Furnival (1961), [c] Baskerville (1972), [d] chosen model

Figure 2.4. Observed and predicted *Tsuga canadensis* mean annual volume increment (AVINC) relative to projected leaf area (PLA). Predicted values obtained from model 3, AVINC = 0.05328 $(1\text{-}\exp(-0.004589\,\mathrm{PLA})^{1.4158})$.

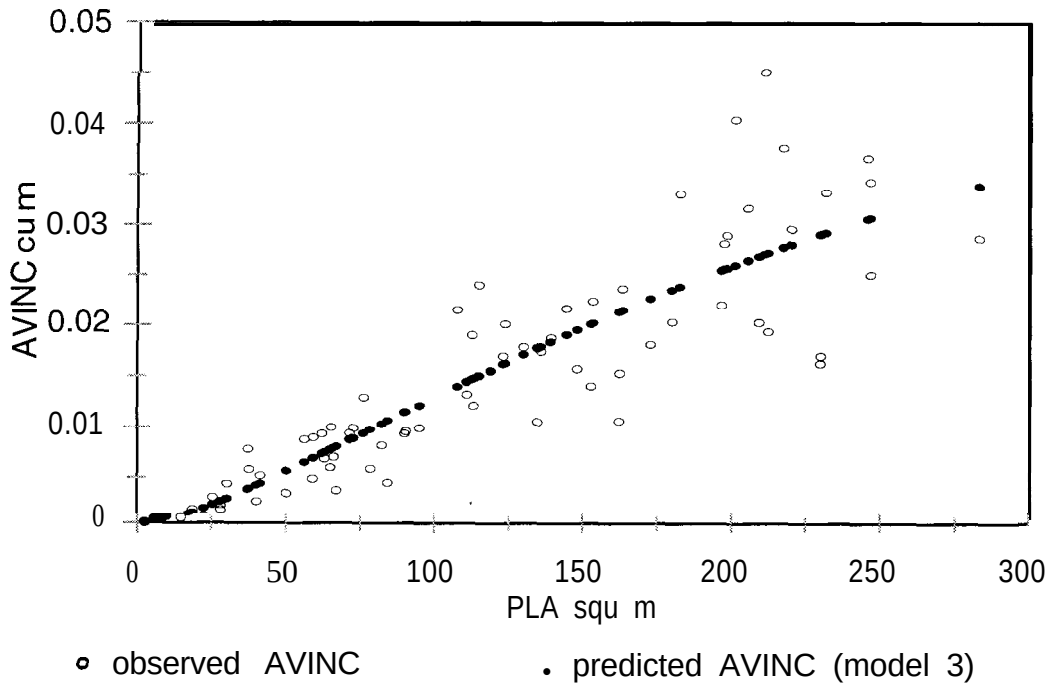

Furnival's Index indicated that Model 2 (Ratkowsky 1990) was optimal for estimation of *A. balsamea* AVINC (R^2 = 0.89, Table 2.4, Figure 2.5). Model 1, used by Gilmore and Seymour (1996) for prediction of *A. balsamea* AVINC in even-aged stands, was an effective and unbiased model, but had somewhat higher FI and lower R^2 values (R^2 = 0.88). Models 3 and 4 failed to yield significant parameter estimates and were not considered for estimation of *A. balsameu* AVINC in this study.

None of the models tested yielded satisfactory results for estimation of *P. rubens* AVINC from PLA. Model 1 represented the upper end of the data well, but overestimated AVINC of trees with < 50 m^2 PLA. Models 2-4 provided more accurate predictions for trees with small amounts of PLA, but underestimated AVINC of trees with > 250 m^2 PLA. Examination of the data suggested that AVINC would be better estimated by models fit to the lower (D and E) and upper (B and C) strata separately (Figure 2.6). Stratifying the data in this way resolved the prediction bias, confirming different trajectories for the upper and lower canopy strata.

AVINC of *P. rubens* in the D and E strata was predicted by model 1, an equation found effective for *A. balsamea* (Gilmore and Seymour 1996), *Pinus contortu* var. *latifolia* (lodgepole pine) (Long and Smith 1990 and 1992) and *P. menziesii* (Brunner and Nigh 2000) (R^2 = 0.69, Table 2.4, Figure 2.7). Models 2 - 4 either failed to converge or failed to yield significant parameter estimates (a = 0.05) for D and E stratum trees. AVINC of *P. rubens* in the B and C strata was also best predicted by model 1 (with an added intercept term), but the parameter estimate for *b,* was not significantly different from zero. A log transformation of a linear variation of model 1, however, yielded

Figure 2.5. Observed and predicted *Abies balsamea* mean annual volume increment (AVINC) relative to projected leaf area (PLA). Predicted values obtained from model 2, AVINC = 0.03368(exp(-92.4196/(PLA + 15.4520))).

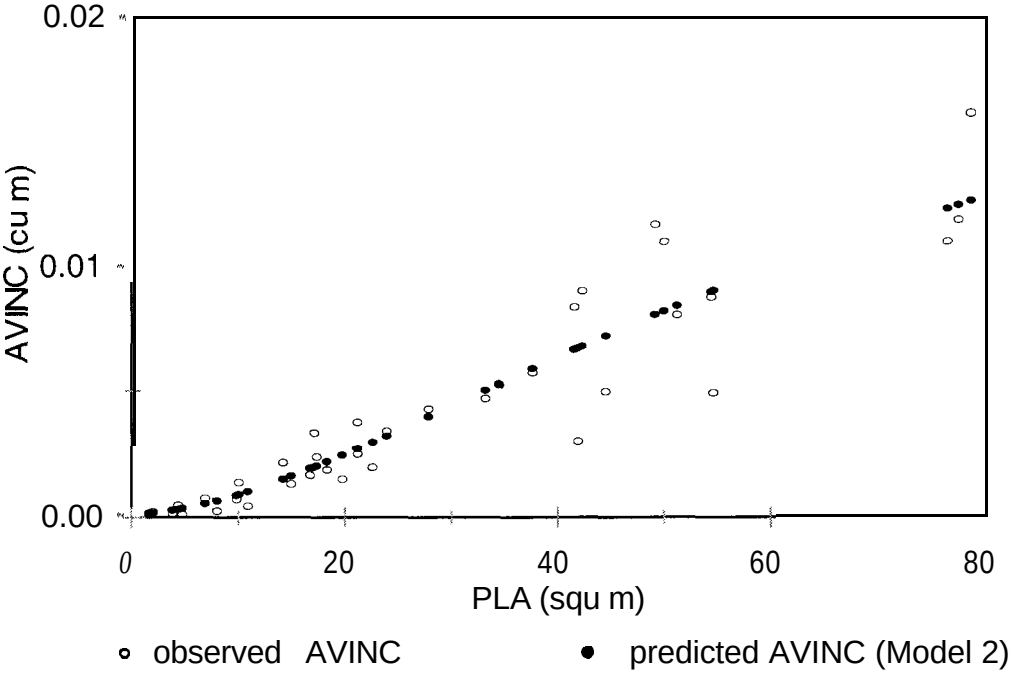

Figure 2.6. Observed *Picea rubens* mean annual volume increment (AVINC) relative to projected leaf area (PLA), with data points identified by stratum, showing (A) all trees used in modeling and (B) an enlarged graph of the boxed area in (A).

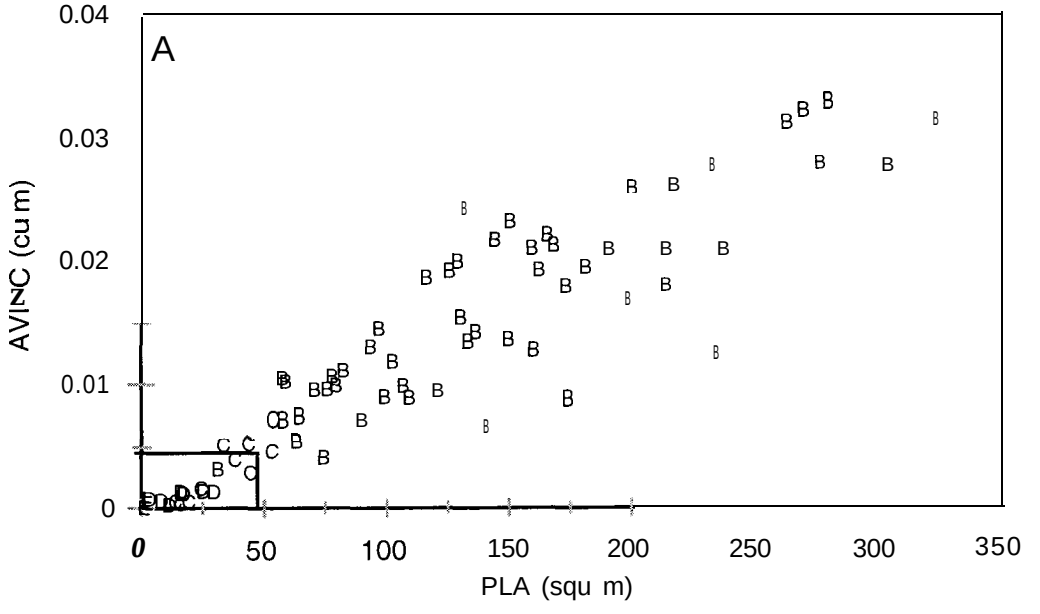

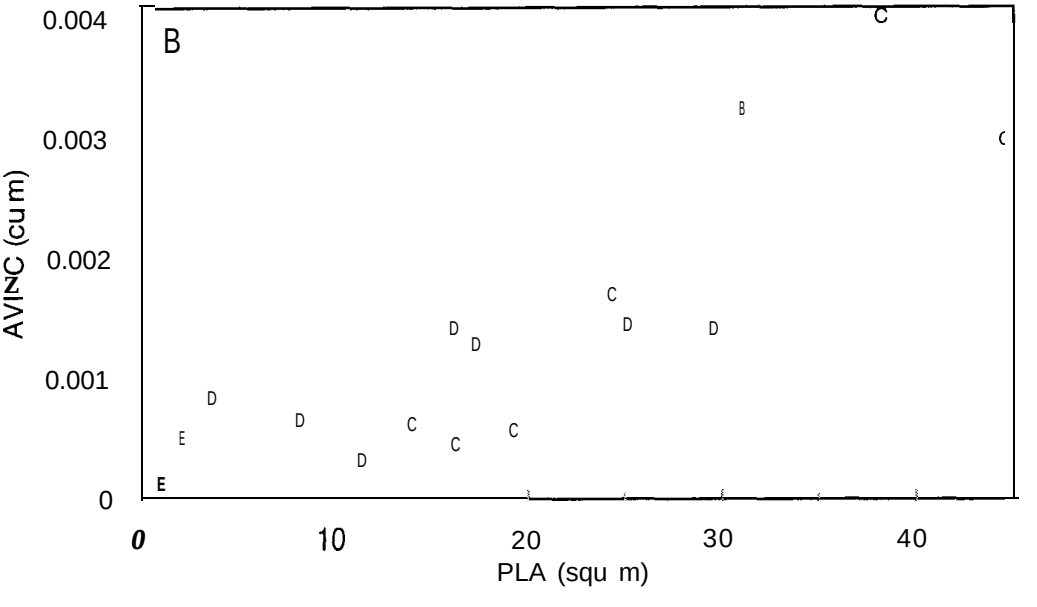

Figure 2.7. Observed and predicted *Picea rubens* mean annual volume increment (AVINC) relative to projected leaf area (PLA). Predicted values for B and C stratum trees (A) obtained from the model 5, AVINC = (exp(-7.3433 + 0.6868 ln(PLA)))-0.003783) x 1.02912. Predicted values for D and E stratum trees (B) obtained from model 1, AVINC = 0.0002446 x $PLA^{0.5384}$.

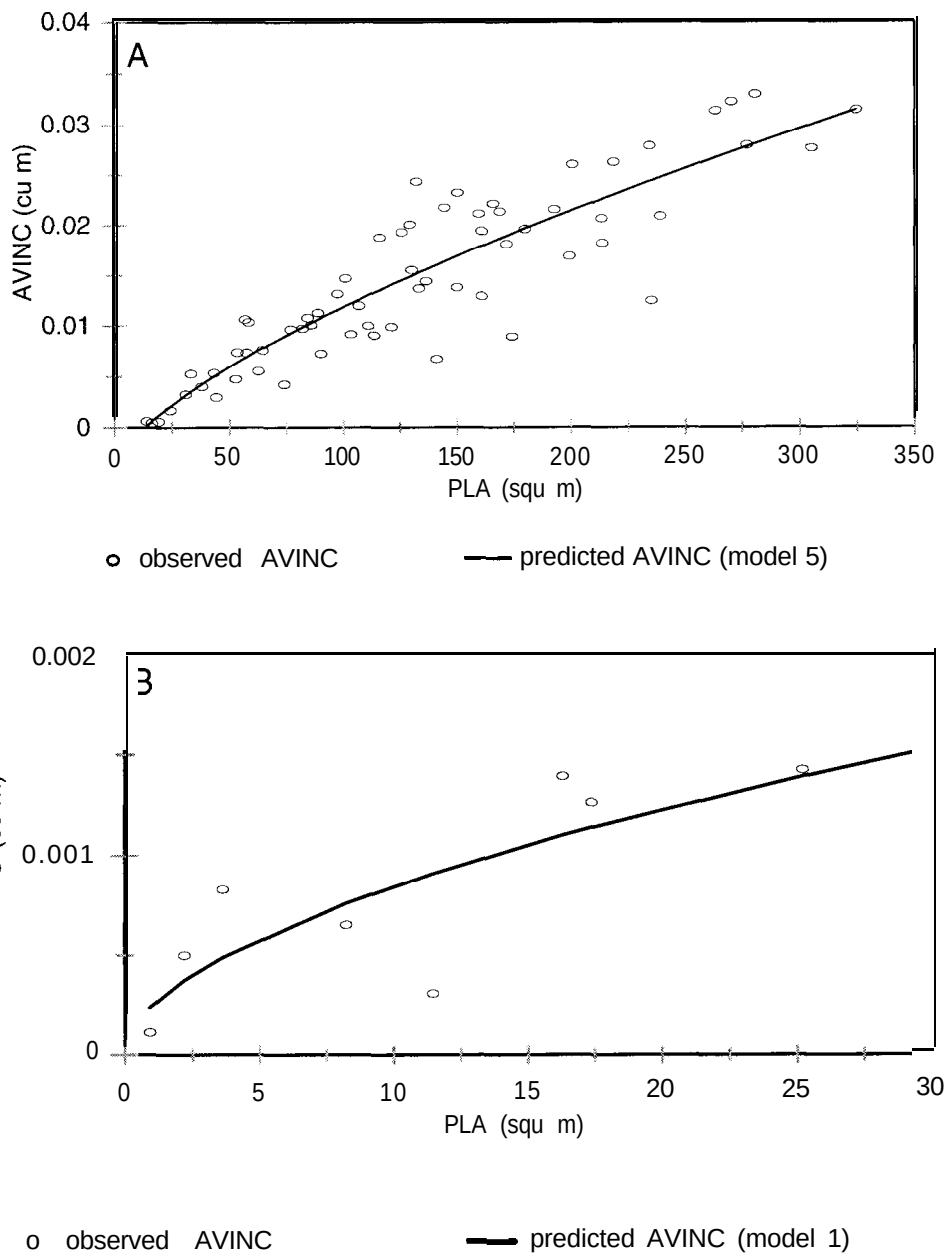

satisfactory results and proved optimal based on FI (model 5, Table 2.4, Figure 2.7). Models 2-4 invariably overestimated AVINC of B and C stratum *P. rubens* with PLA < 50 m^2, and/or underestimated AVINC for PLA > 250 m^2.

Residual analysis did not indicate that other measured variables (dbh, HT, age at breast height (Figure 2.8), or stand BA) would improve prediction of AVINC in the presence of PLA for any of the models applied to the three study species. Maguire et al. (1998), however, found that dbh, HT, and index of past suppression (number of live branch whorls per CL) improved the prediction of *P. rubens* volume increment from PLA (note that suppression was not one of our variables). Further investigation of a potential age - AVINC relationship was undertaken by examining species-specific age - HT and age - PLA relationships, but there was no suggestion of a meaningful relationship between tree age and stemwood volume growth (Figures 2.9 - 2.10).

GE and Canopy Position

Analysis of variance for individual species indicated that mean PLA differs significantly by stratum for *A. balsamea* ($p = 0.0002$), *T. canadensis* ($p = 0.0001$), and *P. rubens* ($p = 0.0001$). Bonferroni multiple comparisons revealed that while mean PLA of the C and D strata do not differ, trees in the B stratum have significantly more PLA (E stratum trees were excluded from ANOVA due to small sample size) ($\alpha = 0.05$, Table 2.5).

Results of ANOVA indicated that mean GE differs significantly by species ($p = 0.0010$) and stratum ($p < 0.0001$), with a marginal ($p = 0.0545$) species by stratum interaction. Bonferroni multiple comparisons established that while mean GE of the B

Figure 2.8. Residuals from nonlinear AVINC - PLA models for (A) *Tsuga canadensis*, (B) *Abies balsamea*, and (C) *Picea rubens*, plotted over age at bh.

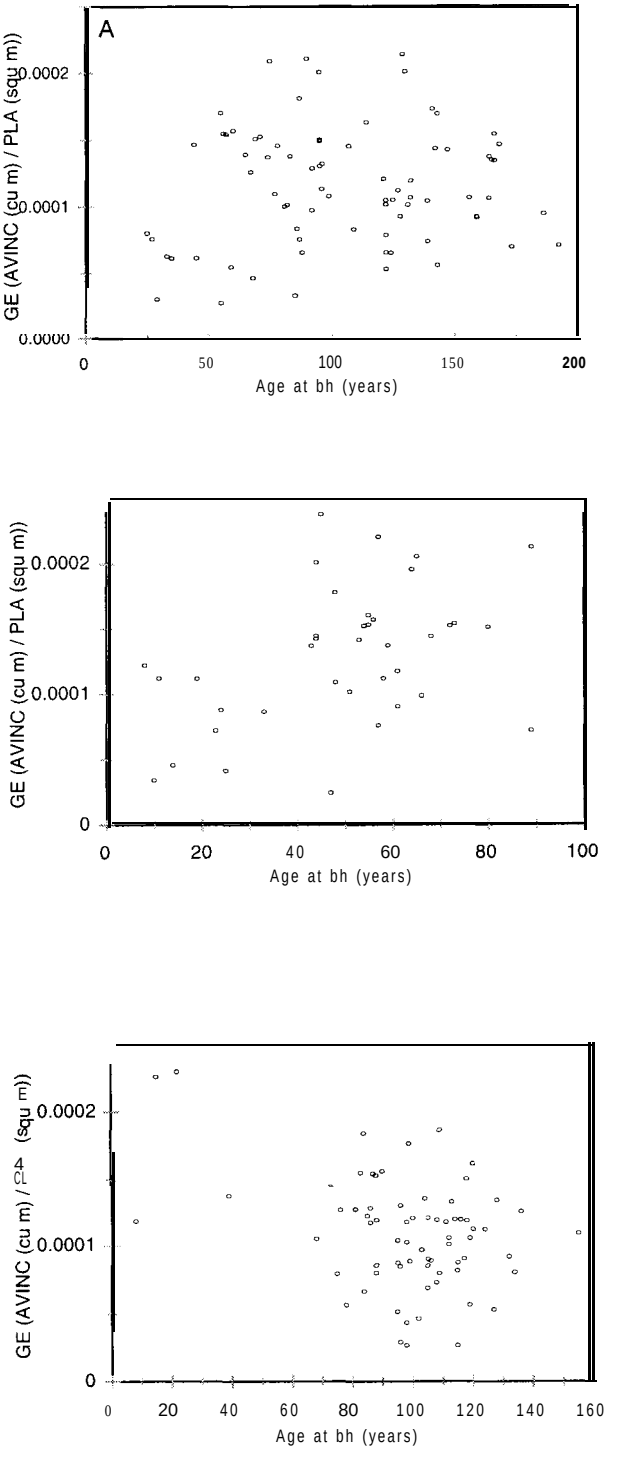

Figure 2.9. Age at bh - tree height relationships for (A) *Tsuga canadensis* (r = 0.78), (B) *Abies balsamea* (r = 0.79), and *(C) Picea rubens* (r = 0.77).

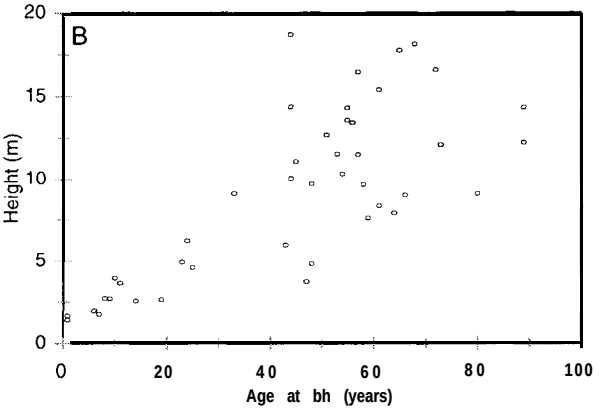

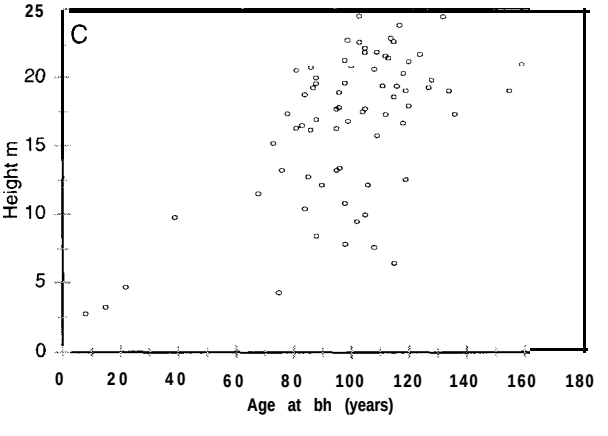

Figure 2.10. Age at bh - projected leaf area (PLA) relationships for (A) *Tsuga canadensis* (r = 0.57), (B) *Abies balsamea* (r = 0.49), and *(C) Piceu rubens* (r = 0.41).

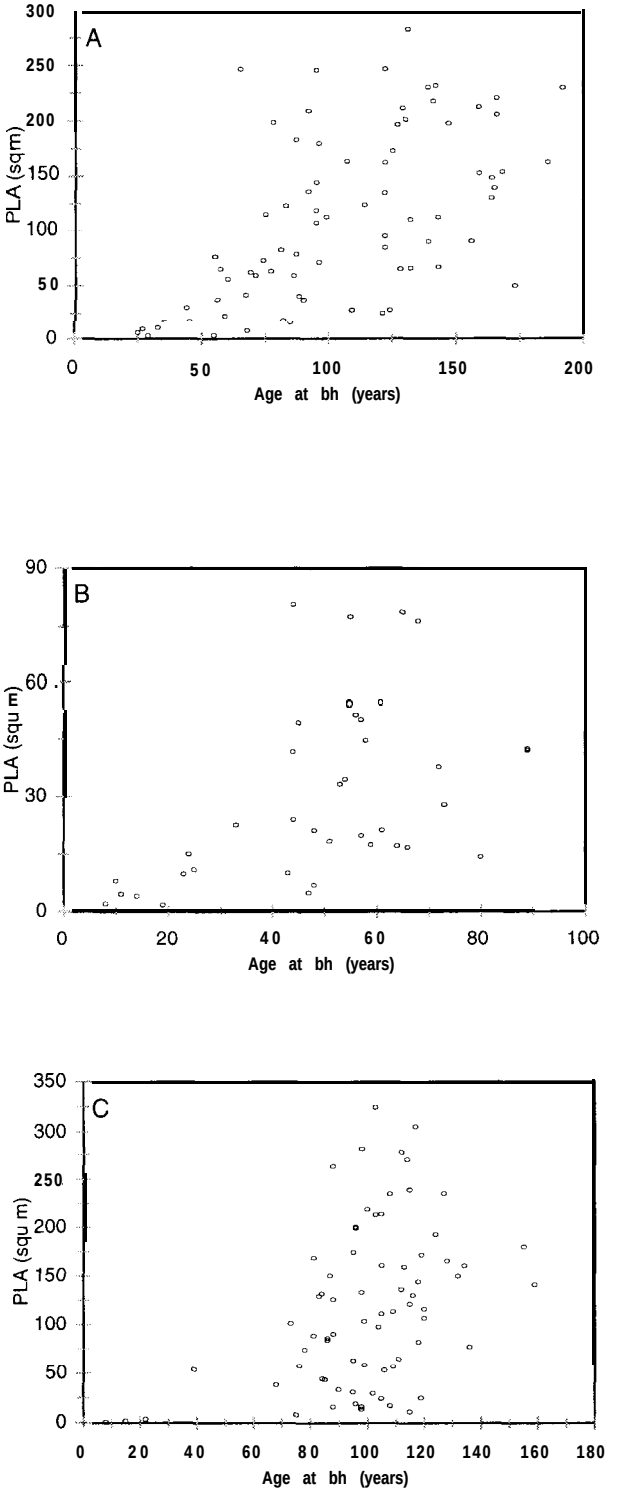

Table 2.5. Results of within-species Bonferroni multiple comparisons of (A) mean projected leaf area (PLA) and (B) mean growth efficiency (GE) by stratum for *Tsuga canadensis, Abies balsamea,* and *Picea rubens*. Within each species, different letters indicate a significant difference in means *(a* = 0.05). SEs in parentheses.

A.

Species	Stratum	Mean PLA		Significance
T. canadensis	B	160.97	(10.18)	a
	C	60.07	(8.34)	b
	D	18.92	(3.34)	b
A. balsamea	B	57.98	(7.98)	a
	C	3 1.70	(4.87)	b
	D	16.73	(3.43)	b
P. rubens	B	151.37	(9.57)	a
	C	34.11	(4.72)	b
	D	15.98	(3.48)	b

B.

Species	Stratum	Mean GE		Significance
T. canadensis	B	1.27×10^{-4}	(6.26×10^{-6})	a
	C	1.47×10^{-4}	(1.20×10^{-5})	a
	D	9.63×10^{-5}	(9.07×10^{-6})	b
A. bulsamea	B	1.59×10^{-4}	(1.63×10^{-5})	a
	C	1.48×10^{-4}	(1.16×10^{-5})	a
	D	8.71×10^{-5}	(1.21×10^{-5})	b
P. rubens	B	1.13×10^{-4}	(4.28×10^{-6})	
	C	8.50×10^{-5}	(1.38×10^{-5})	
	D	8.71×10^{-5}	(2.41×10^{-5})	

and C strata do not differ significantly, trees in these upper strata are significantly more efficient than those in the lower (D) stratum. *A. balsamea* mean GE was found to be significantly greater than *P. rubens* mean GE. ANOVA for individual species indicated that mean GE differs significantly by stratum for *A. balsamea* ($p = 0.0070$), *T. canadensis* ($p = 0.0002$), and *P. rubens* ($p = 0.038$ 1). Bonferroni multiple comparisons, however, failed to detect a difference in mean *P. rubens* GE by stratum *(a* = 0.05, Table 2.5, probably due to the conservative nature of this statistical test.

GE - PLA Relationships

The GE - PLA relationships implied for *A. balsamea*, *T. canadensis*, and *P. rubens* by their respective AVINC - PLA relationships are shown in Figures 2.11 - 2.13. *A. balsamea* GE, implied by model 2, reaches a maximum of 1.65 x 10^{-4} m^3/m^2 at approximately 55 m^2 PLA, though there is little change in GE from 40 m^2 to 80 m^2 (the upper end of the data). Maximum *P. rubens* GE (1.20 x I 0^{-4} m^3/m^2) occurs at a PLA of 70 m^2, though there is little change between 50 - 100 m^2 and a very slight decline thereafter. The GE relationship implied by model *3* for *T. canadensis* increases at a decreasing rate until it reaches a maximum of 1.32 x 10^{-4} m^3/m^2 at 145 m^2 PLA, with predicted GE showing very little change from 120 - 160 m^2 PLA and then slowly declining.

Figure 2.11. Observed and implied *Abies balsamea* growth efficiency (GE) relative to projected leaf area (PLA), and GE - PLA relationships suggested by Gilmore and Seymour (1996). GE is derived from model 2. Data points are identified by stratum.

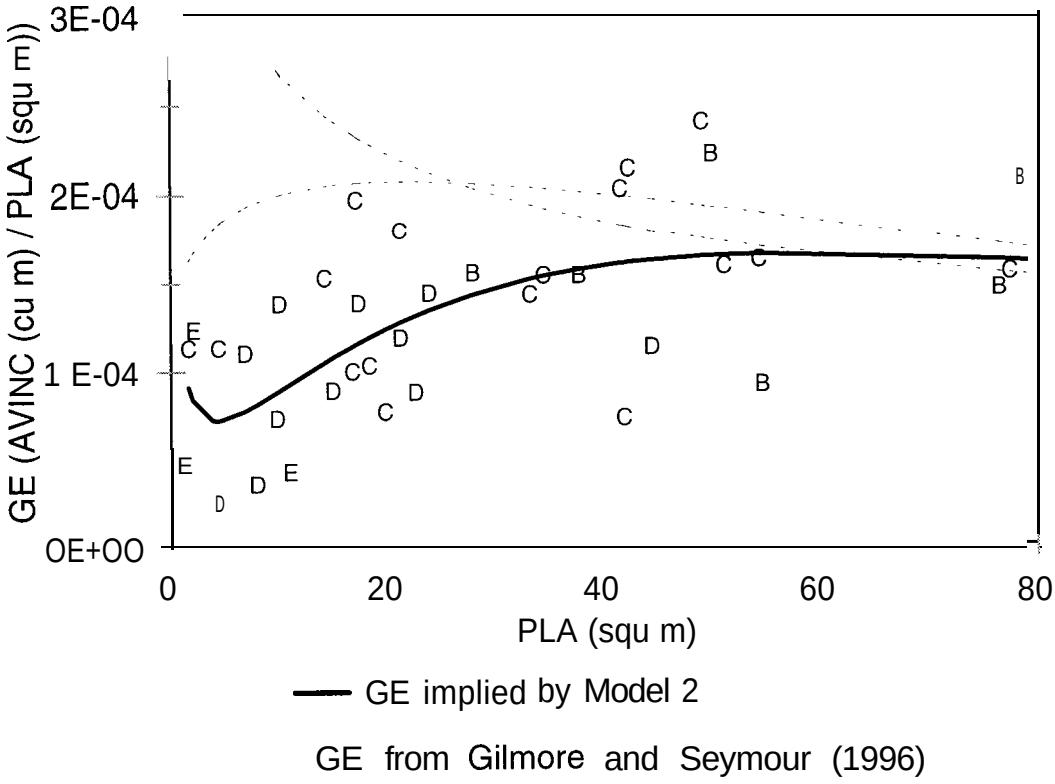

Figure 2.12. Observed and implied *Picea rubens* growth efficiency (GE) relative to projected leaf area (PLA), and GE - PLA relationships suggested by Maguire et al. (1998). GE is derived from model 1 for D and E strata and model 5 for the B and C strata. Data points are identified by stratum.

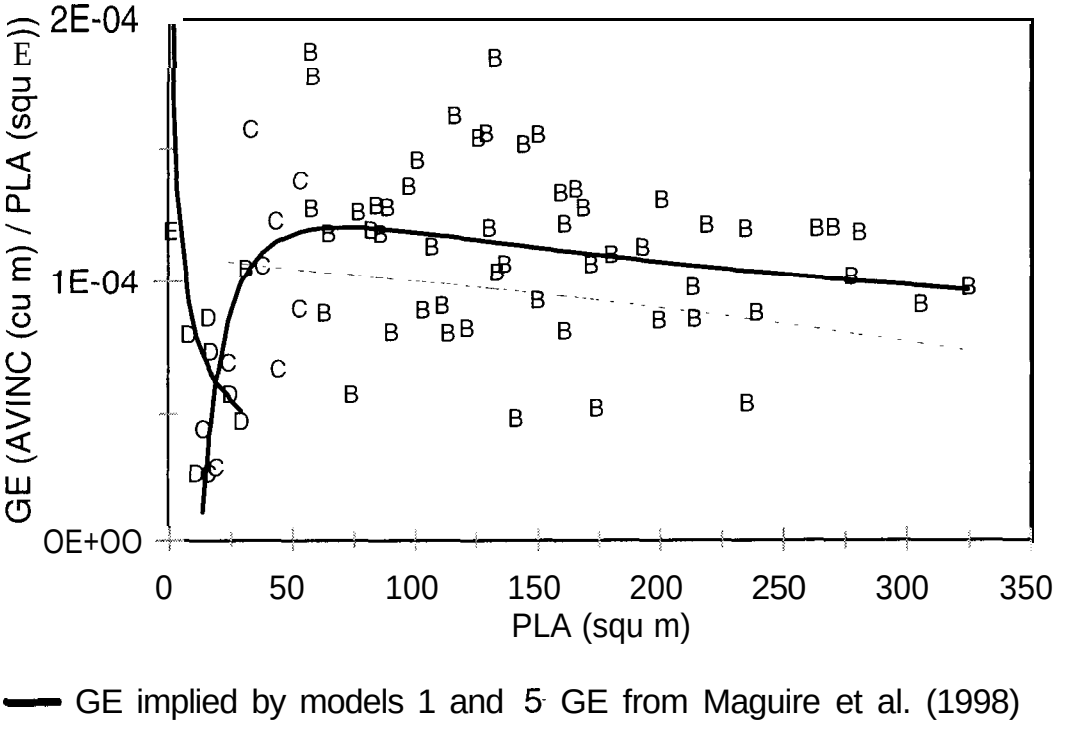

Figure 2.13. Observed and implied *Tsuga canadensis* growth efficiency (GE) relative to projected leaf area (PLA). GE is derived from model 3, and data points are identified by stratum.

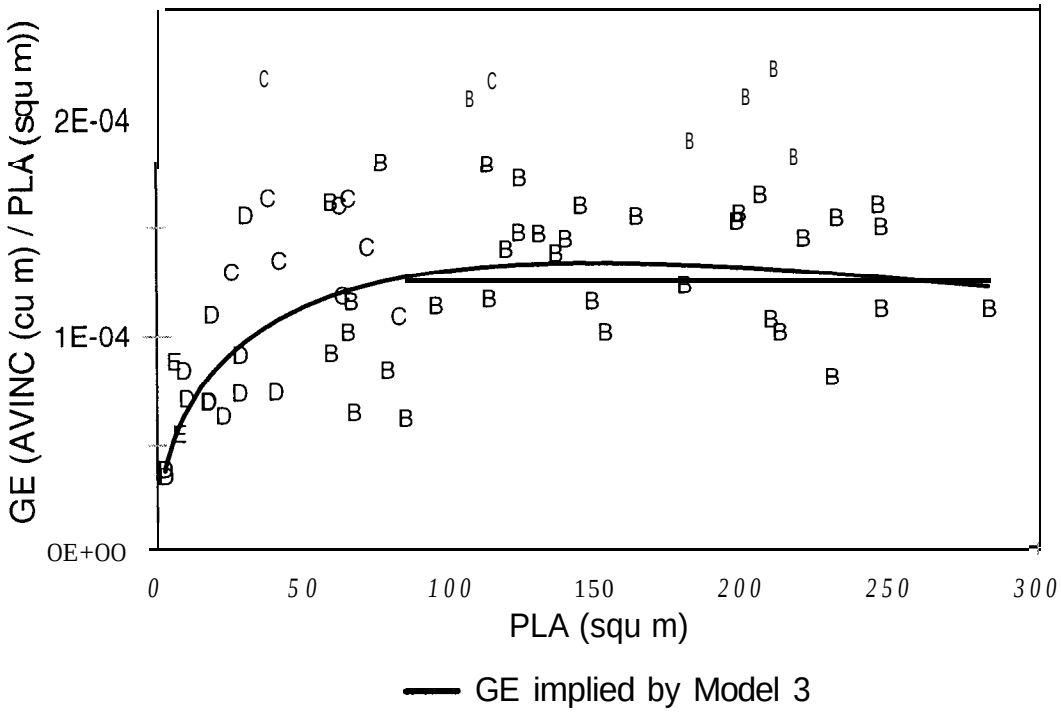

DISCUSSION

Annual Volume Increment

Tree-level PLA was found to be the best predictor of AVINC and, indirectly, GE. This relationship is evidence of the biological link between foliage and stemwood volume increment. Additional measured variables did not contribute significantly to the prediction of AVINC in the presence of PLA. Diameter at breast height and HT were, in fact, components of *T. canadensis*' PLA - AVINC prediction model because they were used in the nonsapwood-based PLA predictor equation (PLA = $f(BA_{bh}, mLCR)$). Neither of these variables were explicit in the *A. balsamea* and *P. rubens* sapwood-based PLA models (PLA = $f(SA_{bh})$), though collinearity may have contributed to the nonsignificant contribution of dbh and HT to the AVINC - PLA. However, the strong biological relationship between the amount of foliage and growth should not be minimized, and apparently accounts for the variation in growth that could be explained by other measured variables.

Growth Efficiency

Abies balsamea

The GE - PLA relationship implied by model 2 for *A. balsamea* exhibits a slight maximum and decline. The AVINC - PLA models tested for *A. bulsumeu* by Gilmore and Seymour (1996) resulted in two different GE - PLA patterns: declining and slightly peaking. Model 1 was found to be effective, though not optimal, for *A. balsamea* in the present study and was one of those used by Gilmore and Seymour (1996). Though the

model form is the same, different parameter estimates result in an increasing GE over PLA pattern within the range of our data, but a declining GE - PLA relationship when evaluated by Gilmore and Seymour (1996).

Model 2 was not explored by Gilmore and Seymour (1996), so we are unable to assess the validity of that model for their data. Gilmore and Seymour (1996) did, however, point out the link between chosen AVINC model form and the shape of the GE - PLA relationship. For *A. balsamea*, the two best models differed little in terms of estimated GE values, but the shape of the GE PLA relationship was notably different. Because model 2 was a better AVINC predictor equation, per its lower FI value, we conclude that the implied GE relationship also better reflects the data. It is important to recognize, however, the key roles that model selection and the vagaries of nonlinear analysis play in the statistical interpretation of biological relationships.

A comparison of the GE - PLA relationship implied by model 2 to those proposed by Gilmore and Seymour (1996) indicates that GE values of trees at the upper end of the PLA distribution are similar in their even- and our multi-aged stands (Figure 2.11). However, GE of trees with small amounts of PLA, and the species' maximum implied GE value, are higher in the even-aged stands (Gilmore and Seymour 1996) (Figure 2.11). This is consistent with Assmann (1970), and supports his suggestion that the growth of small trees in vertically stratified multi-aged stands is negatively affected by increased canopy depth. The trees with the lowest PLA values in even-aged stands are in the suppressed crown class of the main canopy (mean PLA = 3.9 m^2, range 0.8 - 11.8 m^2) (Gilmore and Seymour 1996). Trees with comparable PLA values in the multi-aged stands in the present study, however, are located in the E stratum (mean PLA = 4.8 m^2,

range 2.0 - 10.9 m^2). This distinction is important, because the E stratum trees of multi-aged stands experience competition both within their stratum and from trees of all crown classes of higher strata. Height data from the two studies support this conclusion- mean height of suppressed *A. balsamea* in Gilmore and Seymour's (1996) study of even-aged stands was 7.6 m (range 4.0 to 12.8 m), while E stratum trees of comparable PLA in the present study had a mean height of 2.5 m (range 1.4 to 4.6 m).

There is an alternative, but not unrelated, explanation for the disparate GE values of *A. balsamea* with small amounts of PLA in even- and multi-aged stands. Gilmore and Seymour (1996) report that trees in the suppressed crown classes of even-aged stands have a mean live crown ratio (LCR) of 0.19 (n = 10, range 0.04 - 0.36), equivalent to a mean crown length of 1.4 m. Trees with similar PLA values in multi-aged stands (E stratum trees) have a mean LCR of 0.72 (n = 7, range 0.53 to 0.75) and a mean crown length of 1.8 m. Mean LCR ($p < O.OOOl$), but not mean CL ($p = 0.5537$), differ significantly at $\alpha = 0.05$ (unpublished data courtesy of D.W. Gilmore). Small E stratum trees in multi-aged stands thus have crowns of the same length, with the same PLA, as taller trees in the lower crown class of even-aged stands. The lack of significant mass (i.e. crown or bole) for accumulation of volume growth has been previously recognized as a potential reason for low GE of small trees (Gilmore and Seymour 1996), and may also explain why trees with low amounts of PLA have less volume growth per unit of leaf area in multi-aged stands.

Picea rubens

The different AVINC - PLA trajectories of the split data result in overlapping equations for the upper (B and C) and lower (D and E) strata, and thus overlapping GE relationships for trees in the 15 - 30 m^2 PLA range (Figure 2.12). The differences in behavior of the two models for PLA 15 - 30 m^2 is noteworthy. *P. rubens* in the B and C strata show an increase in GE with increasing PLA for trees in the 15 - 50 m^2 range, supporting the hypothesis that shade-tolerant trees in highly stocked multi-aged stands experience improved light environment, and thus have higher GE values, as they enter the upper canopy (Roberts and Long 1992, Roberts et al. 1993).

Interestingly, *P. rubens* GE declined with increasing PLA up to 30 m^2 in the D and E strata. In fact, the implied GE relationships for small trees of all three species in the present study consistently indicate decreasing and/or low GE values (Figures 2.11-2.13), a finding supported by analysis of variance of mean GE by stratum. This is consistent with research that found that trees in the suppressed crown classes of even-aged stands are less efficient than those in better canopy positions (Waring et al. 1980, O'Hara 1988, Gilmore and Seymour 1996). Assmann (1970) suggested that small trees in multi-aged stands of shade-tolerant species exhibit "impeded development," resulting in lower GE values for lower stratum trees. This appears to be true in our study stands - though all D and E stratum trees of the three species in the present study occupy a codominant or dominant position within their stratum, 80% (29 of 36) are entirely or partially overtopped by foliage on trees in higher strata, though stand-level relative densities are low (most recent pre-cut RD = 0.30 in C9, RD = 0.31 in C16). Thus, it is

not surprising that lower stratum trees in this study exhibit the diminished GE documented in the suppressed trees of even-aged stands.

The monotonically declining GE - PLA relationship implied for *P. rubens* by the model Maguire et al. (1998) fit using PLA as the sole predictor is comparable to that implied by model 5 for B and C stratum trees in the present study (Figure 2.12). In fact, it appears that excluding trees with PLA < 23.8 m^2 (the smallest value used by Maguire et al. 1998) from our data set would have led us to conclude that the *P. rubens* GE - PLA relationship is monotonically declining. Maguire et al. (1998) recognized that a GE peak may exist below their minimum tree size. Though maximum GE implied for B and C stratum trees in the present study occurs at 70 m^2, model form and the existence of this inflection point are strongly influenced by trees with PLA < 25 m^2.

Tsuga canadensis

The *T. canadensis* GE - PLA relationship implied by model 3 (Figure 2.13) approximates the GE peaking behavior suggested for shade-tolerant species (Figure 2.1, Assmann 1970, Roberts et al. 1993). Roberts et al, (1993) hypothesized that beyond a critical leaf area, increases in PLA are associated with decreased LCR, and are offset by increased maintenance respiration for support of woody biomass, or possibly increased carbon allocation to the roots. This results in a peak GE and associated optimal PLA value, and is validated by the implied GE - PLA relationships documented in this study.

Though a decrease in *T. canadensis* GE with increasing PLA above 145 m^2 is consistent with data presented by Assmann (1970), as well as Roberts' et al. (1993) conceptual model, this trend was not seen in previous studies of shade-tolerant northern

conifer species (Gilmore and Seymour 1996, Maguire et al. 1998). In the present study, both *A. balsamea* and *P. rubens* also exhibited slight maxima in otherwise asymptotic curves. Furthermore, the *T. canadensis* maximum GE occurs at a comparatively high PLA relative to *P. rubens* and *A. balsamea.* This may be due, in part, to *T. canadensis'* extraordinary shade tolerance (Burns 1923) and branch retention (Anderson and Gordon 1994). As a result, *T. cunudensis* maintains a longer live crown than either *P. rubens* (Kenefic and Seymour *2000)* or *A. balsamea* of similar height and canopy position. In fact, mean LCR of *T. canadensis* (0.76) is statistically greater than mean LCR of *A. bulsumeu* (0.69) or *P. rubens* (0.60) ($p = 0.0001$). If we accept the proposition that a mechanism for decreased GE with increasing PLA is a decline in LCR (Gilmore and Seymour 1996), the ability of *T. cunudensis* to sustain a longer crown may delay a GE decline in multi-aged stands of this species, relative to *P. rubens* and *A. bulsumeu.*

Species Comparisons

Data for this research were collected from the same sites at the same time, and are free of geographic or temporal complications that may result from inter-species comparisons drawn from the results of earlier published studies. A comparison of the GE relationships implied by the chosen models for *T. cunudensis, A. bulsumeu,* and *P. rubens* reveals important similarities and dissimilarities (Figure 2.14). With the exception of trees with PLA < 10 m^2, *A. bulsumeu* is clearly the most efficient species. *T. cunudensis* GE generally falls between that of *A. balsamea* and *P. rubens* - a finding supported by ANOVA of observed GE data, that indicated that *A. bulsumeu* mean GE was significantly greater than that of *P. rubens* but not *T. cunudensis.* Analysis of variance also indicated

Figure 2.14. Comparison of growth efficiency (GE) - projected leaf area (PLA) relationships implied by the chosen mean annual volume increment (AVINC) - PLA models for *Tsuga* canadensis, *Abies balsamea*, and *Piceu rubens* in the Penobscot Experimental Forest multi-aged stands.

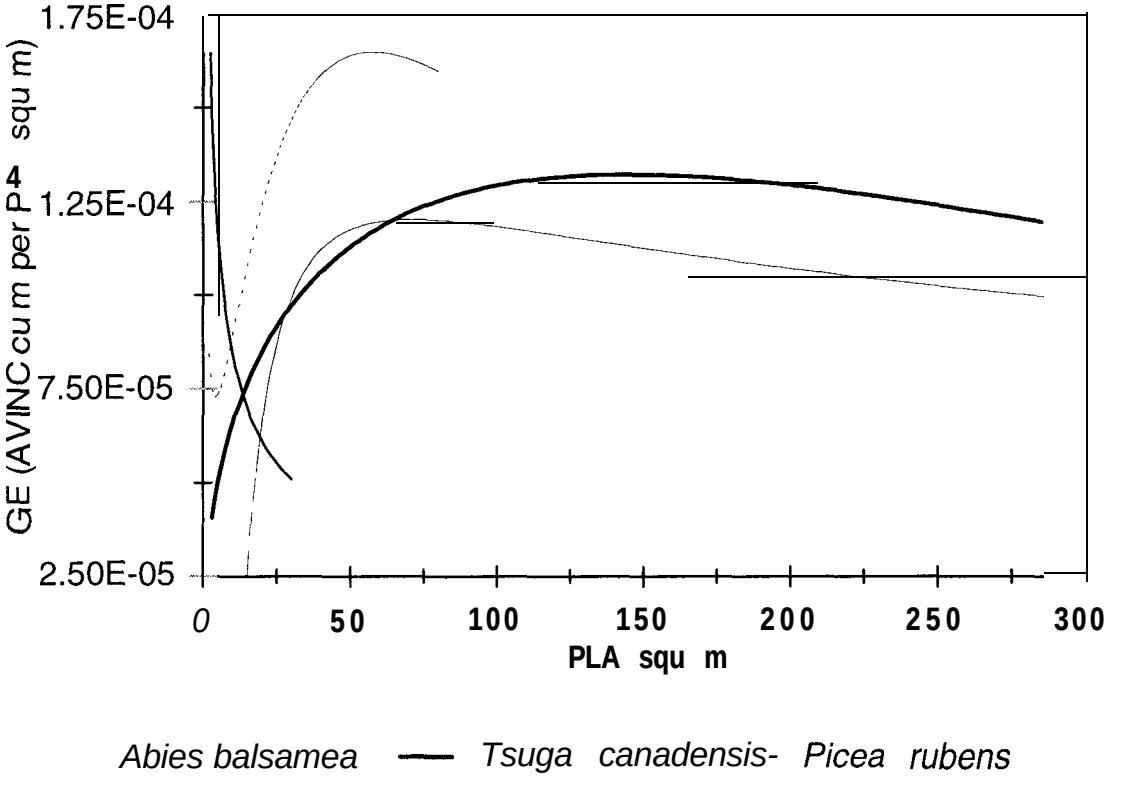

that mean GE is greater in the B and C strata than the D stratum, a conclusion supported by the early upward pattern of GE in all species.

Although the magnitude of GE and range of PLA values differ for *P. rubens* and *A. balsamea*, these two species exhibit similar curve shapes and optimum PLA values. Both species exhibit decreasing GE with increasing PLA for the very smallest trees, followed by a period of increasing GE with increasing PLA. The similarity in the patterns of GE over PLA for these two species is not surprising, considering the frequently cited silvical similarities between them (Seymour 1992). Similarity in silvical properties is associated with similar GE patterns; the relatively higher GE values documented for *A. balsamea* are indicative of this species' more rapid stemwood growth. At a given PLA, *A. bulsumeu* produces more stemwood than *P. rubens*. The link between leaf area and growth dynamics of *A. bulsumeu* and *P. rubens* documented in the present study is also discussed by Aplet et al. (1989), who attribute differences in the stand-level productions of these species to associated differences in leaf area.

The silvicultural implications of these findings are myriad. In mixed-species multi-aged stands, silvicultural treatments that allocate a greater proportion of PLA to *A. bulsumeu* than *P. rubens* should result in increased stand-level stemwood production due to higher observed and implied GE values. There are a number of reasons, however, why this would not be a judicious strategy in the Acadian Forest. The first is that, as suggested by the lower observed maximum PLA and dbh of *A. balsamea*, this species is not as long-lived as *T. canadensis* or *P. rubens*. In fact, the tendency of *A. bulsumeu* to decay restricts it to age classes < 100 years and diameter classes rarely exceeding 25 cm at breast height. It would thus take many more *A. bulsumeu* and a considerably lower

maximum diameter to allocate a substantial portion of a mixed-species stand's PLA to that species. Furthermore, and perhaps most importantly, *A. balsamea* is the preferred host of the spruce budworm (*Choristoneura fumiferana* Clemens) and is subject to extensive mortality during periodic budworm outbreaks (Seymour 1992).

Reducing the proportion of *A. balsamea,* for the reasons cited above, would result in a shift of stand-level PLA to *T. canadensis* and *P. rubens*. *P. rubens* is generally favored due to its greater value for sawlog production. Though *T. canadensis* GE was not significantly different than GE of the other two species, *P. rubens* was significantly less efficient than *A. balsamea*. Theoretically, reducing *A. balsamea* and increasing the component of *P. rubens* would increase the proportion of PLA on less efficient trees and thus reduce stand-level stemwood volume increment.

O'Hara (1996) found increasing GE with increasing leaf area for the oldest cohort of multi-aged stands of shade-intolerant *P. ponderosa* (Figure 2.1). None of the three shade-tolerant species in the present study exhibit this pattern. However, O'Hara's (1996) finding may be questioned based on apparent model bias and extrapolation of the equation used to predict leaf area from SA_{bh}. The volume increment predictor equation proposed by O'Hara (1996, p. 20) exhibits positive bias for trees with low leaf area values, suggesting that GE is overestimated for these trees. Additionally, the maximum predicted leaf area value (1000 m^2) used for volume increment model building far exceeds the upper limit used for development of the leaf area predictor equation (375 m^2, O'Hara and Valappil 1995). In fact, if O'Hara's (1996) leaf area data are restricted to values < 375 m^2, it appears that a differently shaped volume increment ▪ leaf area relationship, and thus GE- leaf area relationship, would be more appropriate.

The slow nature of the decline in GE in the upper range of the PLA data for all three species in the present study indicates that increases in PLA beyond the species' GE maxima are only slightly offset by decreasing GE within the range of our data. Maintaining tree-level PLA values beyond those associated with maximum GE, for *T. canadensis* and *P. rubens* in particular, does not greatly affect stem volume increment per unit leaf area within the range of our data. This is confirmed by ANOVA of mean PLA and mean observed GE, that indicated that GE of B and C stratum trees do not differ significantly, though B stratum trees have significantly more PLA. There is thus little disadvantage to maintaining trees with large amounts of PLA in multi-aged northern conifer stands. Tall, large-crowned trees are in fact quite common in the study stands due to the preponderance of sawtimber trees and discontinuous canopy structure, resulting in frequent side-lighting associated with single-tree or group openings, and the juxtaposition of trees of greatly varying heights.

Mechanistic Explanations

The GE - PLA relationships reported in this study suggest a decrease in GE with increasing PLA above species-specific optima. The peaking behavior of Assmann's (1970) and Roberts' et al. (1993) conceptualized GE models, though more pronounced than the plateau-like slow decline observed in the study stands, was seen in our study of *T. canadensis, A. balsamea*, and *P. rubens*. The difference between our findings and those of Roberts et al. (1993) may be due to differences in even- and multi-aged stand structure. Increased PLA on shade-tolerant trees in even-aged stands would invariably be associated with greater shading of lower branches, resulting in a decrease in LCR,

increase in branch-free bole, and decline in GE. The multi-aged study stands, however, have a discontinuous upper canopy - allowing many trees to grow upward in height and add PLA with little change in the overall light environment experienced by their crown. This is particularly true of *T. canadensis*; many have maintained very long crowns on the edges of gaps (Kenefic and Seymour 1999), with the LCR of some B stratum *T. canadensis* exceeding 90%. With slow branch shedding and frequent side-lighting, short-term increases in such a tree's PLA may not negatively impact the light environment of its lower branches. This may explain why *T. canadensis* has a higher PLA for optimum GE than *A. balsamea* or *P. rubens*.

The mechanisms responsible for the decrease in GE beyond optimal PLA cannot be determined from this study. Plausible explanations for decreasing GE with increasing PLA differ by stratum. For small (D and E stratum) trees, the burden of increased PLA in a shaded or semi-shaded environment where "umbrella" and "candelabrum" trees are common (Davis 198 1), may result in a less favorable ratio of photosynthetic to nonphotosynthetic tissue. In upper stratum trees, however, it remains unresolved whether the causal mechanism is increased maintenance respiration (Yoda et al. 1965), hydraulic resistance (Yoder et al. 1994, Ryan and Yoder 1997), or maturation (Greenwood and Hutchinson 1993, Day et al. 2000).

The question of maturation can be indirectly addressed using our data. Though a decrease in photosynthetic rates has been documented for older *P. rubens* in our study area (Day et al. 2000), examination of residuals from the chosen AVINC models indicated that age did not contribute to the explanation of AVINC in the presence of PLA for *T. canadensis*, *A. bulsumeu,* or *P. rubens* within the range of our data (Figure 2.8). In

fact, upper stratum trees in the present study had higher AVINC and GE values than lower stratum trees, but were the oldest trees in the stands (Table 2.2). This is consistent with research by Vanninen and Mäkelä (2000), who found a high correlation between foliage mass and production for shade-intolerant *Pinus sylvestris* L. (Scots pine), but no indication of age dependence for stemwood production. Additionally, since older trees in our study are also frequently the taller trees (Figure 2.9), it is difficult to separate the influence of increased tree size (and its accompanying increase in hydraulic resistance, nonphotosynthetic tissue, and vapor pressure deficit) and age on AVINC using gross morphological and growth data. We may say, however, that age at breast height did not contribute significantly to estimation of AVINC in our study once a tree's PLA had been accounted for, and that there is only weak to moderate collinearity between age and PLA (Figure 2.10).

SUMMARY

This is the first reported study to assess AVINC - PLA and GE - PLA relationships of three shade-tolerant conifers growing in multi-aged stands. We present new data for *T. canadensis*, and compare our findings for *A. balsamea* and *P. rubens* to those of previous studies (Gilmore and Seymour 1996, Maguire et al. 1998).

Our findings may be summarized with respect to the four stated hypotheses.

Hypotheses 1 and 2. AVINC and GE = f(PLA)

The sole significance of PLA as predictor of AVINC (hypothesis 1), and indirectly GE (hypothesis 2), confirms the biological link between the amount of foliage and stemwood volume increment. In fact, the strength of this relationship was such that additional measured variables did not display potential for significant contribution to AVINC models in the presence of PLA.

Hypothesis 3. GE = f(PLA, stratum)

The three species exhibit GE - PLA relationships similar in concept, if not magnitude, to the peaking models presented by Assmann (1970) for shade-tolerant species in multi-aged stands, and by Assmann (1970) and Roberts et al. (1993) for shade-tolerant trees in even-aged stands. Trees in lower canopy strata were found to be less efficient stemwood producers than those in higher canopy strata, consistent with the lower GE values documented for suppressed trees in even-aged stands (Gilmore and Seymour 1996).

Hypothesis 4. AVINC = f(PLA, species)

Results indicated that A. *balsamea* is significantly more efficient than *P. rubens*, a finding with implications for stand-level production when a greater proportion of PLA is allocated to the latter species via selective removal of the relatively short-lived and budworm-susceptible *A. balsamea*. Though differences in volume growth trajectories of upper and lower stratum *P. rubens* were observed, overall *P. rubens* and *A. balsamea* GE - PLA relationships showed similarities in shape and optimal PLA value, while *T.*

canadensis displayed maximum GE at a higher PLA. Maximum *A. balsamea* GE was found to be less than that observed in a previous study of even-aged stands.

Results of the present study are significant in that they both provide mechanistic explanations for observed patterns of tree growth in complex stands, and because they enable us to better understand, and thus predict, the outcome of leaf area manipulations through silviculture. Findings reported here will enable foresters to improve their understanding of stand dynamics, and therein increase the biological basis, flexibility, and likelihood of success of silvicultural treatments in multi-aged stands.

CHAPTER 3

STRUCTURAL IMPLICATIONS OF STAND-LEVEL *TSUGA CANADENSIS*, *ABIES BALSAMEA*, AND *PICEA RUBENS* STEMWOOD VOLUME GROWTH - LEAF AREA RELATIONSHIPS IN A MIXED-SPECIES, MULTI-AGED NORTHERN CONIFER FOREST

CHAPTER ABSTRACT

Stand-level stemwood volume increment - leaf area index (LAI) relationships were explored in mixed-species, multi-aged stands dominated by shade-tolerant *Tsuga canadensis* (L.) Carr (eastern hemlock), *Abies balsamea* (L.) Mill (balsam fir), and *Piceu rubens* Sarg. (red spruce). Eleven 0.02-ha plots were studied, and exhibited size distributions conceptually associated with even-, two-, and multi-aged stands, including reverse-J diameter distributions with linear and exponential increasing leaf area with increasing canopy stratum (age class surrogate). High inter-plot diversity was attributed to incomplete conversion of the irregular study stands to a balanced multi-aged condition, and applications of a hybrid single-tree and group selection regeneration method.

Compositional and structural characteristics (including LAI, proportion of leaf area by stratum, basal area (BA, m^2/ha), relative density (RD), crown competition factor (CCF), trees per hectare (TPH), and TPH by stratum) were tested for contribution to plot-level stemwood volume increment (PAVINC, m^3/ha) - LAI relationships. PAVINC was effectively modeled for all plots combined using a linear combination of LAI and proportion of midstory leaf area (LAC). Agglomerative hierarchical clustering, canonical variate analysis, and multivariate analysis of variance distinguished two groups of plots with different LAI, PAVINC, BA, LAC, and TPH. Spearman's rank correlation analysis within each cluster indicated a negative correlation between PAVINC and TPH. There was no statistical indication of a difference in quantified structural variables between reverse-J and other structures, and within-cluster regression, though limited by small

sample size, indicated that LAI alone was the best PAVINC predictor. This research establishes LAI as an important, biologically meaningful predictor of PAVINC in mixed-species, multi-aged northern conifer stands, and reveals that vertical structure (as expressed by LAC) explains the variation in growth associated with incomplete conversion to a fully-stocked multi-aged condition and/or the use of a horizontally heterogeneous regeneration method.

INTRODUCTION

The dynamics of mixed-species, multi-aged stands are among the most complicated and incompletely understood aspects of forest ecology. Though numerous studies have explored the structural characteristics of complex stands, information about structural and functional relationships is rare. The relationship between the amount and distribution of leaf area and stand-level stemwood volume growth represents an important link between biological processes and wood production, and is the focus of research reported here.

The inclusion of leaf area relationships in silviculture research represents a critical step toward relating biological processes to stemwood volume growth. The majority of research on this topic has addressed tree-level stemwood volume growth - leaf area relationships (see Chapter 2), or stand-level patterns of one or a few species in even-aged structural arrangements (Waring et al. 198 1, Vose and Allen 1988, O'Hara 1988 and 1989, Smith and Long 1989 and 1992, Long and Smith 1990 and 1992, Jack and Long

199 1, Velazquez-Martinez et al. 1992). Research by O'Hara (1996, 1998) extended physiologically based silviculture research to multi-aged stands of a single shade-intolerant species (*Pinus ponderosa* ex. Laws, ponderosa pine).

Research reported here is the first to explore stand-level leaf area - stemwood volume growth relationships in mixed-species multi-aged stands dominated by shade-tolerant species. This study was conducted on the Penobscot Experimental Forest (PEF) in Maine, the site of a U.S.D.A. Forest Service silviculture experiment and sole source of long-term data on multi-aged silviculture in the Acadian region. Both the U.S.D.A. Forest Service's 45-year data set and newly collected data (1995 - 2000) are used to assess stand-level stemwood volume growth - leaf area relationships in mixed-species multi-aged northen conifer stands dominated by *Tsuga canadensis* (L.) Carr (eastern hemlock), *Abies balsamea* (L.) Mill (balsam fir), and *Piceu rubens* Sarg. (red spruce). Our objectives are to test long-standing assumptions about growth in multi-aged stands, explore the findings of recent research in single-species multi-aged stands (O'Hara 1996), and provide new information about the dynamics of complex stands dominated by shade-tolerant species. We test the hypothesis that stemwood volume growth in multi-aged stands of shade-tolerant species can be predicted from the amount of leaf area alone, without significant contributions by stand structural or compositional characteristics.

STUDY AREA

The two stands sampled in this study, C9 and C16, are part of a long-term silvicultural experiment on the 1540-ha PEF in east-central Maine, located at approximately 44°52'N, 68 °38'W. The PEF was purchased in 1950 by a number of industrial landholders and leased to the U.S.D.A. Forest Service, which began an experiment to study traditional even- and multi-aged silvicultural systems. Treatments and remeasurements have continued to the present and follow a long-term study plan which ensures consistency in management over time. The two stands used for this research are replicates of selection cutting on a 5-year cycle, with nine (C9) and eight (C16) selection cuttings prior to our research. C9 (11.0 ha) and Cl6 (6.6 ha) both have a structural goal defined using the BDq method (Guldin 1991), with a q-factor of 1.96 on 5-cm classes, a residual maximum diameter goal of 48 cm, and a target residual basal area (BA) of 26 m^2/ha. After 40 years of management, both stands had irregular age and diameter distributions (see Chapter 2, Figures 2.2 and 2.3; Kenefic and Seymour 1997, 2000; Seymour and Kenefic 1998).

Marking priorities are to remove cull (> 50 % unmerchantable by volume) and high-risk trees, thin crop trees on at least three sides, and remove trees at financial maturity. Removal of undesirable species and low quality trees have also been a priority. In practice, volume control has taken precedence over structural considerations, often leading to cutting in deficit size classes dominated by high risk or low vigor trees (Seymour and Kenefic 1998). Creation of regeneration openings one-fourth to one-third acre in size began in the 1980s, and cuttings today are most accurately characterized as a

hybrid single-tree and group selection method.

Within- and between-stand species compositions are highly variable due to small-scale differences in soil drainage and stand structural condition. The dominant species on the study sites are *T. canadensis*, *P. rubens*, and A. *balsamea (see* Chapter 2, Table 2.1). Other species include *Pinus strobus* L. (eastern white pine), *Thuja occidentalis* L. (northern white-cedar), *Acer rubrum* L. (red maple), *Betula papyrifera* Marsh. (paper birch), *Picea glauca* (Moench.) Voss (white spruce), and other hardwoods (Kenefic and Seymour 1997, Kenefic 2000). Species composition goals based on species' relative desirability are used to prioritize removals (see Chapter 2, Table 2.1). Treatments to date have emphasized removal of *T. canadensis* and *A. balsamea*, but retention and release of *P. rubens.*

METHODS

Part 1. Random Sampling

A 25-m systematic grid was established in the study stands in 1995. A random sample of 100 *T. canadensis*, 100 *P. rubens*, and 50 *A. balsamea*, stratified by 5-cm diameter at breast height (dbh, 1.3 m) classes, was taken from 12.5-m radius plots centered on the grid points in July and August of 1995 (C 16) and 1997 (C9). These data, obtained for a study of tree-level stemwood volume increment ▪ projected leaf area (PLA, m^2) and growth efficiency (GE) ▪ PLA relationships (Chapter 2), were used in the present study to develop height growth models and supplement published PLA equations for *T. canadensis* (Chapter 1, Kenefic and Seymour 1999) and *P. rubens* (Maguire et al. 1998).

The random sample included trees at least 1.3 m in height, up to a maximum of 50.0 cm dbh (*T. canadensis* and *P. rubens*) or 25.0 cm dbh (*A. balsamea*). Sampling was restricted to areas of somewhat poorly, moderately well, and well drained soils (L.S. Kenefic unpublished data), and excluded the U.S.D.A. Forest Service continuous forest inventory (CFI) plots. Diameter at bh, bark thickness, total height (HT), and height to live crown were recorded for each sample tree, and two increment cores were removed at bh for determination of sapwood radius. In order to be consistent with measurements taken for development of published nonsapwood-based PLA prediction equations, height to live crown was defined as height to lowest branch for *T. canudensis* (Chapter 1, Kenefic and Seymour 1999) and *P. rubens* (Maguire et al. 1998), and height to the lowest whorl consisting of at least three live branches for *A. balsamea* (Gilmore et al. 1996). Tree height and dbh were remeasured on the randomly sampled trees in July 2000.

Sapwood-heartwood boundaries were identified in the field by holding each increment core to the sunlight, and marking the apparent boundary between the translucent (water conducting) and non-translucent zones. Translucent wetwood zones in *T. cunudensis* cores, separated from the sapwood by opaque bands of growth rings, were assumed to be bacterial infection of the heartwood and were ignored. A 0.1 M solution of ferrous ammonium sulfate ($Fe(NH_4)_2(SO_4)_2.6H_2O$) was applied to *T. cunudensis* cores in the laboratory to identify the sapwood colorimetrically (Eades 1958, Chapter 1, Kenefic and Seymour 1999). Field-marked sapwood boundaries were either confirmed or adjusted in favor of the dye for this species.

Each increment core was hand polished with fine grit sandpaper and radial increments and width of the sapwood were measured to 0.01 mm with a Velmex

measuring system (Velmex, Inc.). Sapwood area at bh (SA_{bh}) was determined for each tree as a function of diameter, average sapwood radius, and average bark thickness at bh.

Calculations

Mean Annual Height and Radial Growth. Mean annual height increment (AHINC) was calculated by subtracting 1995 (Cl 6) or 1997 (C9) tree heights from 2000 height remeasurements, and dividing by the number of intervening years. Trees that were cut or damaged were excluded from analysis *(T. canadensis* n = 16, *A. balsamea* n = 8, and *P. rubens* n = 18), with the exception of 15 *T. canadensis* for which height increment had been measured after felling for the PLA study (Chapter 1, Kenefic and Seymour 1999). Mean annual radial increment (ARINC) for the 5-year period prior to sampling was determined for each tree using the average of radial increments from two bh cores. Radial increments from the two cores taken from each tree were first averaged to determine a mean value for each year, then ARINC was calculated by averaging the mean annual values across the 5-year period. Mean ARINC of small trees which had not been cored was determined using year 2000 dbh remeasurements.

Analysis

Regression Modeling;. We compared linear and nonlinear, weighted and unweighted equations (Table 3.1) of the form $y_i = f(\beta | x_i) + \varepsilon_i$, where $\varepsilon_i \overset{iid}{\sim} N(0, x_i^n \sigma^2)$, to identify equations suitable for predicting mean AHINC and ARINC (SAS 1990, PROC REG and PROC NLIN). Only equations with significant parameters (a = 0.05) were considered, and plots of standardized residuals against predicted variables were used to

Table 3.1. Linear and nonlinear equations tested for prediction of *Tsuga canadensis*, *Abies balsamea*, and *Picea rubens* annual height increment (AHINC) from height (HT), live crown ratio (LCR), and annual radial increment (ARINC).

	Model
1.	$AHINC = b_1HT + b_2HT^2$
2.	$AHINC = b_1HT + b_2HT^2 + b_3ARINC$
3.	$AHINC = b_1HT + b_2ARINC$
4.	$AHINC = b_1HT + b_2ARINC + b_3LCR$
5.	$AHINC = b_1HT^{b2} \times ARINC^{b3} \times LCR^{b4}$
6.[a]	$AHINC = \exp(b_0 + (b_1HT) + (b_2ARINC) + (b_3HT^2)$

[a] The HT^2 term in model 6 was included in the A. *balsamea* model only.

verify homogeneous variance. Equations were weighted by x_i^n with n = 0, -1, -2 in order to identify the optimal weighting factor to correct for heteroskedasticity. Cooks' distance was used to evaluate the influence of potential outliers on the estimates of regression coefficients (Graybill and Iyer 1994). Reasonable biological model behavior was taken into consideration, and evaluated using scatter plots of the sample data against the predictor equations.

Generalized R^2 (Kvålseth 1985) was calculated for weighted equations using the corrected sum of squares $(1- (cssresid/\sum(y_i-y_m)^2))$, where the y_i's are the individual sample values and y_m is the sample mean. Graphs of the residuals from the AHINC - HT models were used to determine if predictions were biased relative to other potential predictor variables (dbh, crown length (CL), live crown ratio (LCR), and crown projection area (CPA)). Furnival's (1961) index of fit (FI), a modified maximum likelihood criterion that allows concurrent evaluation of root mean square error, normality, and homoskedasticity, was used to identify optimal model forms. FI has the advantage of simultaneously allowing comparison both across model forms and within models across weighting factors. The lower the FI value, the better the fit based on the criteria listed above.

Other Species. Data were not available to model AHINC for other species on the plots used for this research (see part 2, this chapter - ***A.*** *rubrum*, ***P. strobus, T. occident&is,*** and *Betula alleghaniensis* Britton (yellow birch)). Increment cores obtained from randomly sampled free growing ***P.*** *rubens* (Chapter 2) were used to identify site trees and calculate site index (SI) from published SI curves ***(P.*** *rubens* SI = 40 ft. at age 50, Carmean et al. 1989). The Northeastern TWIGS Variant of the Forest Vegetation Simulator (Bush 1995) was used to generate SI values for other species using known ***P.***

rubens SI (*A. rubrum* SI = *54.7* ft., *P. strobus* SI = *55.0* ft., *T. occidentalis* SI = 34.6 ft., and *B. alleghaniensis* SI = 52.6 ft.). Tree height (in ft) at sample date *t* and SI were then entered into SI equations to solve for age at bh (Carmean et al. 1989), after which HT_{t+}, was determined by entering age at bh + 1 and SI into Carmean's et al. (1989) equations to solve for HT_{+1}. Lastly, AHINC (ft) = HT_{+}, - $HT_{}$, converted to meters using the conversion factor 0.3048.

Part 2. Fixed-radius Plots

Fifteen 8.03-m radius plots, nine in C 16 and six in C9, were measured in July and August of 1997 and 1998 for use in stand-level analysis. The 0.02-ha plots are part of the U.S.D.A. Forest Service CFI network. Each tree > I .27 cm dbh has been numbered and marked with a horizontal line at breast height. Diameter at breast height and tree condition are recorded by the U.S.D.A. Forest Service every five years, and ingrowth are added to the data set. Plots for use in the present study were chosen from somewhat poorly, moderately well, or well drained portions of the study stands (L.S. Kenefic, unpublished data), excluding areas near gravel roads or stand boundaries. Sample plots were subjectively chosen based on species composition determined prior to sampling from CFI data collected on 0.08-ha plots encompassing our 0.02-ha study plots. Four of the fifteen original plots were excluded from analysis due to amount (> 20 % of BA) of species other than *T. canadensis, A. balsamea*, and *P. rubens* (Table 3.2). Species, HT, dbh, crown radii in four cardinal directions, height to crown base (as defined in part 1, this chapter), and canopy stratum (Oliver and Larson 1996, Smith et al. 1997, see Chapter

Table 3.2. Sample plots excluded from analysis due to < *80 % Tsuga canadensis, Abies balsamea,* and/or *Picea rubens*, expressed as percent of total basal area (BA) of trees > 1.27 cm dbh.

		Species composition (percent)			
Plot	**Stand**	***Tsuga canadensis***	***Abies balsamea***	***Picea rubens***	**Other'**
14	c9	49.4	6.1	12.9	31.6
21	c9	9.7	0.0	62.7	27.6
23	C9	39.5	25.2	1.4	33.9
31	c9	1.2	23.3	33.4	42.1

[1] *Acer rubrum*, *Pinus strobus*, and/or *Thuja occidentalis*

2) were recorded for each tree > 1.3 m in height. Saplings < 2.5 cm dbh were excluded from analysis because there are no published PLA or biomass equations for trees of this size.

Calculations

Tree-level Projected Leaf Area.

Tsuga canadensis. Tree-level PLA was predicted for ***T.*** *canadensis* > 6.8 cm dbh on the fixed-radius CFI plots using the nonsapwood-based equation PLA = $b_1 + b_2$ **x** (BA,, x mLCR), where b_1 **= *8.922*** 1, b_2 **=** 0.1789, BA,, = stem cross-sectional area at bh (cm^2), and mLCR (modified live crown ratio) = CL/(HT - 1.3) (Chapter 1, Kenefic and Seymour 1999). An equation was needed for trees outside the range of data used in PLA model building (i.e. trees < 6.8 cm dbh) and/or with mLCR > 1 .O (crown base below bh). Consequently, biomass equations (Young et al. 1980) were used to predict dry leaf weight of trees 2.5 - 6.8 cm dbh (n = 7). Leaf weight of each tree was multiplied by mean ***T.*** *cunudensis* specific leaf area (SLA, 58.43 cm^2/g, Chapter 1, Kenefic and Seymour 1999) to determine PLA. These data were pooled with data from the trees destructively sampled (n = 20) for development of a ***T.*** *canadensis* PLA equation (Chapter 1, Kenefic and Seymour 1999), in order to re-fit a nonsapwood-based equation for use in trees smaller than 6.8 cm and/or with mLCR > 1 .O. The simple linear equation PLA = b_0 **+ *b,*** BA_{bh}, weighted by BA_{bh}^{-1}, where b_0 = 3.6695, ***b,*** = 0.1548, and R^2 = 0.963 was found to be effective (Figure 3.1). Though biased for trees with dbh > 35 cm, this model was unbiased for the 2.5 cm to 6.8 cm range (Figure 3.1), and was used to predict PLA of trees with mLCR > 1 .0, and/or between 2.5 cm - 6.8 cm dbh.

Figure 3.1. (A) Observed and predicted *Tsuga canadensis* projected leaf area (PLA) relative to basal area (BA). Predicted values obtained from the model PLA = 3.6695 + 0.1548 x $BA_{,,}$. (B) Residual plot showing model bias.

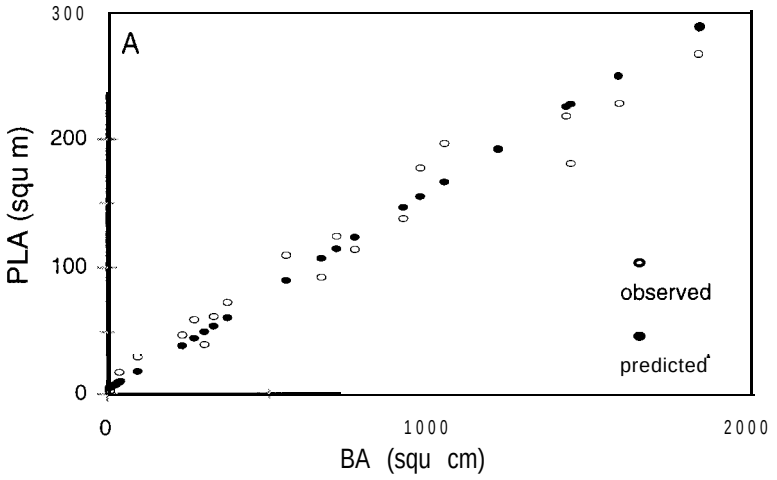

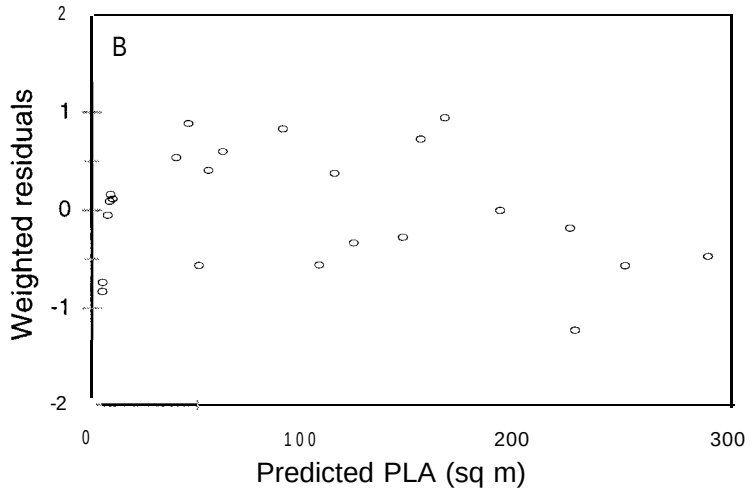

Picea rubens. The nonsapwood-based PLA predictor equation suggested by Maguire et al. (1998) did not encompass the full range of our data (the smallest dbh used in model building was 11 cm), and exhibited bias relative to the sapwood-based equation when applied to our data (Figure 3.2). An alternative nonsapwood-based equation was developed using the leaf area and tree dimension data used by Maguire et al. (1998) (unpublished data courtesy of D.A. Maguire). First, the sapwood-based equation proposed by Maguire et al. (I 998) was applied to our randomly sampled trees between 11 cm and 50 cm dbh. These data were then pooled with Maguire's measured PLA values (unpublished) and the PLA of our randomly sampled trees 2.5 cm to 11 cm dbh, as determined using Young et al.'s (1980) biomass equation and *P. rubens*' SLA (43.5 1 cm^2/g, Maguire et al. 1998). Analysis of FI and regression residuals indicated that PLA was best estimated by the nonlinear equation PLA = b, BA_{bh}^{b2} $mLCR^{b3}$, where b_1 = 0.5553, b_2 = 0.8532, b_3 = 0.4925, and R^2 = 0.849 (Figure 3.3). This equation is a variation of the model form proposed by Valentine et al. (1994), and recommended by Kenefic and Seymour (Chapter 1, 1999) for prediction of *T. canadensis* PLA. The model PLA = b_1 BA^{b2}, where b_1 = 0.2648, b_2 = 0.9145, and R^2 = 0.821 also proved adequate and was chosen to predict PLA of trees with crown base below 1.3 m (mLCR>1 .O) (Figure 3.4). Though biased for large trees (dbh > 40 cm), this equation was unbiased relative to PLA as a function of SA_{bh} for small trees (Figure 3.4).

Abies balsamea. The nonsapwood-based equation PLA = exp(b, + b_2 ln(CL)), where b_1 = 0.250 and b_2 = 1.707 and the log bias correction factor (Baskerville 1972) = 1.173 (Gilmore and Seymour 1996), was used to predict *A. balsamea* tree-level PLA.

Figure 3.2. Projected leaf area (PLA) predicted for randomly sampled *Picea rubens* using sapwood- and nonsapwood-based predictor equations from Maguire et al. (1998).

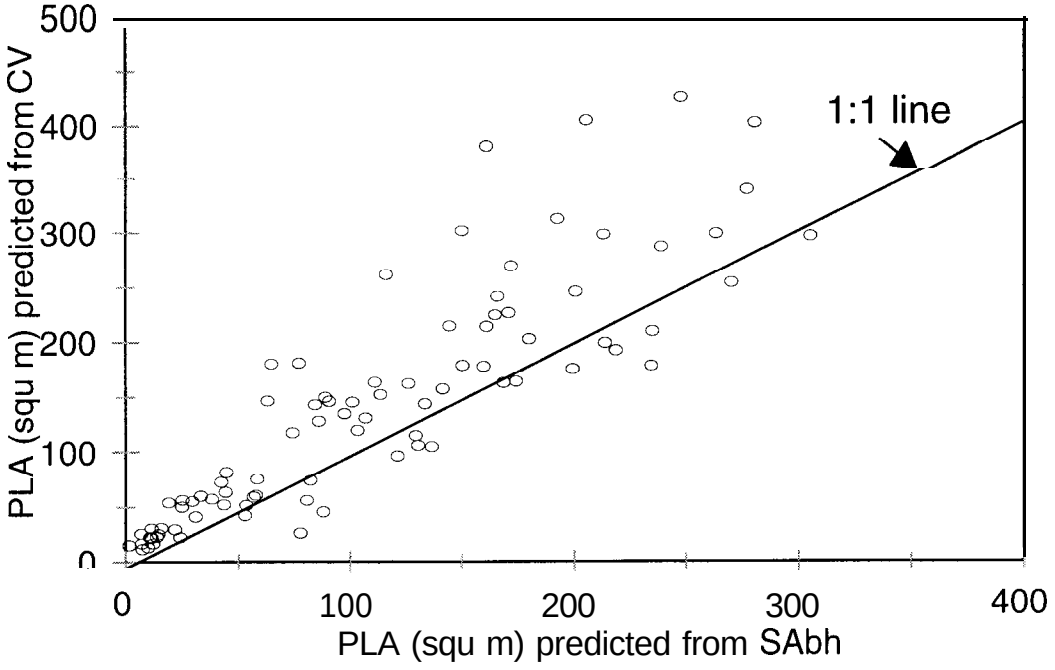

Figure 3.3. Observed and predicted *Picea rubens* projected leaf area (PLA) relative to basal area (BA,,). Predicted values obtained from the model PLA = 0.5553 x (BA,, $^{0.8532}$) x (mLCR $^{0.4925}$).

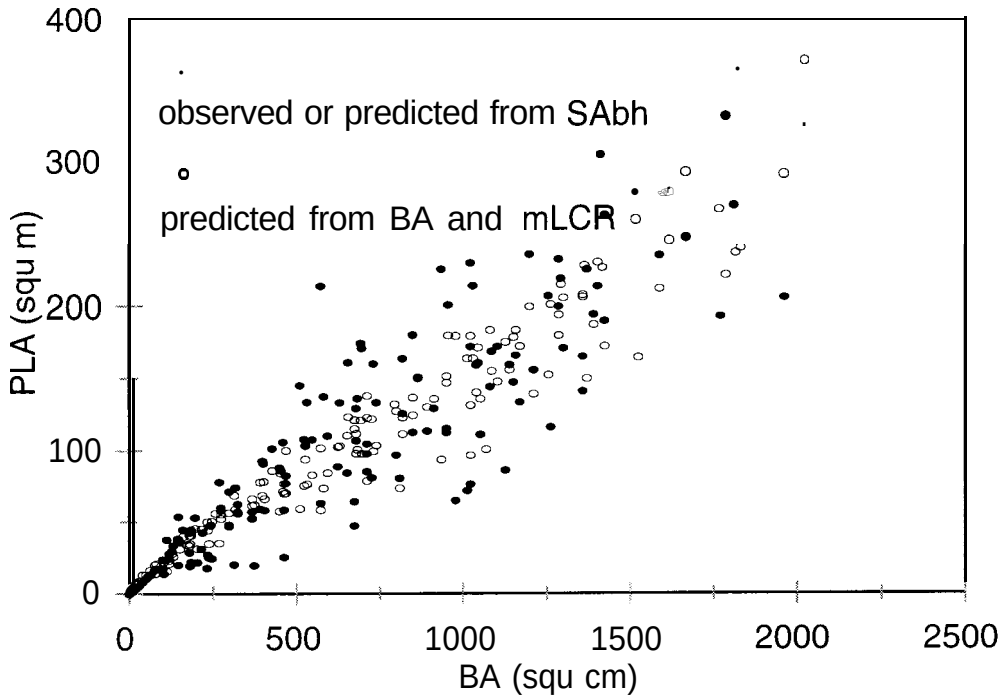

Figure 3.4. (A) Observed and predicted *Picea rubens* projected leaf area (PLA) relative to basal area ($BA_{,}$). Predicted values obtained from the model $PLA = 0.2648 \times (BA_{,}^{0.9145})$. (B) Residual plot showing model bias.

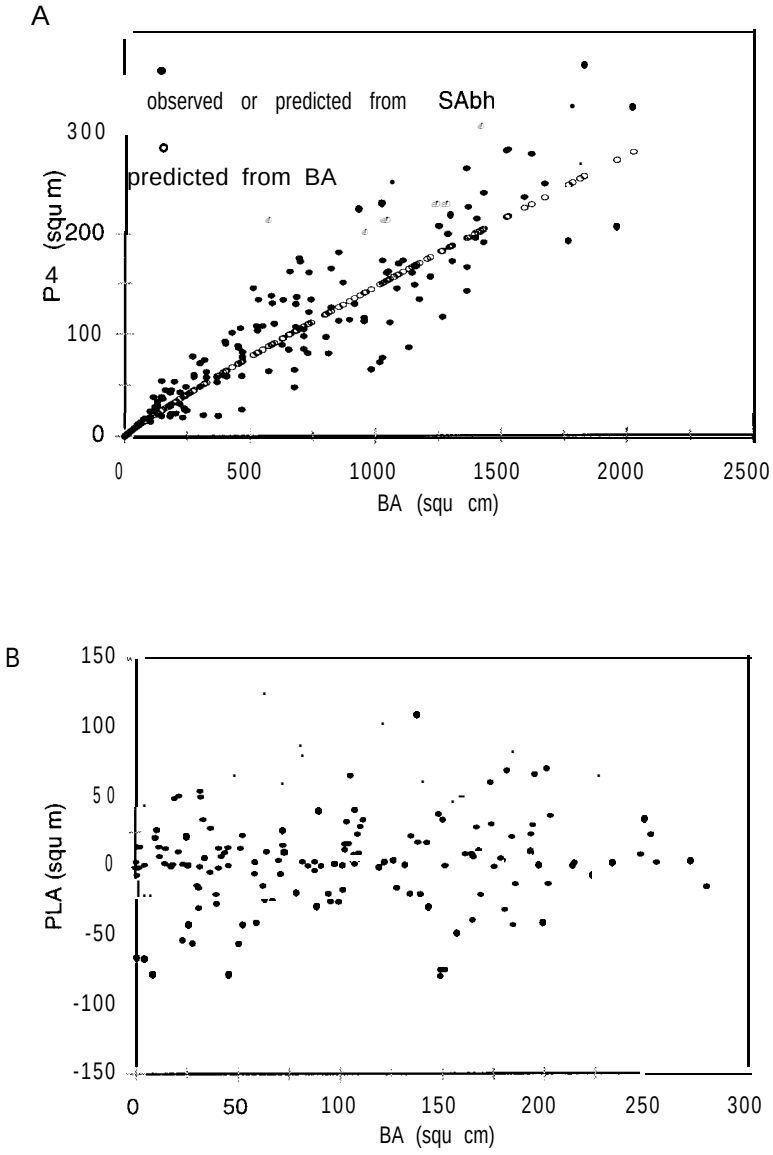

Other Species. Plots with < 20 % BA in species other than *T. canadensis*, *A. balsamea*, and *P. rubens* were included in the analysis. Projected leaf area value of *P. strobus* (n = 1) was predicted using a nonsapwood-based equation (A.A. Barker Plotkin unpublished), with a ratio correction factor of 0.7672 (R.S. Seymour unpublished) to account for overestimation of needle width by the Ag-Image optical analysis system (Decagon Devices, Inc., M. Day unpublished, Chapter 1, Kenefic and Seymour 1999). PLA values for *A. rubrum* (n = 14), *T. occidentalis* (n = 2), and *B. alleghaniensis* (n = 1) were determined by applying species-specific biomass equations (Young et al. 1980) to predict dry leaf weight, and then multiplying by SLA. Though a SLA value was available for *T. occidentalis (48.06* cm^2/g, D.J. McConville unpublished); *A. saccharum* SLA (167 cm^2/g, M.A. Leathers unpublished) was used for both *A. rubrum* and *B. alleghaniensis*.

Mean Annual Radial Increment. Mean ARINC was determined for each tree > 2.5 cm dbh on the 0.02-ha CFI plots used in this study using dbh recorded by the U.S.D.A. Forest Service in the most recent inventory more than three years prior to the measurements taken for the present study. In C 16, dbh measurements from 199 1 were used, while 1994 measurements were used in C9 (inventories occur on different years in these two compartments). Periodic radial growth (diameter growth/2) was divided by the number of growing seasons (R.M. Frank unpublished, Table 3.3) to determine ARINC. In C16, mean ARINC values of trees that grew into the 2.5 cm dbh class between 1991 and our 1997 or 1998 measurement were estimated from 1996 U.S.D.A. Forest Service inventory data, i.e. radial growth was determined from one or two growing seasons. Radial increments of trees that grew into the sapling class after the most recent U.S.D.A. Forest

Table 3.3. Percentages of growing seasons used for periodic growth determination (R.M. Frank, unpublished).

Month of data collection	**Percentage of growth**
January - May	**0**
June	**35**
July	**75**
August	**90**
September - December	**100**

Service inventory but prior to our study (*T. canadensis* n = 8, A. *balsamea* n = 7), were assumed to equal the mean ARINC values of randomly sampled (part 1, this chapter) trees 0 - 4.9 cm dbh, determined from increment cores or dbh remeasurements (*T. canadensis* 0.1 16 ± 0.03 1 cm, *A. balsamea* 0.117 ± 0.013 cm, see Chapter 2 and part 1, this chapter).

Annual Volume Increment. Stem volume (V) was determined in ft' for each sample tree at sampling date t (1997 or 1998) by using the measured dbh and HT (converted to in and ft, respectively) in Honer's (1967) volume equations. Annual stemwood volume increment (AVINC, m^3) was calculated by subtracting ARINC x 2 and AHINC from dbh and HT at time t. The dbh and HT (at time t-l) were entered into Honer's 1967) stem volume equations to calculate volume at t- 1 (V_{t-1}). Finally, AVINC = $V_t - V_{t-1}$, and plot-level volume increment (PAVINC) = $\sum AVINC_i$, converted to m^3/ha.

Plot Summary Statistics. Mensurational, leaf area, and structural statistics calculated for each fixed-radius plot include density (TPH, number of trees/ha), BA (m^2/ha), volume (m^3/ha), relative density (RD, Wilson et al. 1999), PAVINC (m^3/ha), LAI, crown competition factor (CCF), and GE (m^3/m^2) (Table 3.4). Plot species composition and distribution of trees by stratum were also determined. Each plot was assigned to a stand structural category based on inspection of the distribution of trees by diameter class, and distribution of leaf area by canopy stratum.

Table 3.4. Definitions of 0.02-ha continuous forest inventory (CFI) plot summary statistics.

Statistic	Units
Density (trees per hectare, TPH) = number of trees*49.4 19	
Density (basal area, BA) = $(\sum(\pi*dbh_i^2/4))/10\,000*49.4$ 19	m^2/ha
Volume = $\sum V_i*49.4$ 19	m^3/ha
Relative density (RD)" = $(TPH/2.471)/(((\sum V_i/\text{number of trees})*35.31)/33281)^{-0.8231}$	
Plot annual volume increment (PAVINC) = $\sum AVINCi$	m^3/ha
Growth efficiency (GE) = $\sum AVINCi/\sum PLA_i$	m^3/m^2
Leaf area index (LAI) = $(\sum PLA_i)/202.44$	
Crown competition factor (CCF) = $(\sum CPA_i)/202.44*100$	percent
Proportion of leaf area by stratum (LAB, LAC, LAD, LAE)	
Density by stratum (TPHB, TPHC, TPHD, TPHE)	
Species composition (BAEH, BABF, BARS)	

"Wilson et al. (1999)

Analysis

Correlation. Associations between plot stemwood volume growth, leaf area, and structural and compositional variables were explored through correlation analysis. Spearman's rank correlation coefficient (r,), which evaluates correlations between ranked values, was applied to a subset of plot variables (LAI and the distribution of leaf area by stratum, PAVINC, GE, TPH and the distribution of trees by stratum, species composition, BA, and CCF) (PROC CORR, SAS 1990). Spearman's correlation coefficient, which is Pearson's coefficient (r) applied to ranked values, is robust with regard to outliers and able to detect both linear and nonlinear relationships (Devore and Peck 1986).

Regression Modeling. We compared linear multivariate equations of the form $y_i = f(\beta | x_i) + \varepsilon_i$, where $\varepsilon_i \overset{iid}{\sim} N(0, x_i^n \sigma^2)$, to identify equations suitable for predicting plot-level annual volume increment (PAVINC) from the quantitative summary statistics (SAS 1990, PROC REG), (Table 3.5). Criteria for model selection follow those outlined above for prediction of tree-level AHINC from HT and ARINC (see part 1, this chapter).

Multivariate Analysis. Efficacy of stand structural and compositional characteristics for defining plot groupings was explored using clustering and canonical variate analysis. Ward's minimum-variance clustering method (PROC CLUSTER, SAS 1990) was used to group plots with similar structural and/or compositional characteristics. This method of agglomerative hierarchical clustering defines clusters by maximizing between-cluster error sums of squares added over all variables, and minimizing within-cluster sums of squares over all partitions (SAS 1990). The TRIM option was used to remove potentially

Table 3.5. Linear equations tested for prediction of plot-level annual volume increment (PAVINC) from leaf area index (LAI), density (trees per ha, TPH), and proportion of leaf area in the C stratum (LAC).

	Model
1.	$\text{PAVINC} = b_1\text{LAI}$
2.	$\text{PAVINC} = b_1\text{LAI} + b_2\text{LAC}$
3.	$\text{PAVINC} = b_1\text{LAI} + b_2\text{TPH}$
4.	$\text{PAVINC} = b_1\text{LAI} + b_2\text{LAC} + b_3\text{TPH}$

influential outliers (k = 2, $\alpha = 0.05$). The average linkage (group average) clustering method, in which inter-cluster distances are calculated as the average distance between pairs of observations (SAS 1990), was also applied to verify that different clustering methods distinguish the same (robust) clusters.

Variables included in clustering analysis were those which appeared, based on a inspection of plot graphs and multivariate regression analysis of all plots combined, to have potential for separating groups (LAI, TPH, and proportion of plot leaf area in the C stratum). All variables were standardized to a mean of 0 and standard deviation of 1 before and after the TRIM procedure, to reduce the potential effect of large variance on the analysis. Canonical variate analysis and multivariate analysis of variance (PROC CANDISC, SAS 1990) were applied to test for structural and compositional differences between clusters using Wilks' λ, Mahalanobis' distances, and univariate F-tests (a = *0.05).*

RESULTS

Regression

Tree-level Height Increment Models

Tsuga canadensis. Nonlinear and linear regression modeling (PROC REG, PROC NLIN) failed to yield satisfactory models for estimation of *T. canadensis* AHINC, due to low R^2 values (< 0.10). Analysis of variance (ANOVA, PROC GLM) indicated that *T. canadensis* AHINC differed significantly by stratum (p = 0.0415), though Bonferroni

pairwise comparisons failed to detect a difference in means (a = 0.05). Inspection of mean AHINC by stratum suggested that prediction of *T. canadensis* AHINC may be improved by fitting models to the upper (B and C) and lower (D and E) strata separately (Table 3.6). Stratifying the data resulted in improved estimation of D and E stratum AHINC. Model 5, with significant HT, LCR, and ARINC terms, had the lowest (best) FI value of all models tested, though models 3, 4, and 6 were also effective but not optimal (Table 3.7, Figure 3.5). Models evaluated for prediction of AHINC of B and C stratum trees failed to yield significant parameters (a = 0.05). Subsequently, mean AHINC of the randomly sampled B and C stratum trees (0.3 188 ± 0.02497 m) was applied to all upper stratum *T. canadensis* in this study (Figure 3.5).

***Abies balsamea* and *Picea rubens*.** Model 2, a polynomial function of HT, HT^2, and ARINC, proved to be best, in terms of FI, of the equations tested for estimation of both *A. balsamea* and *P. rubens* AHINC (Table 3.7, Figures 3.6 and 3.7). Due to low R^2 values (0.33 for *A. balsamea* and 0.10 for *P. rubens*), ANOVA of the two species' mean AHINC values by stratum was applied to determine if separate AHINC models for upper and lower strata would improve accuracy of prediction. Analysis of variance (PROC GLM) failed to detect a significant difference in mean AHINC by stratum for *A. balsamea* (p = 0.0828) and *P. rubens* (0.19 1 1) (Table 3.6). Residual analysis indicated no model bias relative to dbh, CPA, or CL for either species.

Table 3.6. Results of analysis of variance of mean annual height increment (AHINC, m) by stratum for *Tsuga canadensis*, *Abies balsamea*, and *Picea rubens (a = 0.05)*. SEs in parentheses.

	Tsuga canadensis	***Abies balsamea***	***Picea rubens***
	p = 0.0415	p = 0.0828	p = 0.191 l
B	0.3131 (0.02937)	0.2757 (0.03836)	0.2333 (0.01674)
C	0.3430 (0.0449 1)	0.2994 (0.03923)	0.2411 (0.05123)
D	0.1950 (0.03386)	0.2300 (0.03979)	0.1486 (0.02842)
E	0.1929 (0.023 11)	0.1429 (0.02434)	0.1643 (0.02943)

Table 3.7. Parameter estimates, weighting factors and fit statistics for nonlinear models tested for prediction of *Tsuga* ***canadensis, Abies*** *balsamea*, and *Picea rubens* AHINC. SEs in parentheses.

Model	Parameter estimates	$R^{2\,a}$	FI [b]	Weight
T. canadensis: D and E strata				
1	b_1 = 0.07159 (0.1935), b_2 = -0.005453 (0.0024785)	0.764	0.1334	none
2	b_1 and b_2 are not significant			
3	b_1 = 0.01625 (0.003763), b_2 = 1.09323 (0.10881)	0.903	0.06376	HT^{-1}
4	b_1 = 0.01109 (0.004170), b_2 = 0.08137 (0.03773), b_3 = 0.7752 (0.1775)	0.912	0.05786	HT^{-1}
5 [d]	b_1 = 0.5063 (0.1014), b_2 = 0.4059 (0.1159), b_3 = 0.4851 (0.1184), b_4 = 1.2759 (0.5827)	0.937	0.05499	HT^{-1}
6	b_1 = -1.1470 (0.4539), b_2 = -0.002322 (0.02248), b_3 = 0.3122 (1.3633)	0.908	0.06074	HT^{-1}
T. canadensis: B and C strata				
	No models yielded all significant parameters.			
A. balsamea				
1	b_1 = 0.05529 (0.007008), b_2 = -0.0052353 (0.0004975)	0.225	0.1264	none
2 [d]	b_1 = 0.03746 (0.01039), b_2 = -0.001682 (0.0006160), b_3 = 0.6472 (0.2462)	0.333	0.1178	HT^{-1}
3 - 4	b_1 is not significant			
5	b_1 and b_4 are not significant			
6	b_1 = -2.8882 (0.2798), b_2 = 0.2480 (0.06804), b_3 = -0.01258 (0.1184), b_4 = 1.2759 (0.5827)	0.307	0.1189	HT^{-1}
P. rubens				
1	b_1 = 0.03906 (0.004630), b_2 = -0.001375 (0.0002470)	0.019	0.1404	HT^{-1}
2 [d]	b_1 = 0.01812 (0.004885), b_2 = -0.000556 (0.0002343), b_3 = 0.7746 (0.1136)	0.102	0.1112	HT^{-1}
3	b_1 = 0.006847 (0.001189), b_2 = 0.9189 (0.09896)	0.0341	0.1145	HT^{-1}
4 - 5	b_3 and b_4 (respectively) are not significant			
6	b_1 = -2.3018 (0.1811), b_2 = 0.02228 (0.007235), b_3 = 3.1846 (0.8651)	0.0819	0.1156	HT^{-1}

[a] Kvålseth (1985), [b] Furnival (1961), [c] Baskerville (1972), [d] chosen model

Figure 3.5. Observed and predicted *Tsuga canadensis* annual height increment (AHINC) relative to height. (A) Predicted values obtained from the model AHINC = 0.5063 x (HT $^{0.4059}$) x (ARINC $^{0.4851}$) x (LCR $^{1.2759}$) for D and E stratum trees. (B) Predicted values = 0.3188 (mean) for B and C stratum trees.

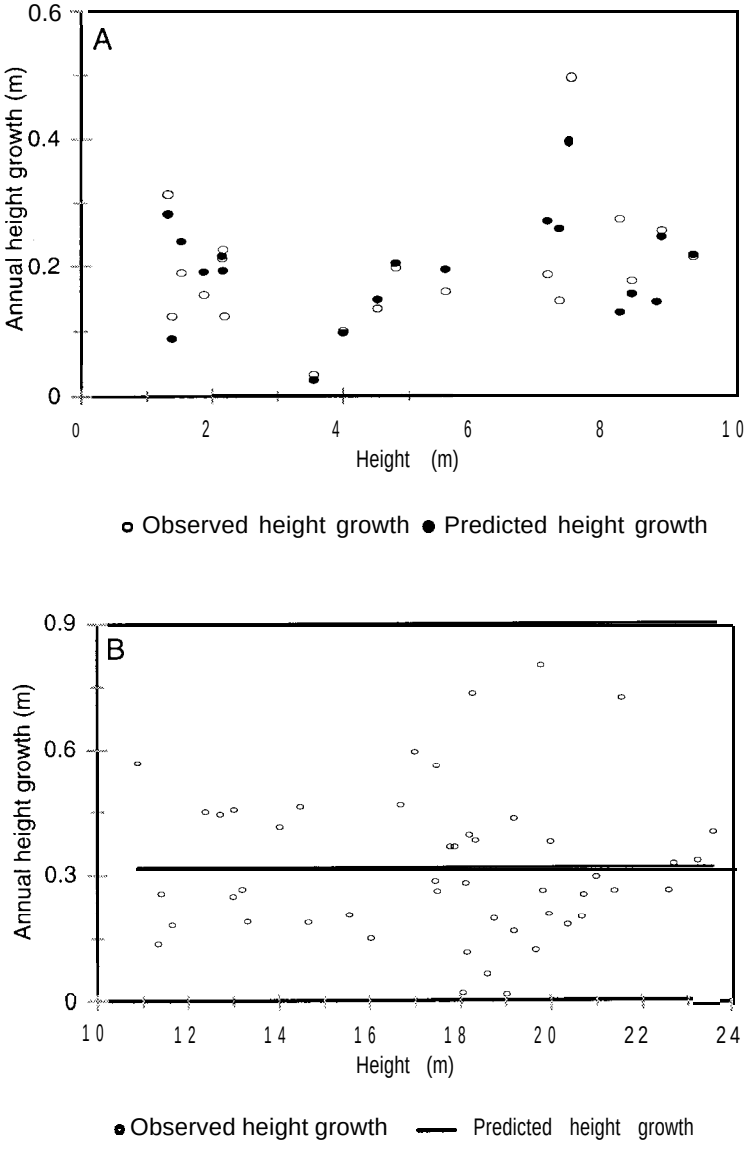

Figure 3.6. Observed and predicted *Abies balsamea* annual height increment (AHINC) relative to height. Predicted values obtained from the model AHINC = 0.03746 x HT - *0.001682* x HT^2 + 0.6472 x ARINC.

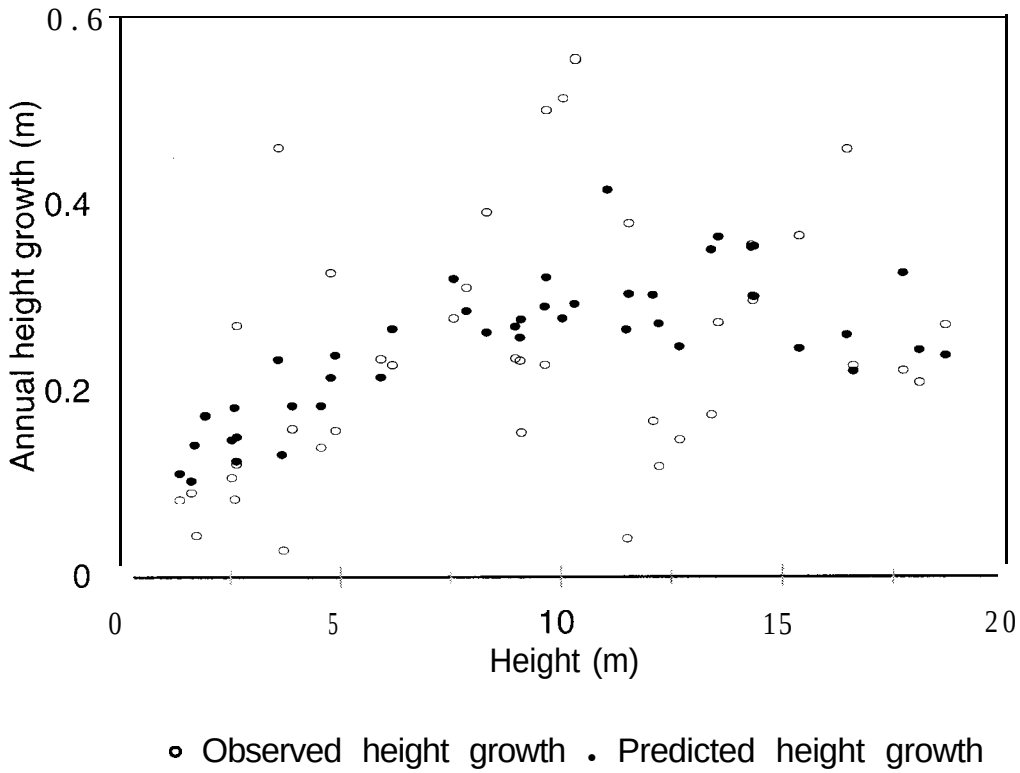

Figure 3.7. Observed and predicted *Picea rubens* annual height increment (AHINC) relative to height. Predicted values obtained from model AHINC = 0.018 12 x HT - *0.000556* x HT^2 + 0.7746 x ARINC.

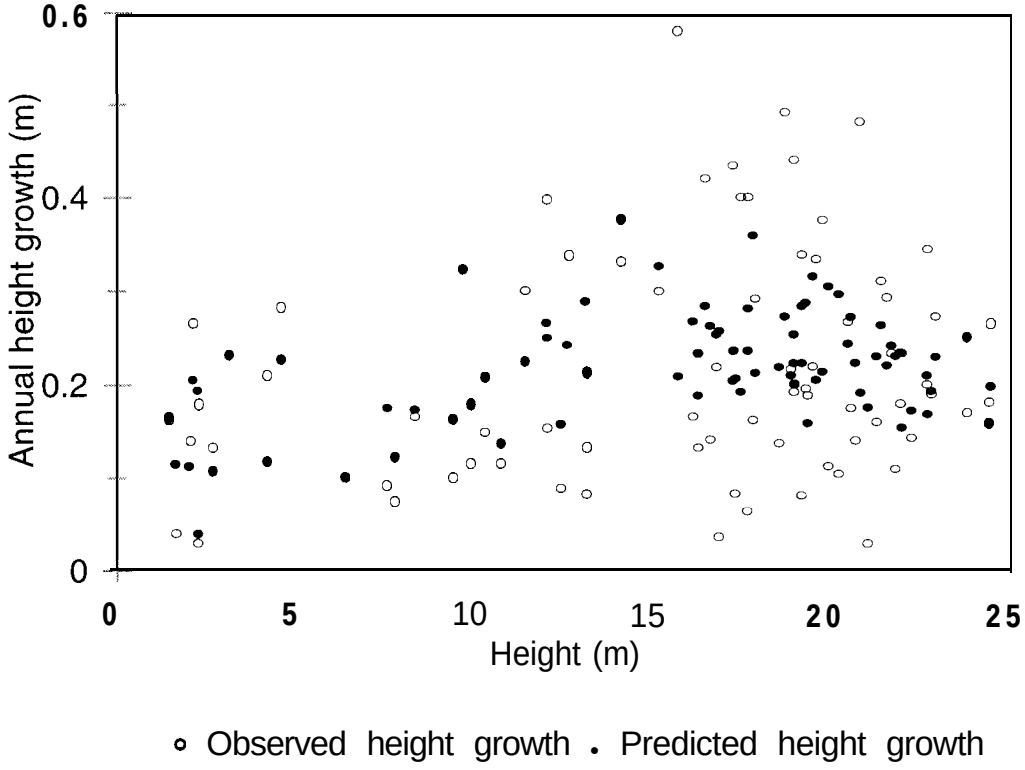

Plot-level Volume Increment Models

Plot-level AVINC was adequately predicted by the simple linear model PAVINC = b_1 LAI, where b_1 = 1.5 167 ± 0.03654, R^2 = 0.9245, and FI = 0.513] (Figure 3.8). Examination of the residuals plotted against the quantitative plot variables (Table 3.4) suggested model bias relative to plot density (TPH) and the proportion of plot leaf area in the C stratum (LAC). However, a density term (b_2 TPH) was not significant when added to the LAI-only model (p = 0.5074, a = 0.05). The equation PAVINC = $\boldsymbol{b}$, LAI + b_2 LAC, where $\boldsymbol{b}$, = 1.7402 ± 0.07352 and b_2 = -0.03888 ± 0.01196, proved optimal. This model had a higher R^2 (0.9652) and lower FI (0.3668) than the LAI-only model, and was unbiased across the range of data (Figure 3.8).

Plot Characteristics

Mensurational data for each of the eleven sample plots (Figure A. 1.) are summarized in Table 3.8, and species compositions are shown in Figure 3.9. Inspection of the data revealed that the majority (n = 6) of the sample exhibited monotonic decreasing (reverse-J) diameter distributions and linear or exponential increasing leaf area distributions (Figures 3.10 and 3.11). The remaining plots had structures conceptually associated with two- or even-aged stands: monotonic decreasing diameter distributions with unimodal distributions of leaf area (n = 1); bi-modal diameter distributions with leaf area distributions heavily skewed to upper (A and B) stratum trees (n = 2); and bimodal diameter distributions with an even distribution of leaf area between separated upper (A or B) and Iower (C or D) stratum trees (n = 2). Analysis of data from all plots indicated a linear relationship between RD and LAI (Figure 3.12).

Figure 3.8. Observed and predicted plot-level annual volume increment (PAVINC) relative to LAI for all plots combined. Predicted values obtained from the models (A) PAVINC = 1.5 167 x LAI and (B) PAVINC = (1.7402 x LAI) - (0.03888 x LAC).

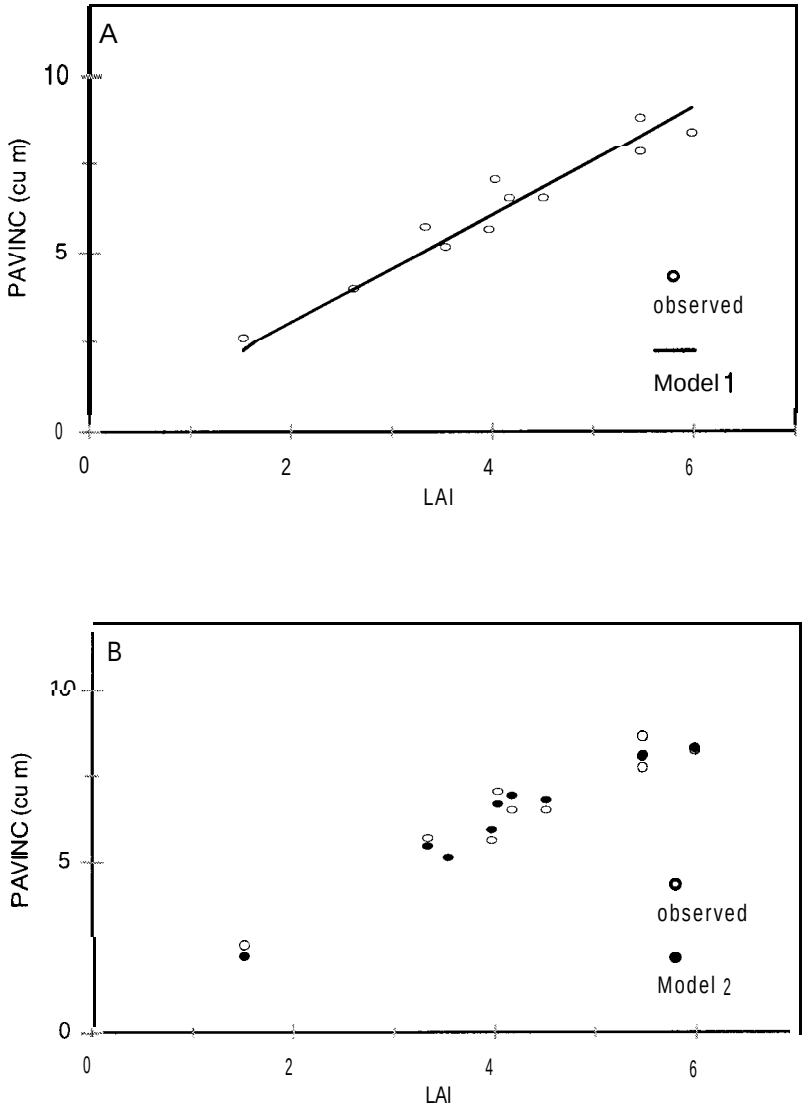

Table 3.8. Summary data for eleven sample plots in multi-aged stands on the Penobscot Experimental Forest.

PLOT	11	12	21	31	32	33
TPH	642.5	1186.1	1334.3	1087.2	1680.3	1235.5
BA (squ per ha)	25.69	16.06	28.68	33.52	23.45	4.62
Volume (cu m per ha)	172.18	107.99	229.97	215.84	131.33	20.16
RD	0.31	0.24	0.45	0.41	0.30	0.06
CCF (percent)	117.4	119.1	170.7	216.1	157.7	43.7
PAVINC (cu m per ha)	7.04	5.16	7.82	8.76	6.52	2.58
LAI	4.02	3.53	5.46	5.45	4.50	1.52
GE (cu m per squ m)	1.7E-04	1.5E-04	1.4E-04	1.6E-04	1.4E-04	1.7E-04

PLOT	41	42	43	52	53
TPH	1186.1	1186.1	1087.2	1037.8	593.0
BA (squ m per ha)	20.08	27.73	14.70	24.44	20.65
Volume (cu m per ha)	149.65	201.47	86.28	189.98	145.26
RD	0.31	0.40	0.19	0.37	0.27
CCF (percent)	134.0	191.6	106.7	130.3	127.2
PAVINC (cu m per ha)	5.65	8.36	3.97	6.52	5.72
LAI	3.96	5.96	2.61	4.16	3.33
GE (cu m per squ m)	1.4E-04	1.4E-04	1.5E-04	1.6E-04	1.7E-04

Figure 3.9. Species compositions of eleven 0.02-ha plots sampled in multi-aged stands C9 and Cl6 on the Penobscot Experimental Forest (PEF), expressed as percent of total basal area (BA) of trees > 1.27 cm dbh. Species abbreviations are BF, *Abies balsamea*; HEM, *Tsuga canadensis;* NWC, *Thuja occidentalis;* RM, *Acer rubrum*; RS, *Picea rubens*; WP, *Pinus strobus;* YB, *Betula alleghaniensis.*

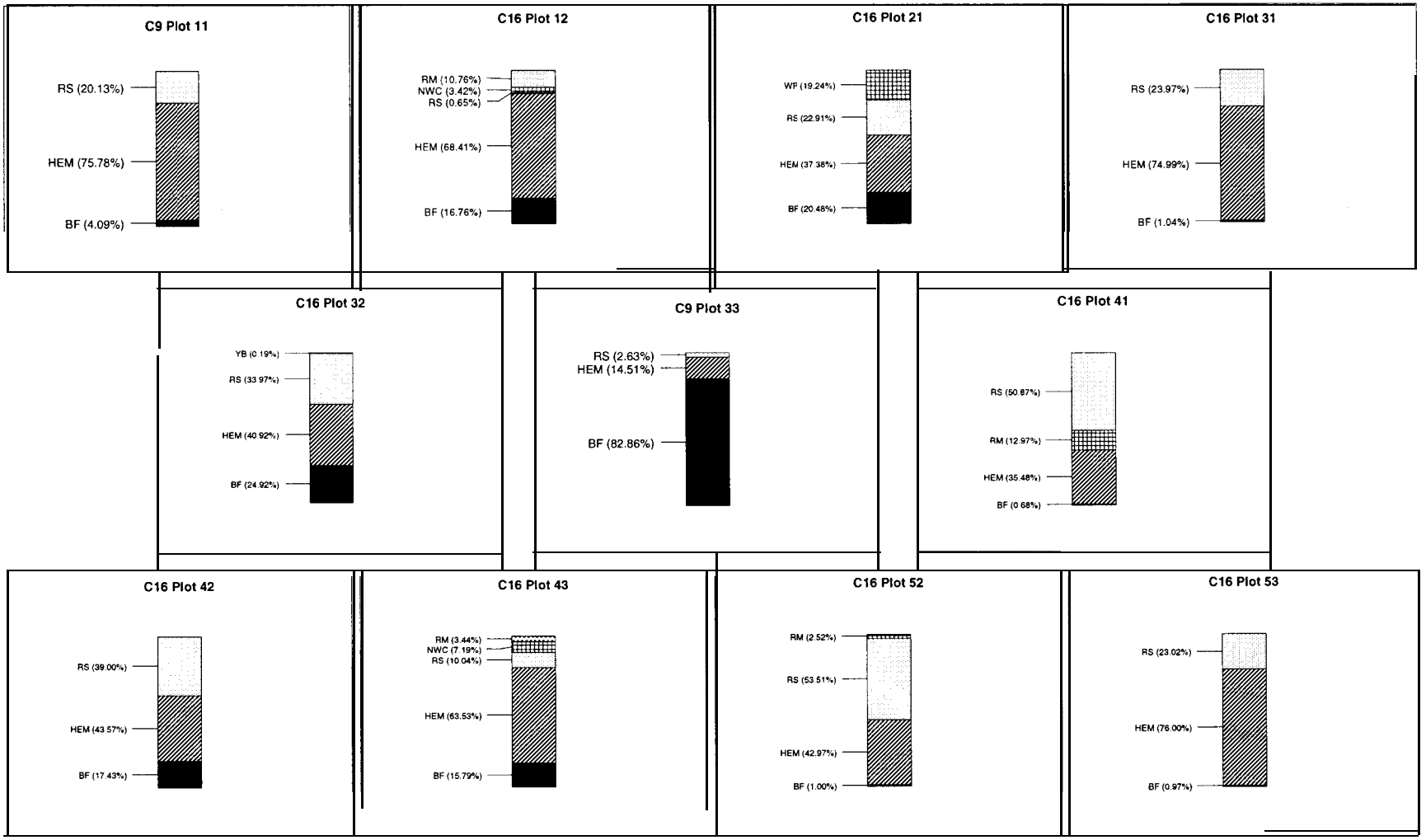
C9 Plot 11
RS (20.13%)
HEM (75.78%)
BF (4.09%)
C16 Plot 12
RM (10.76%)
NWC (3.42%)
RS (0.65%)
HEM (68.41%)
BF (16.76%)
C16 Plot 21
WP (19.24%)
RS (22.91%)
HEM (37.38%)
BF (20.48%)
C16 Plot 31
RS (23.97%)
HEM (74.99%)
BF (1.04%)
C16 Plot 32
YB (0.19%)
RS (33.97%)
HEM (40.92%)
BF (24.92%)
C9 Plot 33
RS (2.63%)
HEM (14.51%)
BF (82.86%)
C16 Plot 41
RS (50.87%)
RM (12.97%)
HEM (35.48%)
BF (0.68%)
C16 Plot 42
RS (39.00%)
HEM (43.57%)
BF (17.43%)
C16 Plot 43
RM (3.44%)
NWC (7.19%)
RS (10.04%)
HEM (63.53%)
BF (15.79%)
C16 Plot 52
RM (2.52%)
RS (53.51%)
HEM (42.97%)
BF (1.00%)
C16 Plot 53
RS (23.02%)
HEM (76.00%)
BF (0.97%)

Figure 3.10. Diameter distributions of eleven 0.02-ha plots sampled in multi-aged stands C9 and Cl6 on the Penobscot Experimental Forest (PEF). Species abbreviations are BF, *Abies balsamea;* HEM, *Tsuga canadensis;* NWC, *Thuja occidentalis;* RM, *Acer rubrum*; RS, *Picea rubens*; WP, *Pinus strobus;* YB, *Betula alleghaniensis.*

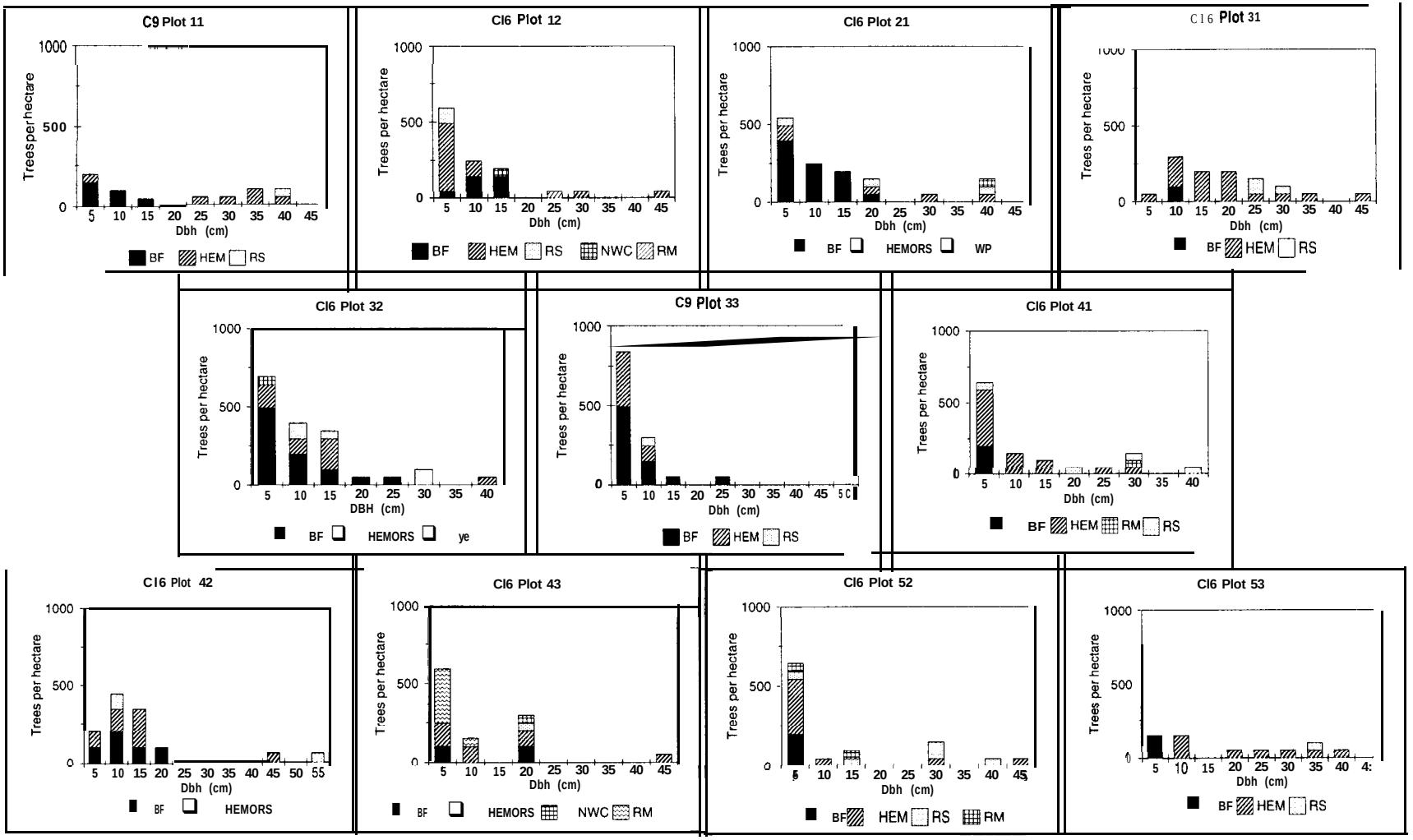
C9 Plot 11
Trees per hectare
1000
500
0
5 10 15 20 25 30 35 40 45
Dbh (cm)
BF HEM RS
Cl6 Plot 12
Trees per hectare
1000
500
0
5 10 15 20 25 30 35 40 45
Dbh (cm)
BF HEM RS NWC RM
Cl6 Plot 21
Trees per hectare
1000
500
0
5 10 15 20 25 30 35 40 45
Dbh (cm)
BF HEMORS WP
C16 Plot 31
Trees per hectare
1000
500
0
5 10 15 20 25 30 35 40 45
Dbh (cm)
BF HEM RS
Cl6 Plot 32
Trees per hectare
1000
500
0
5 10 15 20 25 30 35 40
DBH (cm)
BF HEMORS ye
C9 Plot 33
Trees per hectare
1000
500
0
5 10 15 20 25 30 35 40 45 5C
Dbh (cm)
BF HEM RS
Cl6 Plot 41
Trees per hectare
1000
500
0
5 10 15 20 25 30 35 40
Dbh (cm)
BF HEM RM RS
C16 Plot 42
Trees per hectare
1000
500
0
5 10 15 20 25 30 35 40 45 50 55
Dbh (cm)
BF HEMORS
Cl6 Plot 43
Trees per hectare
1000
500
0
5 10 15 20 25 30 35 40 45
Dbh (cm)
BF HEMORS NWC RM
Cl6 Plot 52
Trees per hectare
1000
500
0
5 10 15 20 25 30 35 40 45
Dbh (cm)
BF HEM RS RM
Cl6 Plot 53
Trees per hectare
1000
500
0
5 10 15 20 25 30 35 40 4:
Dbh (cm)
BF HEM RS

Figure 3.11. Distributions of projected leaf area (PLA) by canopy stratum in eleven 0.02-ha plots sampled in multi-aged stands C9 and C 16 on the Penobscot Experimental Forest (PEF). Species abbreviations are BF, *Abies balsamea*; HEM, *Tsuga canadensis*; NWC, *Thuja occidentulis;* RM, *Acer rubrum*; RS, *Picea rubens*; WP, *Pinus strobus;* YB, *Betula alleghaniensis*.

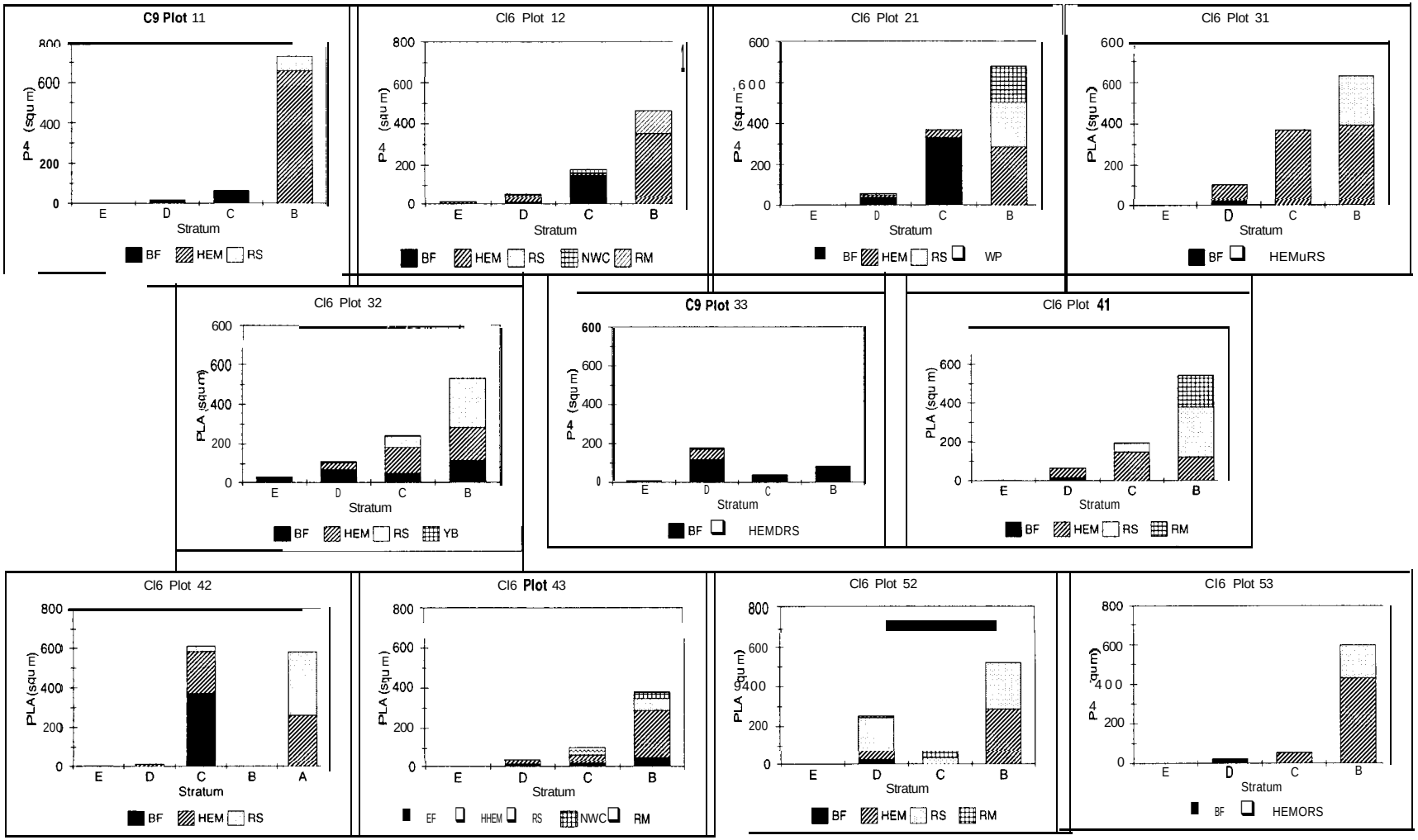
C9 Plot 11
PLA (squ m)
800
600
400
200
0
E D C B
Stratum
BF HEM RS
Cl6 Plot 12
PLA (squ m)
800
600
400
200
0
E D C B
Stratum
BF HEM RS NWC RM
Cl6 Plot 21
PLA (squ m)
600
400
200
0
E D C B
Stratum
BF HEM RS WP
Cl6 Plot 31
PLA (squ m)
600
400
200
0
E D C B
Stratum
BF HEMuRS
Cl6 Plot 32
PLA (squ m)
600
400
200
0
E D C B
Stratum
BF HEM RS YB
C9 Plot 33
PLA (squ m)
600
400
200
0
E D C B
Stratum
BF HEMDRS
Cl6 Plot 41
PLA (squ m)
600
400
200
0
E D C B
Stratum
BF HEM RS RM
Cl6 Plot 42
PLA (squ m)
800
600
400
200
0
E D C B A
Stratum
BF HEM RS
Cl6 Plot 43
PLA (squ m)
800
600
400
200
0
E D C B
Stratum
EF HHEM RS NWC RM
Cl6 Plot 52
PLA (squ m)
800
600
400
200
0
E D C B
Stratum
BF HEM RS RM
Cl6 Plot 53
PLA (squ m)
800
600
400
200
0
E D C B
Stratum
BF HEMORS

Figure 3.12. Leaf area index (LAI) - relative density (RD) relationships in multi-aged stands on the Penobscot Experimental Forest (PEF) and nearby fully-stocked, even-aged *Tsuga canadensis* stands.

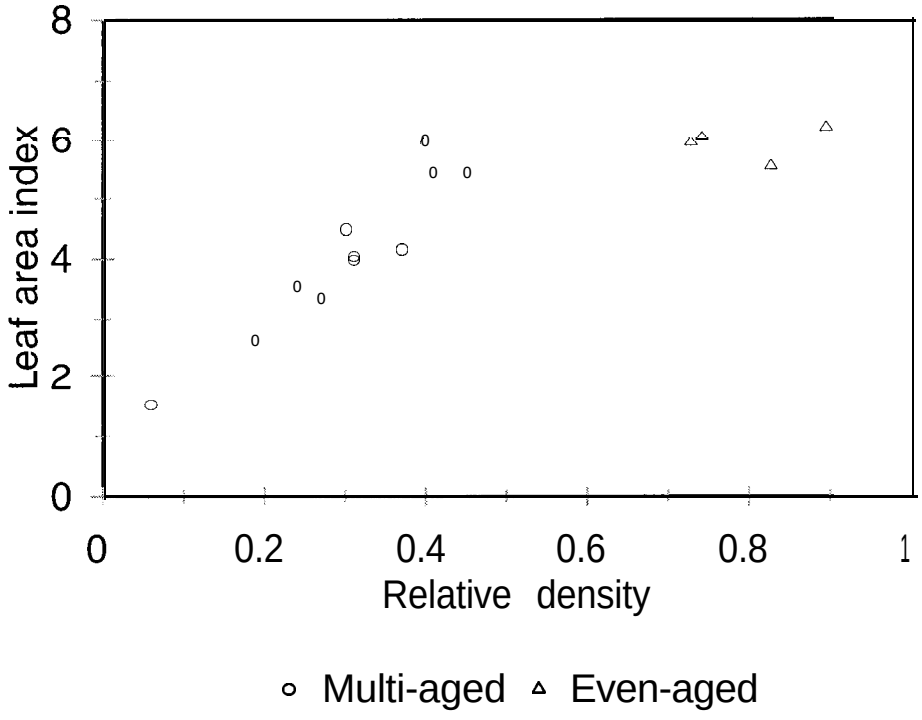

Clustering and Canonical Variate Analysis

Cluster analysis using Ward's minimum-variance method separated sample plots into two clusters (Table 3.9). Two plots (32 and 42) were determined to be outliers using the TRIM option (SAS 1990), but were not excluded from analysis because the significance of the results from both clustering and canonical variate analysis were unchanged by the inclusion of these two plots. Cluster robustness was verified by the average linkage method, which identified the same plot groupings as Ward's method.

Canonical Variate Analysis. Collective comparison of variables between clusters using multivariate ANOVA (Wilks' λ statistic), and pairwise comparisons using Mahalanobis' distances, indicated a significant difference in clusters ($p = 0.0160$, $\alpha = 0.05$). Univariate F tests ($\alpha = 0.05$) indicated highly significant differences in mean plot LAI, PAVINC, BA, and LAC by cluster, with a marginally nonsignificant difference in mean TPH (Table 3.9). The significant between-cluster differences in these plot variables verified that the two groups defined in PROC CLUSTER have distinct structural characteristics. Cluster 1 ($n = 7$) consists of relatively low density (BA) plots with low LAI, a low proportion of midstory foliage, and low PAVINC. Plots in cluster 2 ($n = 4$) have relatively high density, high LAI, a high proportion of midstory foliage, and high PAVINC (Table 3.9, Figure 3.13).

Table 3.9. Results of clustering, canonical variate analysis, and analysis of variance (univariate F-tests) using quantified plot structural characteristics. SEs in parentheses, $\alpha = 0.05$.

	Cluster 1	Cluster 2	
Plots	11, 12, 33, 41, 43, 52, 53	21, 31, 32, 42	
			p-value
PAVINC (m^3/ha)	5.2343 (0.5766)	7.8650 (0.4879)	0.0134
LAI	3.3043 (0.3583)	5.3425 (0.3050)	0.004 1
LAC (percent)	15.0714 (2.9330)	36.0000 (5.1350)	0.0039
BA (m^2/ha)	18.0343 (2.6976)	28.3450 (2.0662)	0.0282
TPH	995.4457 (100.8355)	132 1.9700 (129.7750)	0.0803

Figure 3.13. Distributions of mean trees per hectare (TPH) per diameter class and mean projected leaf area (PLA) per canopy stratum for sample plots in (A) cluster 1 and (B) cluster 2 in multi-aged stands on the Penobscot Experimental Forest.

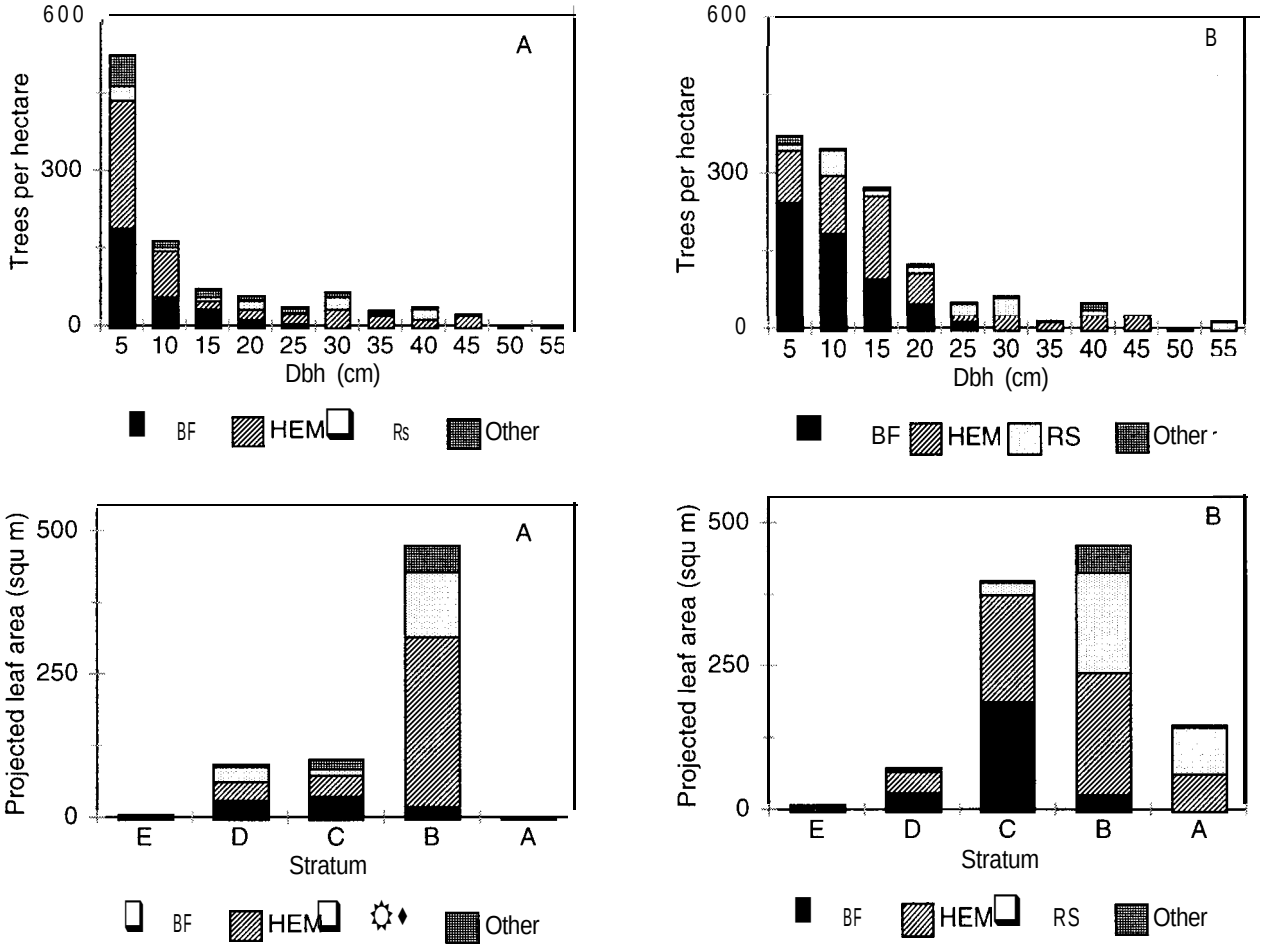

Regression Analysis

Plot-level AVINC within each cluster was effectively modeled with the equation PAVINC = b_1LAI, where b_1 = 1 .5808 ± 0.05 116 and R^2 = 0.908 in cluster 1, and b_1 = 1.47 11 ± 0.04726 and R^2 = 0.730 in cluster 2 (Figure 3.14). These models imply constant GE over increasing LAI within each cluster (Figure 3.14). Though residual analysis suggested possible PAVINC model bias relative to LAC and TPH, parameter estimates were not significantly different from zero for either variable when added to the within-cluster LAI-only models (a = 0.05).

Correlation Analysis

Spearman's rank correlation coefficient (r,) was calculated to assess within-cluster correlations between stemwood volume growth and quantified structural and compositional plot variables. Significant associations between variables, but not the direction of these associations, differed between plots (Tables A.1 and A.2).

A few significant correlations were common to both clusters, and indicate stand-level patterns, such as inverse relationships between TPH and PAVINC (cluster 1 p = 0.0408, cluster 2 p = 0.0001) and between CCF and the proportion of *A. balsamea* (cluster 1 p = 0.0269, cluster 2 p = 0.0001). Additional significant negative associations were found between GE and proportion of midstory foliage (p = 0.0056), LAI and midstory density (p = 0.0362), and PAVINC and midstory density (p = 0.0068) in cluster 1. A significant negative association was also found between TPH and CCF in cluster 2 (p = 0.0001). Significant positive associations of interest include BA and PAVINC (p =

Figure 3.14. Observed and predicted plot-level annual volume increment (PAVINC) (A) and implied growth efficiency (GE) (B) relative to LAI. Predicted values obtained from the models PAVINC = 1.5808 x LAI for cluster 1, and PAVINC = 1.4711 x LAI for cluster 2.

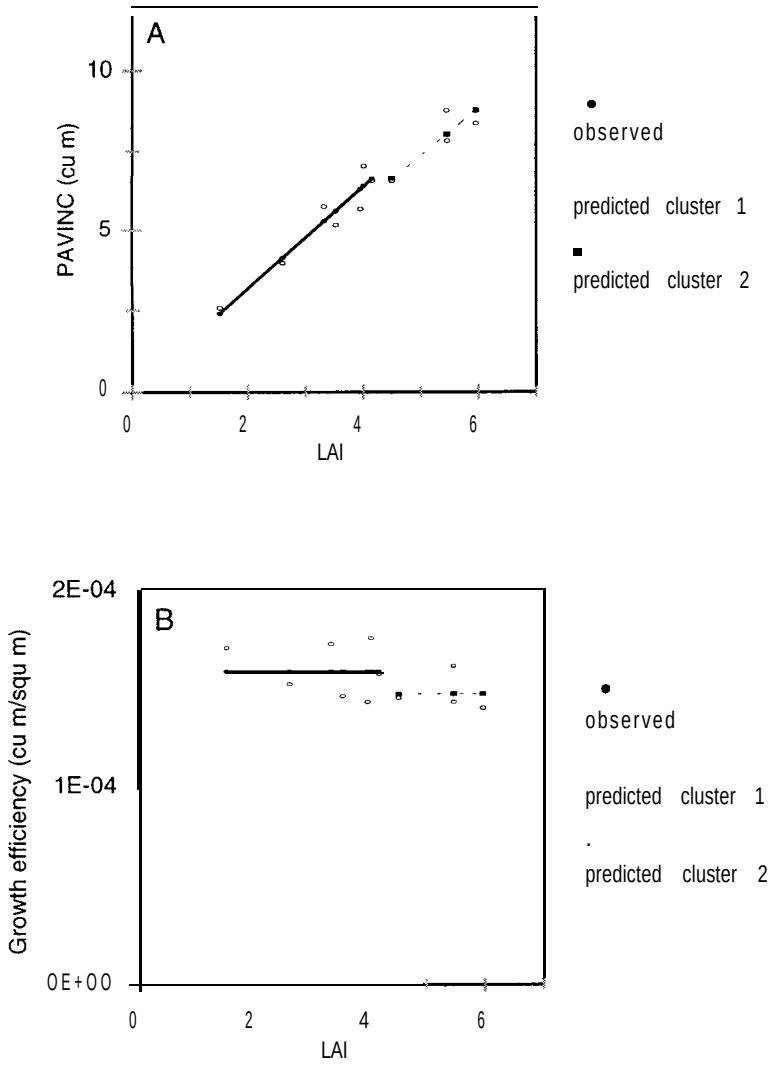

O.OOOl), proportion of *T. canadensis* and B-stratum density (p = 0.0457) in cluster l, and proportion of *A. balsamea* and TPH (p = 0.0001) in cluster 2.

DISCUSSION

Traditional multi-aged silviculture has been criticized due to the tendency of selection cuttings to homogenize horizontal composition and structure. Research reported here reveals small-scale (inter-plot) structural diversity within the multi-aged study stands. Diameter and leaf area distributions encountered on the eleven sample plots approximate those conceptually associated with even-, two-, and multi-aged silvicultural systems (Figures 3.10 and 3.11). Despite high inter-plot variability in structure and composition, a sufficient number of common characteristics exist to allow discussion of growth relationships in multi-aged stands. We begin by posing and answering a single question about growth and leaf area relationships.

Do structural and/or compositional characteristics of multi-aged northern conifer stands improve prediction of stemwood volume growth from LAI?

Though regression analysis of all plots combined indicated that PAVINC was effectively modeled as a function of LAI alone (R^2 = 0.945), residual analysis suggested model bias relative to two structural characteristics: number of stems per ha and leaf area distribution. Though the parameter estimate for TPH was not statistically significant when added to the LAI-only model for all plots combined, the proportion of plot leaf area

in the C stratum (LAC) improved prediction of PAVINC. This finding is consistent with O'Hara and Valappil (1995) and O'Hara (1996, 1998), who documented linear relationships between LAI and stand-level annual volume increment in multi-aged ***P. ponderosa*** stands. Though structural attributes were not explicitly included in O'Hara's (1996) regression equation, he determined that different age structures had different growth efficiencies and that calculation of leaf area per cohort and cohort-specific AVINC improved prediction of stand-level volume increment.

In the present study, the negative parameter estimate for LAC in the PAVINC model for all plots combined indicates that at a given LAI, a greater proportion of midstory foliage is associated with lower plot-level stemwood volume increment. This is presumably because plots with the same LAI but different proportions of midstory foliage have different structural arrangements. The plots with higher proportions of C-stratum leaf area in this study were those with more TPH (for all plots combined, $r_s = 0.6037$, $p = 0.0492$), and lower plot-level GE (for all plots combined, $r_s = 0.7397$, $p = 0.0093$).

Structural characteristics proved meaningful for grouping sample plots. Clustering and canonical variate analysis revealed that the data set actually consisted of two distinct groups - one in which BA, LAI, LAC, and PAVINC are high, and one in which BA, LAI, LAC, and PAVINC are low (Table 3.9, Figure 3.13). It is noteworthy that the proportion of midstory leaf area contributes significantly to both the prediction of stemwood volume increment and the identification of structurally distinct clusters. This finding suggests that vertical foliage distribution may be an important indicator of functionally significant differences in structure. This is supported by research in multi-aged stands of shade-tolerant northern hardwoods, which established relationships

between vertical foliage distribution and conceptual sustainability of silvicultural treatment (Kenefic and Nyland 1996, 2000).

Regression analysis within each cluster indicated that the proportion of midstory did not contribute significantly to estimation of PAVINC once plots were grouped based on similar amounts of LAI and LAC. The significance of this finding should be interpreted with caution due to small sample size (cluster 1 n = 7, cluster 2 n = 4). Nevertheless, the implication of within-cluster regression analysis is that the proportion of midstory foliage, within our data range of 7.9 - 50.6 %, is not explicitly important to the determination of stemwood volume growth in multi-aged stands with density and LAI values similar to those of our clusters.

Plot-level AVINC differed significantly between clusters, with higher annual stemwood volume increment on high-BA, high-LA1 plots (Table 3.9). This finding is not surprising, since regression analysis established a relationship between LAI and PAVINC that overwhelms the contribution of most other structural variables to the prediction of plot-level stemwood volume growth. The result is that, within the range of our data, plots with higher BA have higher LAI, and plots with higher LAI have higher stemwood production. This can be simplified by linking BA and PAVINC directly, but, through the inclusion of the BA - LAI and LAI - PAVINC associations we have verified the physiological basis of an otherwise artificial "wood grows wood" relationship.
Jack and Long (1991) established a positive relationship between density and LAI for shade-tolerant *Abies lasiocarpa* (Hook.) Nutt. (subalpine fir), and numerous studies have linked LAI and stemwood growth (O'Hara 1989, Smith and Long 1989 and 1992, Long and Smith 1992). Our analysis has clarified that, on multi-aged plots of shade-tolerant

species with ranges of density and LAI similar to those within our clusters, increases in LAI are positively related to growth regardless of the vertical foliage distribution.

Species Composition. Aplet et al. (1989) found that stemwood production in mixed-species multi-aged stands of *Picea engelmannii* (Parry) (Englemann spruce) and *Abies lasiocarpa* (Hook.) Nutt. (subalpine fir) was directly related to LAI, and that LAI and stemwood production varied in response to *A. lasiocarpa* diameter distribution. Though species composition is, conceptually, an important component of multi-aged growth relationships, we did not find a significant stemwood volume growth - species composition relationship in our plot-level data. This finding is supported by species-specific, tree-level GE - PLA relationships, which indicate that neither *A. balsamea* nor *P. rubens* GE differs significantly from that of *T. canadensis* (Chapter 2). Though GE of *A. balsamea* and *P. rubens* do differ significantly from one another, these species' influences on growth may have been obscured by small sample size compounded by, or in addition to, gross structural variability. Alternatively, by limiting analysis to plots with > 80% *T. canadensis*, *A. balsumea,* and/or *P. rubens* we may have restricted our sample to a range of species variability that does not exhibit a significant explicit relationship to stand-level stemwood volume growth.

Rank correlation analysis within each cluster indicated that plots with a large proportion of *A. balsamea* (BABF) had relatively low PAVINC, but also low CCF and high TPH (Table A.2). These associations, with inspection of plot summary graphs, suggest that the apparent inverse relationship between PAVINC and BABF may be a

function of structure (lower canopy closure and more small stems) rather than species composition (amount of *A. balsamea*).

Scaling Up: Stand-level Applicability of Plot-level Findings

The study stands, though unquestionably multi-aged, are far from balanced in terms of diameter, age class, or leaf area distributions (Kenefic and Seymour 1997, 1999, and 2000, Seymour and Kenefic 1998). Both stands are dominated by older cohorts, with overstory trees that show prolonged and/or multiple periods of suppression (Kenefic and Seymour 1997, 2000), slow ingrowth, excesses of sawtimber and deficits of pole sized trees (Seymour and Kenefic 1998), and potentially nonsustainable species compositions due to *P. rubens* age class imbalances in both stands (Kenefic et al. 1999, Kenefic 2000) and a single cohort of large sawtimber *P. strobus* in C9. It is thus likely that the plots examined in this study represent, in part, different points along the continuum of stand-level conversion from an irregular multi-aged condition to a balanced multi-aged stand. The diversity of plot structures is also likely due to the horizontal structural heterogeneity that results from a hybrid group and single-tree regeneration method. Though our analysis of the sample plots reveals a diversity of structures, including some conceptually even-or two-aged, all of these contribute to the overall multi-aged condition and are appropriately included in an assessment of multi-aged stand structure and growth. This conclusion is supported by the distributions of mean TPH by diameter class for each of the two clusters (Figure 3.13). Diameter distributions resemble a reverse-J in cluster 1 and a rotated sigmoid in cluster 2, indicating that, on average, cluster structures are similar to common multi-aged size class distributions.

Management Considerations

Research reported here established LAI as the most important predictor of PAVINC in mixed-species multi-aged northern conifer stands. Furthermore, results indicated that including the proportion of midstory leaf area in the regression equation improved growth prediction when plots with markedly different structures were analyzed together. This is consistent with O'Hara (1996) who found that stand structure (leaf area distribution by age class) improved prediction of stand-level AVINC relative to using LAI alone. For all plots combined in the present study, increases in the proportion of midstory were associated with higher stem density and lower GE (from correlation analysis), and decreased PAVINC at a given LAI (from regression analysis).

Within clusters of plots of similar density and LAI, structural variables (Table 3.4) did not prove relevant to PAVINC. The implication of this is that within the range of structural diversity encompassed by each cluster, structural goals designed to maximize stemwood volume increment should have as much leaf area as possible regardless of vertical arrangement. Because there is a positive relationship between RD and LAI (Figure 3.12), increasing RD by increasing number or size of stems would result in higher LAI within the range of our data. Data collected from fully stocked even-aged *T. canadensis* stands in the area of the PEF indicated that plots with RD 0.73 - 0.90 have mean LAI 5.97 (range 5.57 - 6.26) (Figure 3.12). The sample plots in the present study have RD 0.06 - 0.45 and mean LAI 4.05 (range 1.52 - 5.96), suggesting that RD and LAI could be increased. While a few (i.e. plot 42 with LAI = 5.96) appear to be at or close to maximum LAI, others (i.e. plot 33 with LAI = 1.52) appear to be grossly understocked.

It is possible to increase plot-level RD and LAI through recruitment of small trees and increases in lower stratum leaf area (LA), or the retention of higher upper stratum density and LA. The latter alternative may prove more effective for increasing growth than allocating additional leaf area to the lower (less efficient) strata (Chapter 2). The potential problem inherent to this approach is that increasing overstory LA inevitably increases competition for light in lower stratum trees. The degree to which LAI can be increased via allocation of leaf area to large trees without endangering the sustainability of growth and structure is a topic that deserves attention in future research and modeling of PAVINC - LAI relationships.

SUMMARY

The study reported here explores quantitative relationships between leaf area, stemwood volume increment, growth efficiency, and structure in mixed-species, multi-aged northern conifer stands. It is apparent that these factors are inextricably linked at the tree and stand levels, and that the dynamics of multi-aged stands are in fact the outcome of a multitude of interrelated processes driven by highly correlated tree and stand characteristics. From the tangle of ecological relationships, we have successfully unraveled a few, key relationships.

In **Chapter 1,** the validity of nonsapwood-based equations for prediction of *T. canadensis* projected leaf area was established. A model suggested by Valentine et al. (I 996) was recommended, and bridged the gap between highly theoretical discussion and practical application of structural control by leaf area allocation. This equation links standard inventory data (diameter at breast height and live crown ratio) to leaf area - a biologically meaningful expression of growing space occupancy and predictor of growth. A variation of this model form was later applied to *P. rubens* in Chapter 3.

Chapter 2 addressed tree-level volume increment - leaf area relationships for three shade-tolerant species growing in multi-aged stands. Regression analysis established strong relationships between tree-level volume increment and projected leaf area (PLA). The growth efficiencies implied by these models revealed that *A. balsamea* and trees in the upper canopy were the most efficient stemwood producers. All three species' growth efficiency (GE) - PLA relationships exhibited slight maxima, thus conforming in shape if not magnitude to the conceptualized pattern of GE for shade-

tolerant species in multi-aged stands. Age was not found to be an important determinant of growth or growth efficiency.

Chapter 3 utilized the established PLA and annual stemwood volume increment relationships to assess the structure and growth of different multi-aged structures obtained from sample plots within irregularly multi-aged stands. Stand-level analysis revealed that leaf area index (LAI) is the best predictor of stand-level volume increment, though the vertical distribution of leaf area (proportion of midstory leaf area) improved prediction of growth when plots of significantly different densities were combined. Clusters of plots with like-structures were identified, and differed significantly in terms of LAI, basal area, and volume growth. Within these clusters, LAI alone was the best predictor of growth and average diameter distributions were typical of multi-aged stands. Comparison of data from these and fully-stocked even-aged *T. canadensis* plots suggested that LAI and volume growth could be increased, based on the relationship between relative density and LAI.

Increasing short-term stemwood volume increment by increasing LAI and the proportion of the most efficient (upper stratum) leaf area was suggested, but further research is needed to determine the highest proportion of upper stratum leaf area that can be maintained without reducing regeneration and lower stratum tree growth to nonsustainable levels.

REFERENCES

Anderson, H.W. and A.G. Gordon. 1994. The tolerant conifers: eastern hemlock and red spruce, their ecology and management. Ministry of Natural Resources, Ontario Forest Research Institute. Ontario. 46 pp.

Aplet, G.H., F.W. Smith, and R.D. Laven. 1989. Stemwood biomass and production during spruce fir stand development. J. Ecology 77:70-77.

Applequist, M.B. 1958. A simple pith locator for use with off-center increment cores. J. For. 56: 141.

Assmann, E. 1970. Principles of forest yield study: studies in the organic production, structure, increment, and yield of forest stands. Pergamon Press Ltd. Oxford. 506 pp.

Baskerville, G.L. 1972. Use of logarithmic regression in the estimation of plant biomass. Can. J. For. Res. 2:49-53.

Belsley, D.A., E. Kuh, and R.E. Welsh. 1980. Regression diagnostics: identifying influential data and sources of collinearity. John Wiley & Sons, New York.

Bormann, B.T. 1990. Diameter-based biomass regression models ignore large sapwood variation in Sitka spruce. Can. J. For. Res. 20: 1098-l 104.

Brunner, A. and G. Nigh. 2000. Light absorption and bole volume growth of individual Douglas-fir trees. Tree Physiology 20:323-332.

Burns, G.P. 1923. Studies in tolerance of New England forest trees: IV. Minimum light requirement referred to a definite standard. Vt. Agric. Exp. Stn. Bull. No. 235.

Carmean W.H., J.T. Hann, and R.D. Jacobs. 1989. Site index curves for forest tree species in the eastern United States. USDA Forest Service NC Forest Experiment Stn. Gen. Tech. Rpt. NC-128. 142 pp.

Coyea, M.R., and H.A. Margolis. 1992. Factors affecting the relationship between sapwood area and leaf area of balsam fir. Can. J. For. Res. 22: 1684-1693.

Davis, W.C. 198 1. The role of advance growth in regeneration of red spruce and balsam fir in east central Maine. In: C.M. Simpson (Editor), Proc. of the Conf. on Natural Regeneration. Forestry Canada. 17- 19 March 1990. Fredericton, N.B. pp. 157-168.

Day, M.E., M.S. Greenwood, and A.S. White. 2000. Abstract: Long-term maturational changes in foliar morphology and physiology in red spruce in relation to declining net primary productivity with tree age. In: Communicating and advancing ecology: The Ecological Society of America 85th Annual Meeting. 6- 10 August 2000. Snowbird, Utah. p. 84.

Dean, T.J. and J.N. Long. 1986. Variation in sapwood-leaf area relations within two stands of lodgepole pine. For. Sci. 32:749-758.

Dean, T.J., J.N. Long, and F.W. Smith. 1988. Bias in leaf area - sapwood area ratios and its impact on growth analysis in *Pinus contorta*. Trees 2: 104-109.

Devore, J. and R. Peck. 1986. Statistics: the exploration and analysis of data. West Publishing Company. St. Paul, MN. 699 pp.

Eades, H.W. 1958. Differentiation of sapwood and heartwood in western hemlock by color tests. For. Prod. J. 8: 104-106.

Espinosa Bancalari, M.A., D.A. Perry, and J.D. Marshall. 1987. Leaf area - sapwood area relationships in adjacent young Douglas-fir stands with different early growth rates. Can. J. For. Res. 17: 174-180.

Furnival, G.M. 196 1. An index for comparing equations used in constructing volume tables. For. Sci. 7:337-34 1.

Gilmore, D.W. and R.S. Seymour. 1996. Alternative measures of stem growth efficiency applied to *Abies balsamea* from four canopy positions in central Maine, USA. For. Ecol. Manage. 84:209-2 18.

Gilmore, D.W., R.S. Seymour, and D.A. Maguire. 1996. Foliage - sapwood area relationships for *Abies balsamea* in central Maine, U.S.A. Can. J. For. Res. 26:207 *l-2079.*

Graybill, F.A. and H.K. Iyer. 1994. Regression analysis: concepts and applications. Wadsworth Publishing Company. Belmont, CA. 701 pp.

Greenwood, M.S. and K.W. Hutchinson. 1993. Maturation as a developmental process. In: Clonal forestry: Genetics and biotechnology. Edited by M.R. Ahuja and W.J. Libby. Springer-Verlag, Berlin. pp. 14-33.

Gregoire, T.G. and H.T. Valentine. 1995. A sampling strategy to estimate the area and perimeter of irregularly shaped planar regions. For. Sci. 41: 470-476.

Guldin, J.M. 199 1. Uneven-aged BD*q* regulation of Sierra Nevada mixed conifers. W. J. Appl. For. 6:27-32.

Holmes, R.L. 1983. Computer assisted quality control in tree-ring dating and measurement. Tree-Ring Bull. 43:69-78.

Honer, T.G. 1967. Standard volume tables and merchantable conversion factors for the commercial tree species of central and eastern Canada. Forest Manage. Res. and Services Inst. Ottawa, Canada. 84 pp.

Huang, S. and S.J. Titus. 1995. An individual tree diameter increment model for white spruce in Alberta. Can. J. For. Res. 25: 1455-1465.

Jack, S.B. and J.N. Long. 1991. Response of leaf area index to density for two contrasting tree species. Can. J. For. Res. 21: 1760-1764.

Jack, S.B. and J.N. Long. 1991. Structure, production and leaf area dynamics: a comparison of lodgepole pine and sunflower. Annals of Botany 68:247-252.

Jack, S.B. and J.M. Long. 1992. Forest production and the organization of foliage within crowns and canopies. For. Ecol. Manage. 49:233-245.

Jensen, W.A. 1962. Botanical histochemistry: Principles and practice. W.H. Freeman and Company, San Fransisco.

Kenefic, L.S. 2000. Multi-aged silviculture in the Acadian Forest of Maine. In: Proceedings of the Tolerant Softwood Workshop. Compiled by: G. Harrison, R. Whitney, and E. Swift. 13- 15 April 1999, Fredericton, N.B. Maritime Forest Ranger School. Not paginated.

Kenefic, L.S., J.C. Brissette, and R.S. Seymour. 1999. Dynamics of overstory species composition in managed uneven-aged northern conifer stands (Abstract). In: Program and Abstracts. Second North American Forest Ecology Workshop. Edited by: J.D. Eckhoff. 27-30 June 1999, Orono, ME. p. 136.

Kenefic, L.S. and R.D. Nyland. 1996. Structural development and consistency in uneven-aged northern hardwood stands. In: Proceedings of the Society of American Foresters Convention. 28 Oct.-l Nov. 1995, Portland, ME. pp. 441-442.

Kenefic, L.S. and R.D. Nyland. 2000. Habitat diversity in uneven-aged northern hardwood stands: a case study. Res. Pap. NE-714. Newtown Square, PA: U.S. Department of Agriculture, Forest Service, Northeastern Research Station. 4 p.

Kenefic, L.S. and R.S. Seymour. 1997. Patterns of tree growth and structural development in uneven-aged northern conifer stands in the Acadian forest of Maine. In: Proceedings of the IUFRO Symposium on Uneven-aged Silviculture. 15-19 Sept. 1997, Corvalis, OR. pp. 554-568.

Kenefic, L.S. and R.S. Seymour. 1999. Leaf area prediction models for *Tsuga canadensis* in Maine. Can. J. For. Res. 29:1574-1582.

Kenefic, L.S. and R.S. Seymour. 2000. Growth patterns of *Tsuga canadensis* in managed uneven-aged northern conifer stands. In: Proceedings: Symposium on Sustainable Management of Hemlock Ecosystems in Eastern North America; 1999 June 22-24; Durham, NH. Edited by: K.A. McManus, K.S. Shields, and D.R. Souto. Gen Tech Rep. 267. Newtown Square, PA. U.S. Dept. Agric., Forest Service, Northeastern Res. Stn. pp. 29-33.

Kvålseth, T.O. 1985. Cautionary note about R^2. Amer. Stat. 39:279-285.

Long, J.N. and F.W. Smith. 1989. Estimating leaf area of *Abies lasiocarpa* across ranges of stand density and site quality. Can. J. For. Res. 19:930-932.

Long, J.N. and F.W. Smith. 1990. Determinants of stemwood production in *Pinus contortu* var. *latifolia* forests: the influence of site quality and stand structure. J. Appl. Ecol. 27:847-856.

Long, J.N. and F.W. Smith. 1992. Volume increment in *Pinus contortu* var. *latifolia*: the influence of stand development and crown dynamics. For. Ecol. Manage. 53:53-64.

Maguire, D.A. and J.L.F. Batista. 1996. Sapwood taper models and implied sapwood volume and foliage profiles for coastal Douglas-fir. Can. J. For. Res. 26:849-863.

Maguire, D.A. and W.S. Bennett. 1996. Patterns in vertical distribution of foliage in young coastal Douglas-fir. Can. J. For. Res. 26: 1991-2005.

Maguire, D.A. and D.W. Hann. 1989. The relationship between gross crown dimensions and sapwood area at crown base in Douglas-fir. Can J. For. Res. 19:557-565.

Maguire, D.A. J.C. Brissette, and L.Gu. 1998. Canopy structure and growth efficiency of red spruce in uneven-aged, mixed-species stands in Maine. Can. J. For Res. 28:1233-1240.

Marchand, P.J. 1984. Sapwood area as an estimator of foliage biomass and projected leaf area for *Abies balsamea* and *Piceu rubens*. Can. J. For. Res. 14:85-87.

Marshall, J.D. and R.H. Waring. 1986. Comparison of methods of estimating leaf-area index in old-growth Douglas-fir. Ecology 67:975-979.

O'Hara, K.L. 1988. Stand structure and growing space efficiency following thinning in an even-aged Douglas-fir stand. Can. J. For. Res. 18:859-866.

O'Hara, K.L. 1989. Stand growth efficiency in a Douglas-fir thinning trial. Forestry 62:409-4 18.

O'Hara, K.L. 1996. Dynamics and stocking-level relationships of multiaged ponderosa pine stands. For. Sci. 42, Monogr. 33.

O'Hara, K.L. 1998. Silviculture for structural diversity: A new look at multiaged systems. J. For. 96:4-10.

O'Hara, K.L. and N.I. Valappil. 1995. Sapwood-leaf area prediction equations for multi-aged ponderosa pine stands in western Montana and central Oregon. Can. J. For. Res. 25: 1553-1557.

Oliver, CD. and B.C. Larson. 1996. Forest stand dynamics. John Wiley and Sons, Inc. New York. 520 pp.

Ratkowsky, D.A. 1990. Handbook of nonlinear regression models. Marcel Dekker, Inc. New York. 241 pp.

Roberts, S.D. and J.N. Long. 1992. Production efficiency of *Abies lasiocarpa*: influence of vertical distribution of leaf area. Can. J. For. Res. 22: 1230-1234.

Roberts, S.D., J.N. Long, and F.W. Smith. 1993. Canopy stratification and leaf area efficiency: a conceptualization. For. Ecol. and Manage. 60: 143-156.

Ryan, S.D. and B.J. Yoder. 1997. Hydraulic limits to tree height and tree growth. Bioscience 47:235-242.

SAS Institute Inc. 1990. SAS/STAT User's guide. SAS Institute Inc., Cary, NC. 1686 pp.

Schlotzhauer, S.D. and R.C. Littell. 1997. SAS System for elementary statistical analysis. Second edition. SAS Institute, Inc. Cary, NC. 440 pp.

Seymour, R.S. 1992. The red spruce-balsam fir forest of Maine: Evolution of silvicultural practice in response to stand development patterns and disturbances. In: The ecology and silviculture of mixed-species forests. Edited by: M.J. Kelty. Kluwer Academic Publishers. Netherlands. pp. 2 17-244.

Seymour, R.S. and L.S. Kenefic. 1998. Balance and sustainability in multi-aged stands: a northern conifer case study. J. For. 96: 12-17.

Shvets, V. and B. Zeide. 1996. Investigating the parameters of growth equations. Can. J. For. Res. 26: 1980- 1990.

Smith, D.M., B.C. Larson, M.J. Kelty, and P.M.S. Ashton. 1997. The practice of silviculture: Applied forest ecology. Ninth Ed. John Wiley & Sons, Inc. New York. 537 pp.

Smith, F.W. and J.N. Long. 1989. The influence of canopy architecture on stemwood production and growth efficiency of *Pinus contorta* var. *latifolia*. J. Appl. Ecol. 26:681-691.

Smith, F.W. and J.N. Long. 1992. A comparison of stemwood production in monocultures and mixtures of *Pinus contorta* var. *latifolia* and *Abies lasiocarpa*. In: The ecology of mixed-species stands of trees. M.G.R. Cannell, et al. Blackwell Sci. Publ. Inc. Cambridge, MA. pp. 87-98.

Swain, T. 1965. The tannins. In: Plant biochemistry. Edited by: J. Bonner and J.E. Varner. Academic Press, Inc. New York. pp. 552-580.

Valentine, H.T., V.C. Baldwin Jr., T.G. Gregoire, and H.E. Burkhart. 1994. Surrogates for foliar dry matter in loblolly pine. For. Sci. 40:576-585.

Vanninen, P. and A. Mäkelä. 2000. Needle and stem wood production in Scots pine (*Pinus sylvestris*) trees of different age, size and competitive status. Tree Physiology 20:527-533.

Velazquez-Martinez, A., D.A. Perry, and T.E. Bell. 1992. Response of aboveground biomass increment, growth efficiency, and foliar nutrients to thinning, fertilization, and pruning in young Douglas-fir plantations in the central Orgeon Cascades. Can. J. For. Res. 22: 12781289.

Vose, J.M. and H.L. Allen. 1988. Leaf area, stemwood growth, and nutrition relationships in loblolly pine. For. Sci. 34:547-563.

Waring, R.H., K. Newman, and J. Bell. 198 1. Efficiency of tree crowns and stemwood production at different canopy leaf densities. Forestry 54: 129- 137.

Waring, R.H., P.E. Schroeder, and R. Oren. 1982. Application of the pipe model theory to predict canopy leaf area. Can. J. For. Res. 12:556-560.

Wilson, D.S., R.S. Seymour, and D.A. Maguire. 1999. Density management diagram for northeastern red spruce and balsam fir forests. N. J. Appl. For. 16:48-56.

Yang, R.C., A. Kozak, and J.H.G. Smith. 1978. The potential of Weibull-type functions as flexible growth curves. Can. J. For. Res. 8:424-43 1.

Yoda, K., K. Shinozaki, H. Ogawa, K. Hozumi, and T. Kira. 1965. Estimation of the total amount of respiration in woody organs of trees and forest communities. J. Biol. 16: 15-26.

Yoder, B.J., M.G. Ryan, R.H. Waring, A.W. Schoettle, and M.R. Kaufmann. 1994. Evidence of reduced photosynthetic rates in old trees. For. Sci. 40:5 13-527.

Young, H.E., J.H. Ribe, and K. Wainwright. 1980. Weight tables for tree and shrub species in Maine. Life Sciences and Agriculture Exper. Stn. Univ. of Maine, Orono. Misc. Rep. 230. 21 pp.

APPENDIX

Figure A. 1. Plot summary data (A) - (K) for eleven 0.02-ha plots sampled in multi-aged stands C9 and Cl6 on the Penobscot Experimental Forest. Species abbreviations are BF, *Abies balsamea;* HEM, *Tsuga canadensis;* NWC, *Thuja occidentalis;* RM, *Acer rubrum*; RS, *Picea rubens*; WP, *Pinus strobus;* YB, *Betula alleghaniensis.*

A

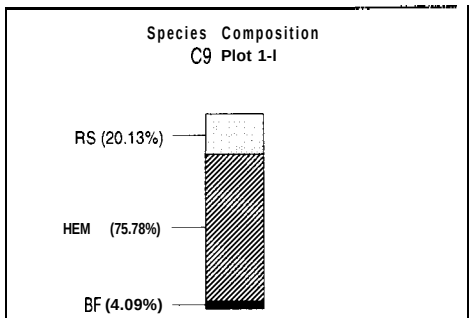

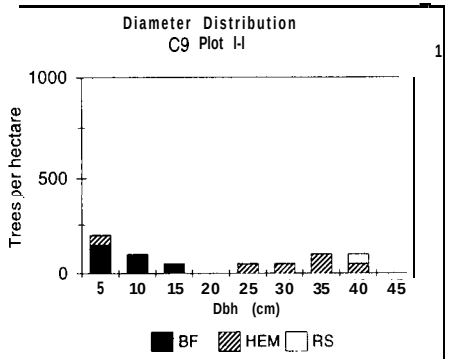

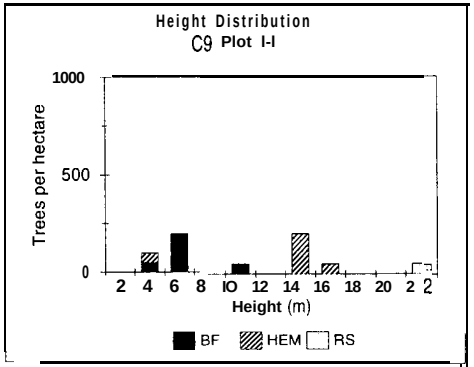

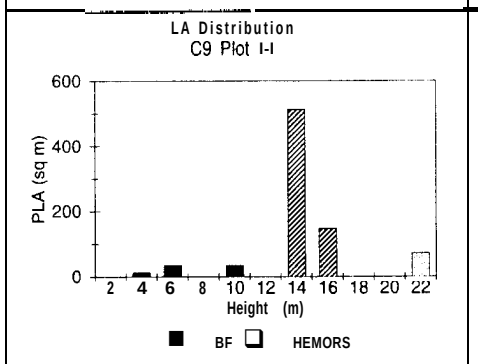

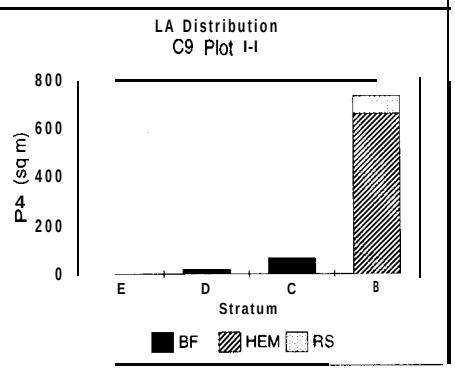

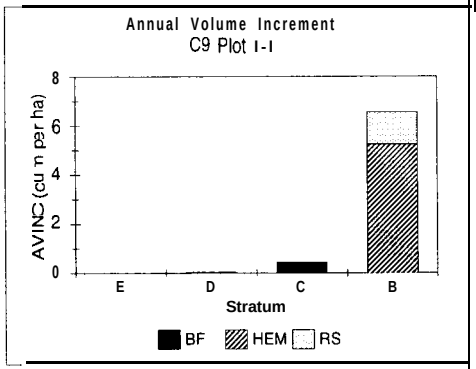

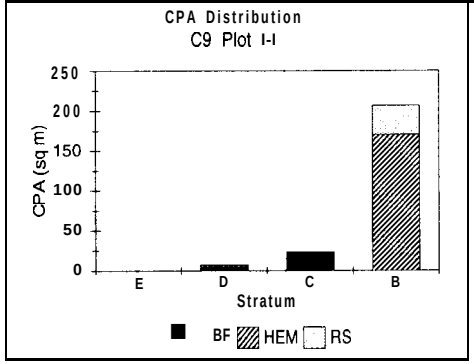

Density	642.45 trees per ha
BA	25.69 squ m per ha
Volume	172.18 cu m per ha
RD	0.31
PAVINC	7.04 cu m per ha
GE	1.7E-04 cu m per squ m
LAI	4.02
CCF	117.35 percent

Bimodal diameter distribution
LA distribution skewed toward upper stratum

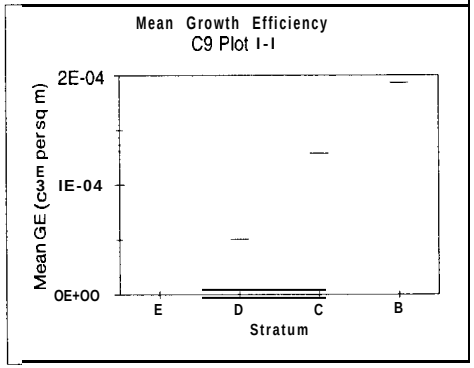

B

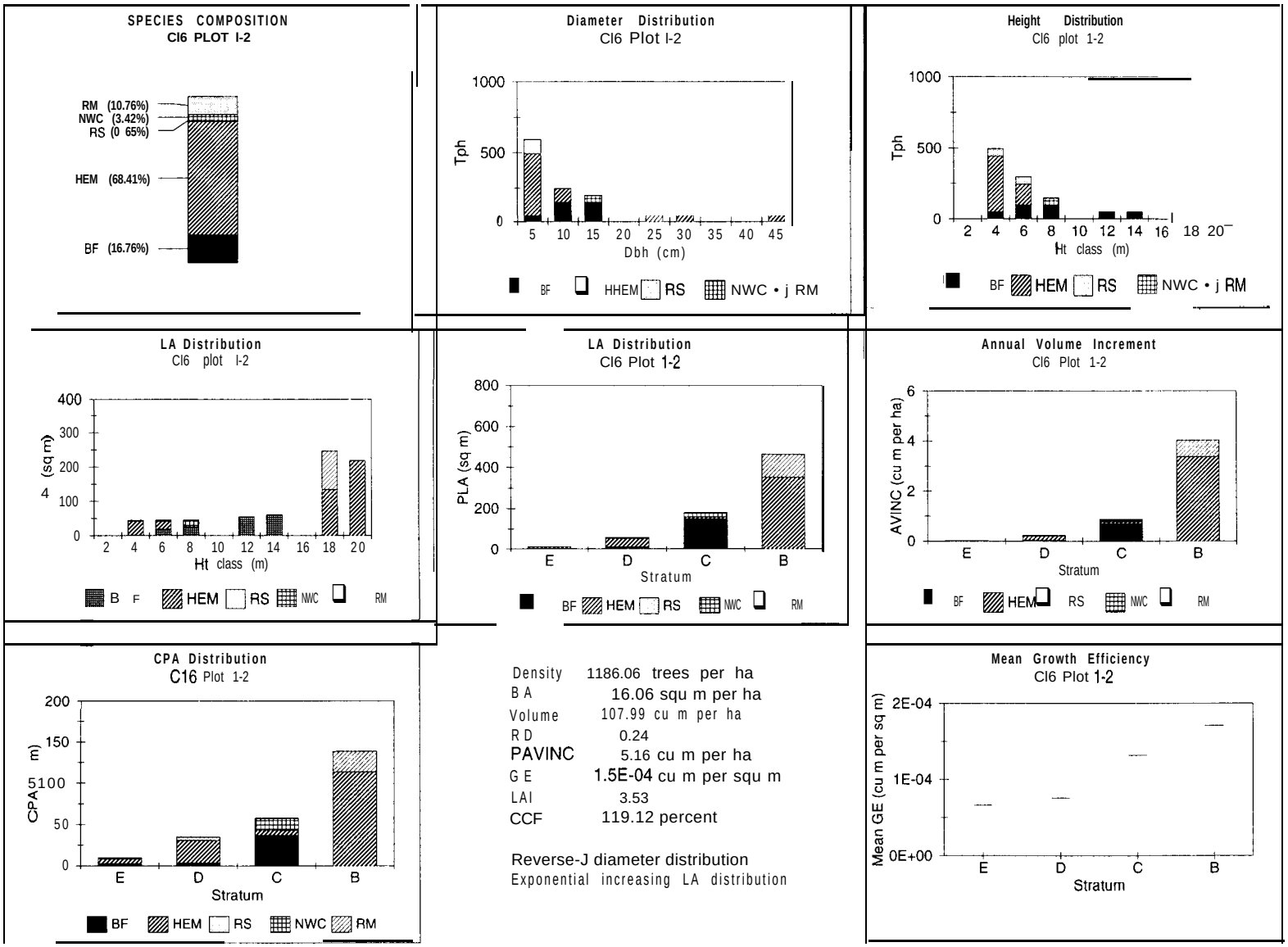
SPECIES COMPOSITION
CI6 PLOT I-2
RM (10.76%)
NWC (3.42%)
RS (0 65%)
HEM (68.41%)
BF (16.76%)
Diameter Distribution
Cl6 Plot I-2
Tph
Dbh (cm)
BF HHEM RS NWC • j RM
Height Distribution
Cl6 plot 1-2
Tph
Ht class (m)
BF HEM RS NWC • j RM
LA Distribution
Cl6 plot I-2
(sq m)
Ht class (m)
B F HEM RS NWC RM
LA Distribution
Cl6 Plot 1-2
PLA (sq m)
Stratum
BF HEM RS NWC RM
Annual Volume Increment
Cl6 Plot 1-2
AVINC (cu m per ha)
Stratum
BF HEM RS NWC RM
CPA Distribution
C16 Plot 1-2
CPA m)
Stratum
BF HEM RS NWC RM
Density 1186.06 trees per ha
B A 16.06 squ m per ha
Volume 107.99 cu m per ha
R D 0.24
PAVINC 5.16 cu m per ha
G E 1.5E-04 cu m per squ m
LAI 3.53
CCF 119.12 percent
Reverse-J diameter distribution
Exponential increasing LA distribution
Mean Growth Efficiency
Cl6 Plot 1-2
Mean GE (cu m per sq m)
Stratum

C

SPECIES COMPOSITION
C16 PLOT 2-I

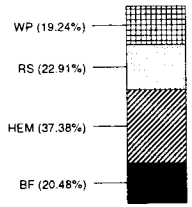

DIAMETER DISTRIBUTION
Cl6 **PLOT** 2-I

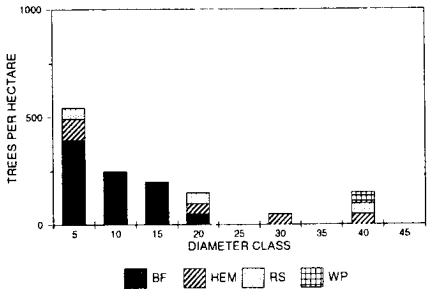

HEIGHT DISTRIBUTION
Cl6 PLOT 2-I

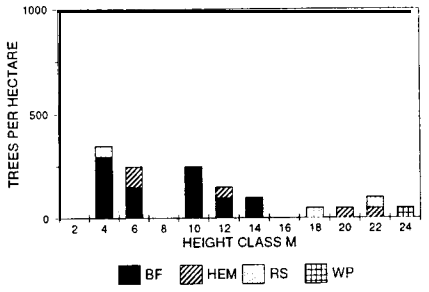

LA DISTRIBUTION
Cl6 PLOT 2-1

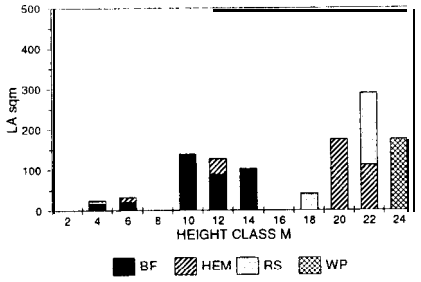

LA Distribution
Cl6 Plot 2-1

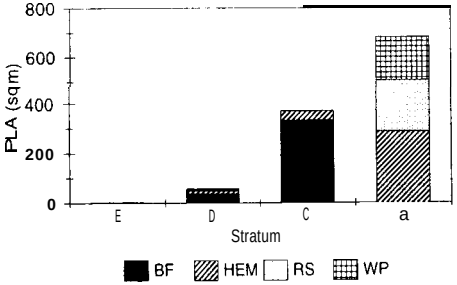

Annual Volume Increment
Cl6 Plot 2-1

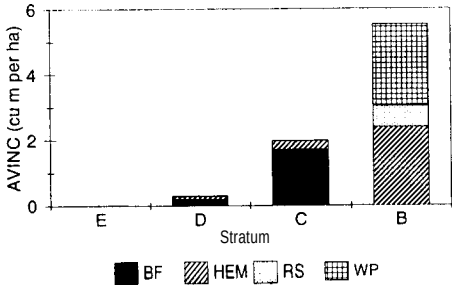

CPA Distribution
Cl6 Plot 2-1

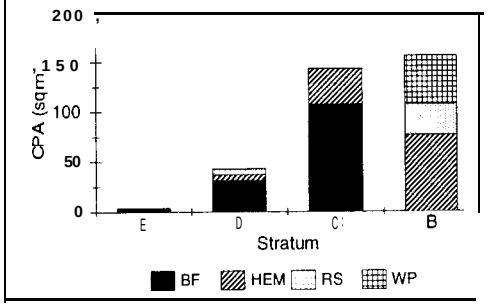

Density	1334.32 trees per ha
BA	28.68 squ m per ha
Volume	229.97 cu m per ha
R D	0.45
PAVINC	7.82 cu m per ha
GE	1.4E-04 cu m per squ m
LAI	5.46
CPA	170.67 percent

Reverse-J diameter distribution
Linear increasing LA distribution

Mean Growth Efficiency
Cl6 Plot 2-1

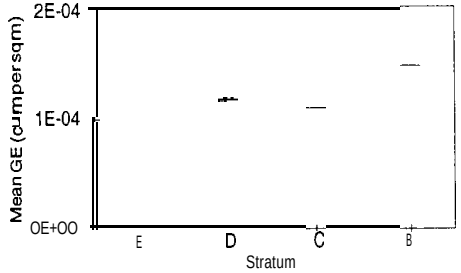

D

SPECIES COMPOSITION
Cl6 PLOT 3-1

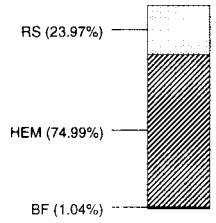

Diameter Distribution
C16 Plot 3-1

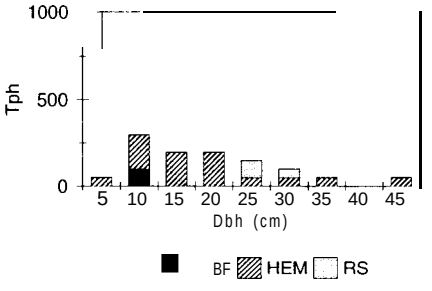

Height Distribution
Cl6 plot 3-1

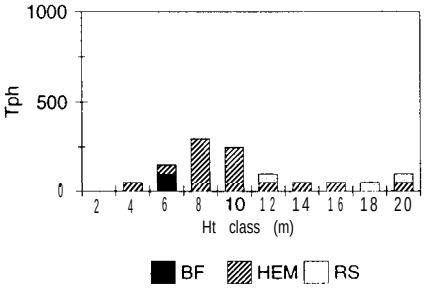

LA Distribution
C16 plot 3-1

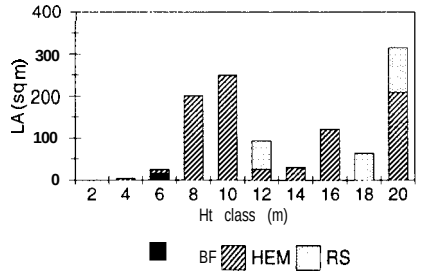

LA Distribution
C16 Plot 3-1

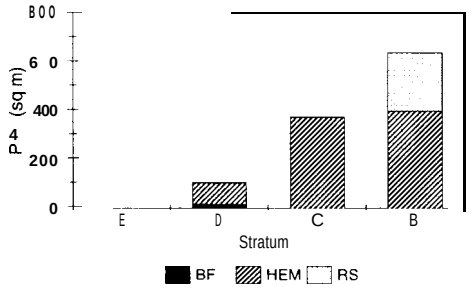

Annual Volume Increment
Cl6 Plot 3-1

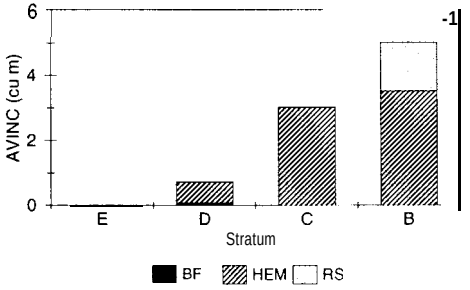

CPA Distribution
Cl6 Plot 3-1

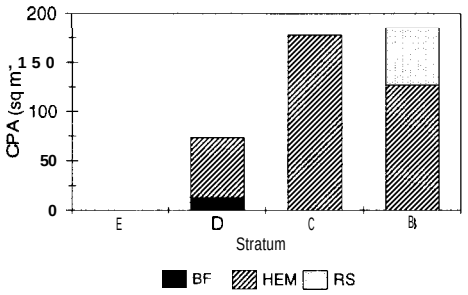

Density	1087.23 trees per ha
BA	33.52 squ m per ha
Volume	215.84 cu m per ha
RD	0.41
PAVINC	8.76 cu m per ha
G E	1.6E-04 cu m per squ m
LAI	5.45
CCF	216.13 percent

Reverse-J diameter distribution (truncated)
Linear increasing leaf area distribution

Mean GE
Cl6 Plot 3-l

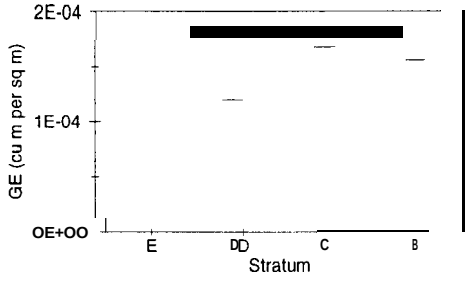

E

SPECIES COMPOSITION
COMPARTMENT 16 PLOT 3-2

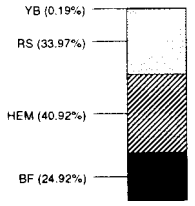

DIAMETER DISTRIBUTION
COMPARTMENT 16 PLOT 3-2

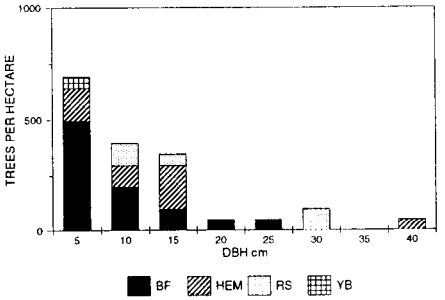

HEIGHT DISTRIBUTION
C16 Plot 3-2

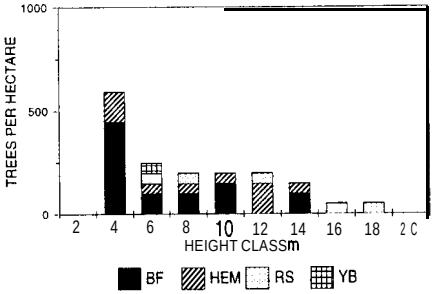

LA Distribution
Cl6 Plot 3-2

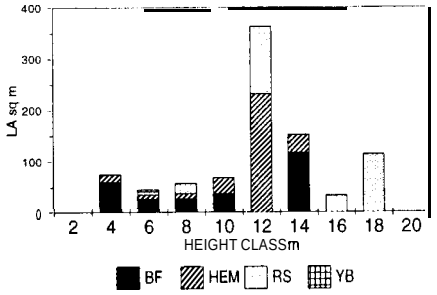

LA Distribution
Cl6 Plot 3-2

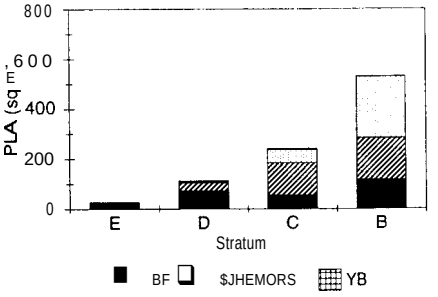

Annual Volume Increment
C1 6 Plot 3-2

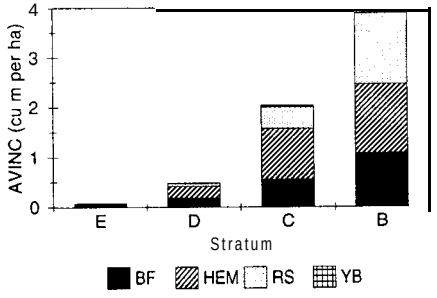

CPA Distribution
Cl6 Plot 3-2

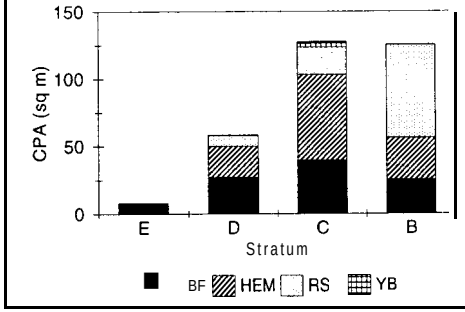

Density	1680.26 trees per ha
BA	23.45 squ m per ha
Volume	131.33 cu m per ha
RD	0.30
PAVINC	6.52 cu m per ha
GE	1.4E-04 cu m per squ m
LAI	4.50
CPA	157.66 percent

Reverse-J diameter distribution
Exponential increasing LA distribution

Mean Growth Eff iciency
Cl6 Plot 3-2

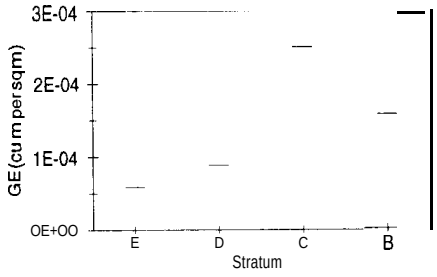

F

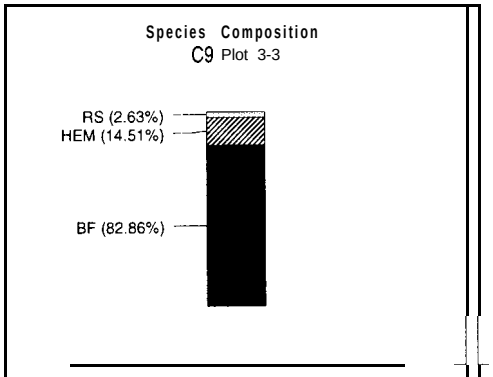

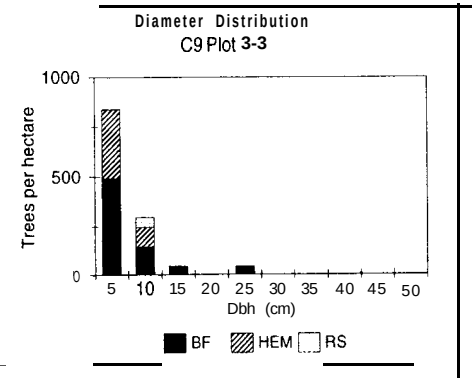

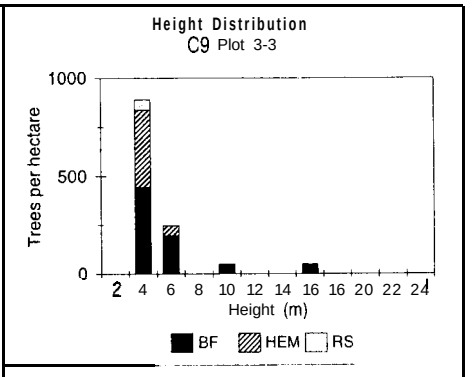

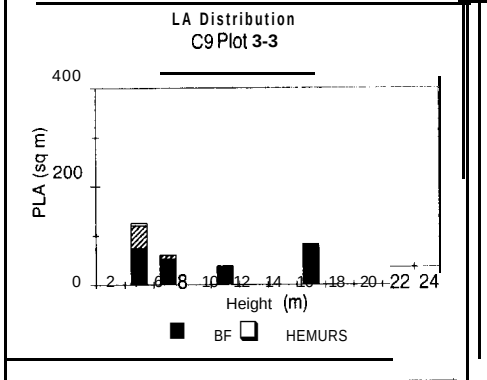

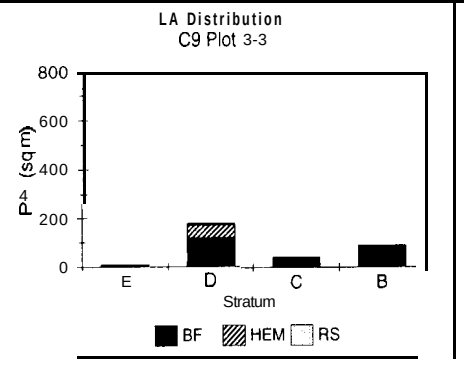

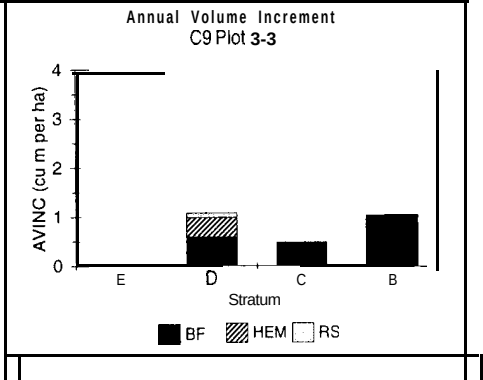

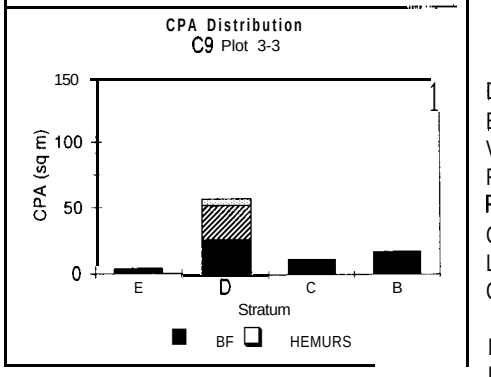

Density	1235.48	trees per ha
BA	4.62	squ m per ha
Volume	20.16	cu m per ha
RD	0.06	
PAVINC	2.58	cu m per ha
GE	1.7E-04	cu m per squ m
LAI	1.52	
CCF	43.67	percent

Decreasing diameter distribution
Unimodal LA distribution

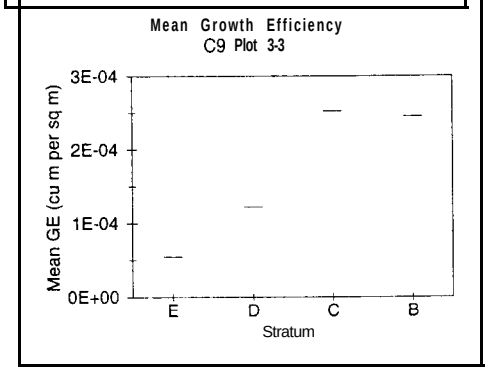

PERCENT SPECIES COMPOSITION
COMPARTMENT 16 PLOT 4-I

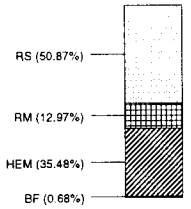

DIAMETER DISTRIBUTION
CI6 PLOT 4-1

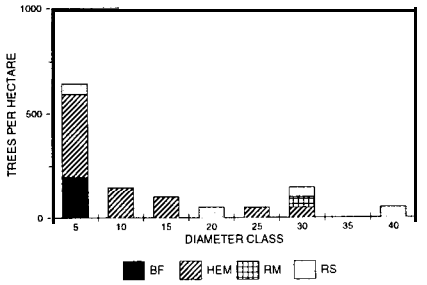

HEIGHT DISTRIBUTION
CI6 Plot 4-1

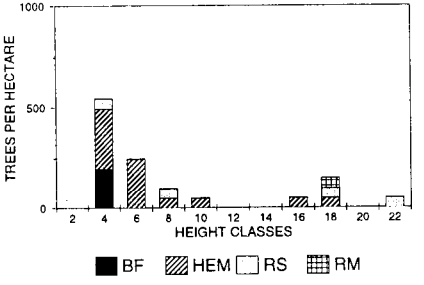

LA DISTRIBUTION
CI6 Plot 4-1

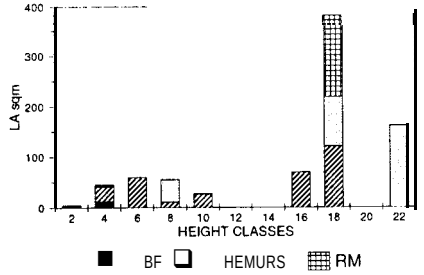

LA Distribution
CI6 Plot 4-1

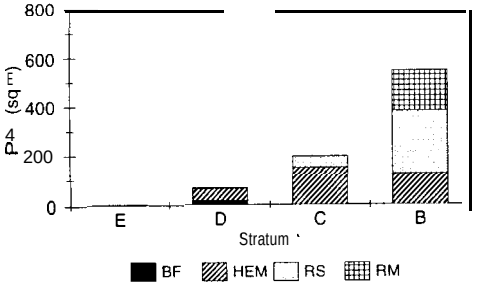

Annual Volume Increment
CI6 Plot 4-1

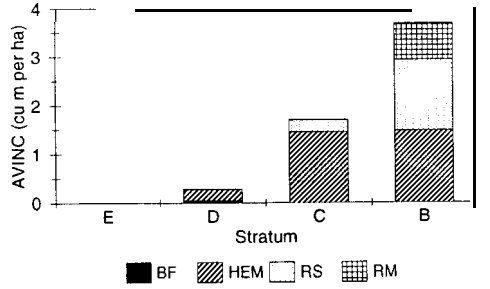

CPA Distribution
CI6 Plot 4-1

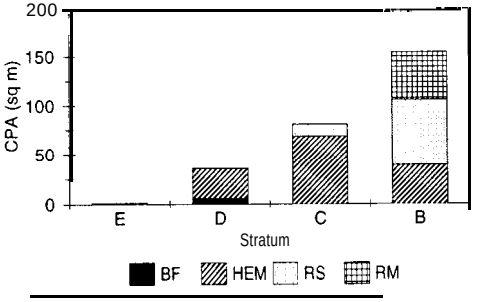

Density	1166.06	Trees per ha
BA	20.08	squ m per ha
Volume	149.65	cu m per ha
RD	0.31	
PAVINC	5.65	cu m per ha
GE	1.4E-04	cu m per sq m
LAI	3.96	
CCF	134.01	percent

Reverse-J diameter distribution
Exponential increasing LA distribution

Mean Growth Efficiency
CI6 Plot 4-1

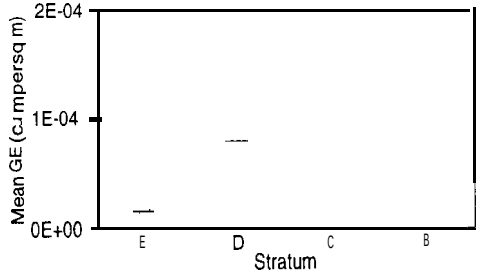

SPECIES COMPOSITION
Cl6 PLOT 4-2

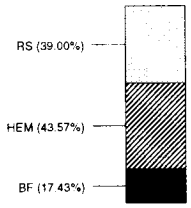

DIAMETER DISTRIBUTION
Cl6 PLOT 4-2

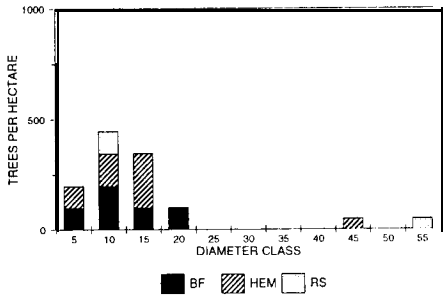

HEIGHT DISTRBUTION
Cl6 PLOT 4-2

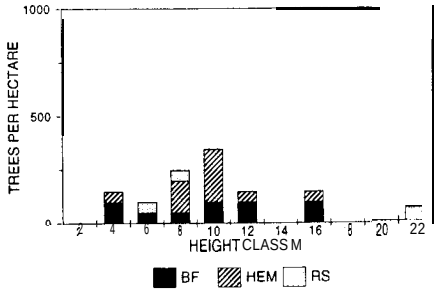

LA DISTRIBUTION
Cl6 PLOT 4-2

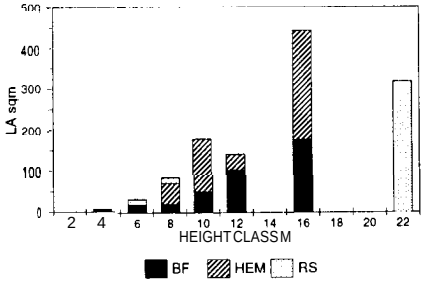

LA Distribution
Cl6 Plot 4-2

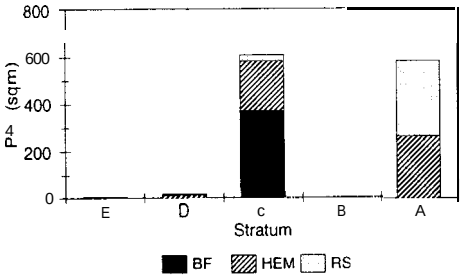

Annual Volume **Increment**
Cl 6 Plot 4-2

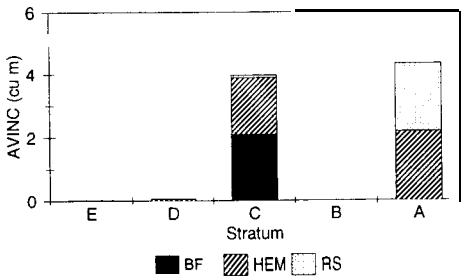

CPA Distribution
Cl 6 Plot 4-2

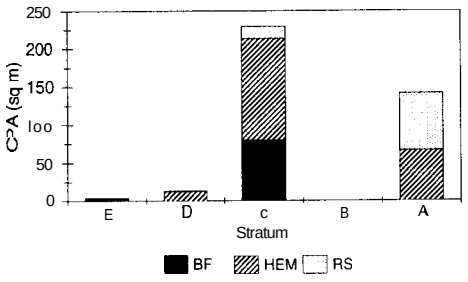

Density 1186.06 trees per ha
BA **27.73** squ m per ha
Volume 201.47 cu m per ha
RD **0.40**
PAVINC **8.36** cu m per ha
GE 1.4E-04 cu m per sq m
LAI 5.96
CPA 191.56 percent

Bimodal diameter distribution
Bimodal LA distribution

Mean Growth Efficiency
Cl 6 Plot 4-2

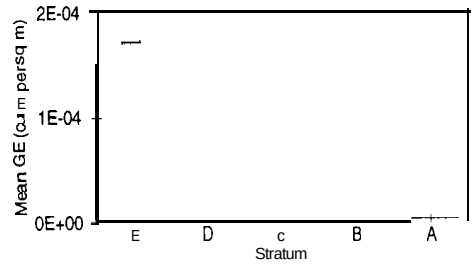

SPECIES COMPOSITION
C16 PLOT 4-3

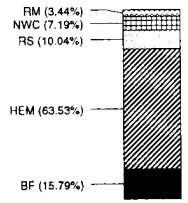

DIAMETER DISTRIBUTION
C16 PLOT 4-3

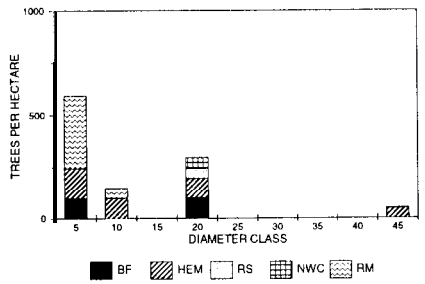

HEIGHT DISTRIBUTION
C16 PLOT 4-3

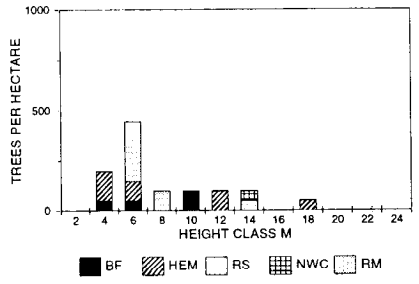

LA DISTRIBUTION
C16 PLOT 4-3

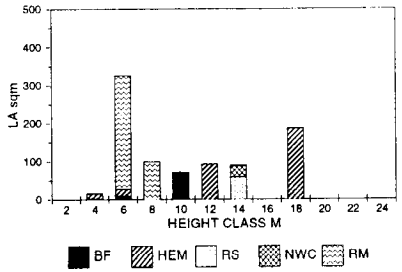

LA Distribution
Cl 6 Plot 4-3

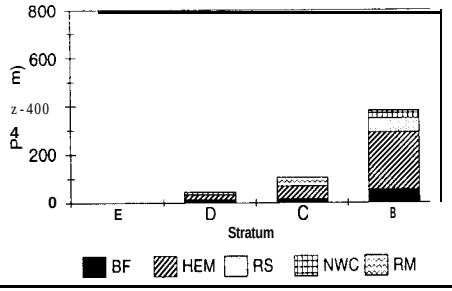

Annual Volume Increment
Cl 6 Plot 4-3

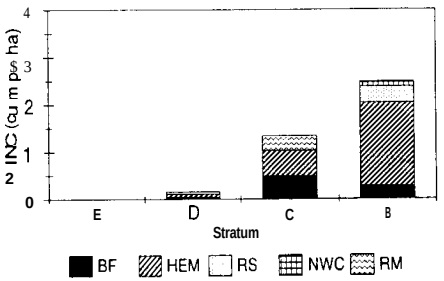

CPA Distribution
Cl6 Plot 4-3

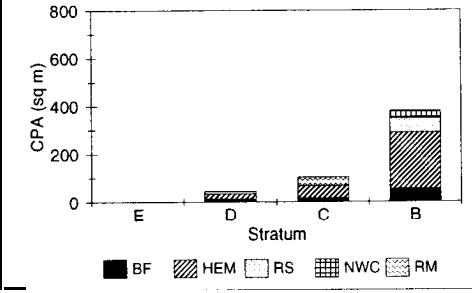

Density	1087.23	**trees per ha**
BA	**14.70**	**squ m per ha**
Volume	86.28	**cu m per ha**
RD	**0.19**	
PAVINC	**3.97**	**cu m per ha**
GE	1.5E-04	**cu m per squ m**
LAI	2.61	
CCF	**106.68**	**percent**

Reverse-J diameter distribution
Exponential increasing LA distribution

Mean Growth Efficiency
Cl 6 Plot 4-3

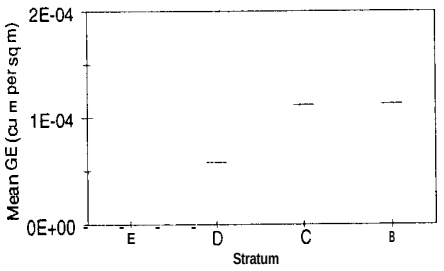

J

SPECIES COMPOSITION
C16 PLOT 5-2

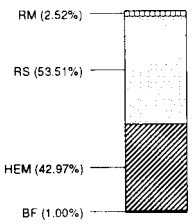

DIAMETER DISTRIBUTION
C16 PLOT 5-2

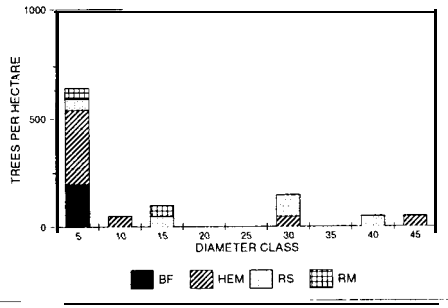

HEIGHT DISTRBUTION
C16 **PLOT 5-2**

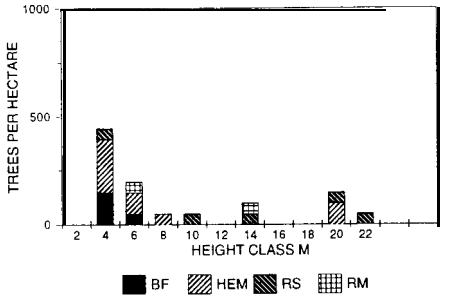

LA DISTRIBUTION
C16 PLOT 5-2

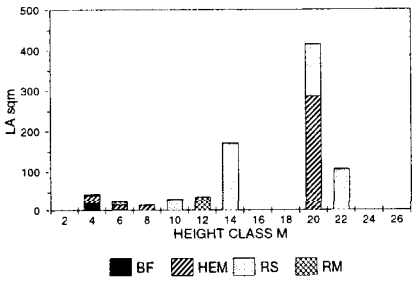

LA Distribution
C16 Plot 5-2

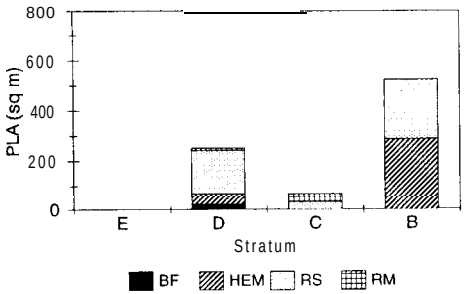

Annual Volume Increment
C16 Plot 5-2

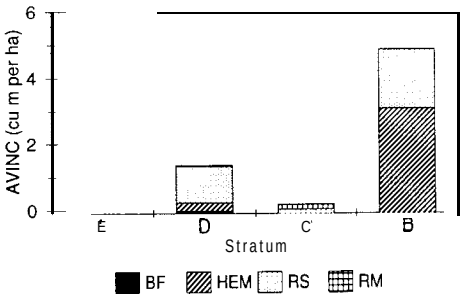

CPA Distribution
C16 Plot 5-2

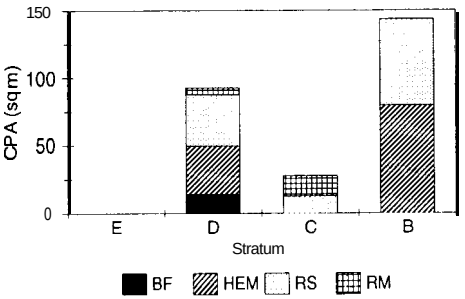

Density	1037.81 trees per ha
BA	24.44 squ m per ha
Volume	189.98 cu m per ha
RD	0.37
PAVINC	6.52 cu m per ha
GE	1.6E-04 cu m per sq m
LAI	4.16
CCF	130.34 percent

Bimodal diameter distribution
Bimodal LA distribution

Mean Growth Efficiency
C16 Plot 5-2

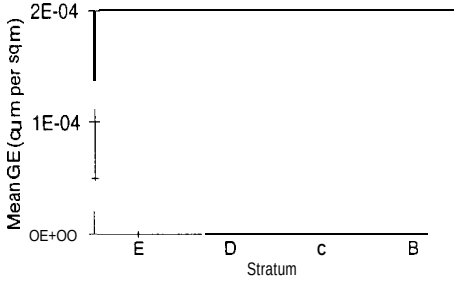

K

SPECIES COMPOSITION
C16 PLOT 5-3

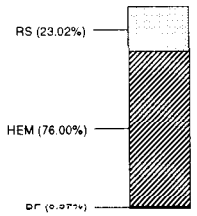

DIAMETER DISTRIBUTION
Cl6 PLOT 5-3

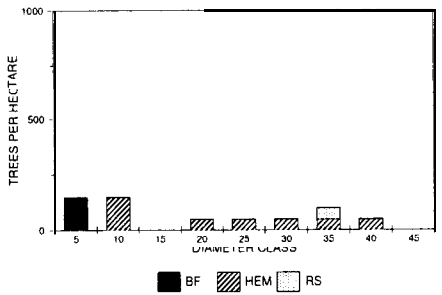

HEIGHT DISTRIBUTION
Cl6 PLOT 5-3

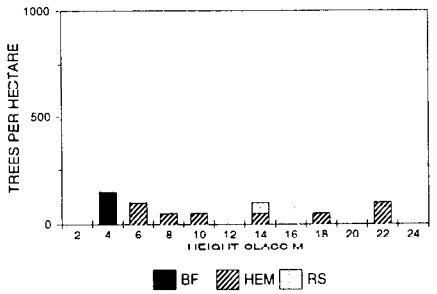

LA DISTRIBUTION
C16 PLOT 5-3

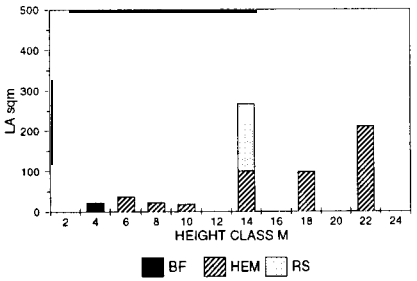

LA Distribution
Cl6 Plot 5-3

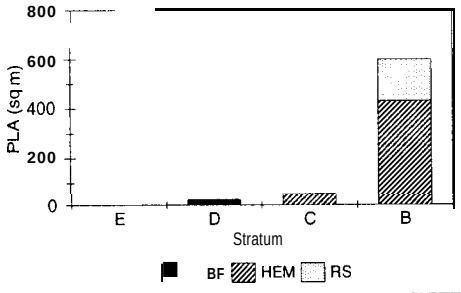

Annual Volume Increment
Cl6 Plot 5-3

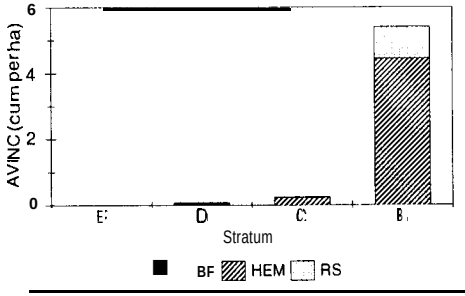

CPA Distribution
Cl 6 Plot 5-3

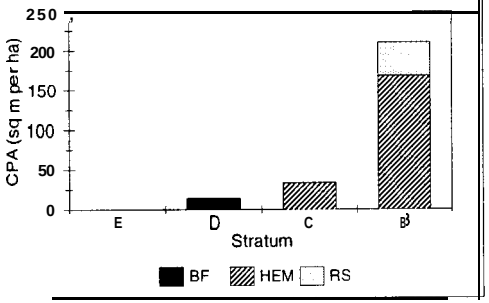

Density	593.03	trees per **ha**
BA	20.65	squ m per ha
Volume	145.26	cu m per ha
RD	0.27	
PAVINC	5.72	cu m per ha
GE	1.7E-04	cu m per squ m
LAI	3.33	
CCF	**127.24**	**percent**

Bimodal diameter distribution
LA distribution skewed toward upper stratum

Annual Volume Increment
Cl 6 Plot 5-3

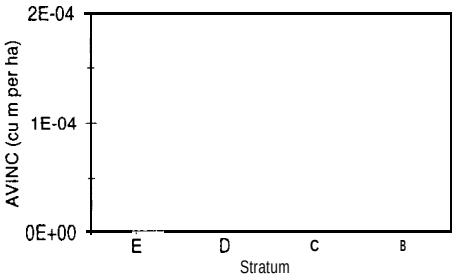

Table A. 1. Cluster 1. Spearman's correlations coefficient (r,) for plot variables, with p-values in parentheses (a = 0.05).

	PAVINC	GE	TPH	CCF	BA	BAEH	BABF	BARS
LAI	0.8571 (0.0137)	0.0000 (I .0000)	-0.4144 (0.3553)	0.6786 (0.0938)	0.8571 (0.0137)	0.1786 (0.7017)	-0.6126 (0.1436)	0.6429 (0.1194)
PAVINC		0.4286 (0.3374)	-0.7748 (0.0408)	0.5357 (0.2152)	1 .oooo (0.0001)	0.5357 (0.2152)	-0.6307 (0.1289)	0.6429 (0.1194)
GE			-0.5946 (0.1591)	-0.3929 (0.3833)	0.4286 (0.3374)	0.4643 (0.2939)	0.1442 (0.7578)	0.0357 (0.9394)
TPH				-0.2703 (0.5577)	-0.7748 (0.0408)	-0.8108 (0.0269)	0.4909 (0.2633)	-0.4865 (0.2682)
CCF					05357 (0.2 152)	0.0714 (0.8790)	-0.8829 (0.0085)	0.7500 (0.0522)
BA						0.5357 (0.2152)	-0.6307 (0.1289)	0.6429 (0.1194)
BAEH							-0.1442 (0.7578)	-0.0357 (0.9394)
BABF								-0.9009 (0.0056)

Table A.1. Cluster 1. Continued.

	LAC	LAD	LAE	TPHB	TPHC	TPHD	TPHE
LAB	-0.3964 (0.3786)	-0.8929 (0.0068)	-0.6699 (0.0997))	0.9274 (0.0026)	0.4286 (0.3374)	-0.9550 (0.0008)	-0.59 11 (0.1622)
LAC		0.2883 (0.5307)	0.6163 (0.1405))	-0.6055 (0.1496)	0.5586 (0.1925)	0.3364 (0.4604)	0.7356 (0.0595)
LAD			0.4335 (0.3313)	-0.7638 (0.0457)	-0.3214 (0.482 1)	0.8469 (0.0162)	0.3152 (0.49 10)
LAE				-0.8728 (0.0103)	-0.1576 (0.0997)	0.6362 (0.1245)	0.9565 (0.0007)
TPHB					0.2182 (0.6383)	-0.8808 (0.0088)	-0.8327 (0.0201)
TPHC						-0.4505 (0.3 104)	0.0394 (0.9332)
TPHD							0.5169 (0.2348)

Table A.1. Cluster 1. Continued.

	LAB	LAC	LAD	LAE	TPHB	TPHC	TPHD	TPHE
LAI	0.1786 (0.7017)	-0.3243 (0.4779)	-0.357 1 (0.43 16)	-0.4335 (0.3313)	0.2728 (0.5540)	-0.0357 (0.9394)	-0.0900 (0.8477)	-0.3152 (0.4910)
PAVINC	0.5357 (0.2152)	-0.6667 (0.1019)	-0.6429 (0.1194)	-0.6699 (0.0997)	0.6547 (0.1106)	-0.1429 (0.7599)	-0.4685 (0.2890)	-0.5911 (0.1622)
GE	0.3929 (0.3833)	-0.9009 (0.0056)	-0.2857 (0.5345)	-0.3941 (0.3817)	0.5092 (0.243 1)	-0.5357 (0.2 152)	-0.4144 (0.3553)	-0.5 123 (0.2398)
TPH	-0.7388 (0.0579)	0.709 1 (0.0744)	0.6307 (0.1289)	0.8947 (0.0065)	-0.9083 (0.0047)	0.0182 (0.9694)	0.7636 (0.0457)	0.8350 (0.0194)
CCF	0.0714 (0.8790)	0.090 1 (0.8477)	-0.3214 (0.482 1)	-0.2364 (0.6097)	0.1637 (0.7259)	0.0357 (0.9394)	0.0000 (1.0000)	-0.1182 (0.8007)
BA	0.5357 (0.2152)	-0.6667 (0.1019)	-0.6429 (0.1194)	-0.6699 (0.0997)	0.6547 (0.1106)	-0.1429 (0.7599)	-0.4685 (0.2890)	-0.59 11 (0.1622)
BAEH	0.7857 (0.0362)	-0.3604 (0.427 1)	-0.7500 (0.0522)	-0.59 11 (0.1622)	0.7638 (0.0457)	0.2857 (0.5345)	-0.9189 (0.0034)	-0.4335 (0.3313)
BABF	-0.3604 (0.427 1)	0.2000 (0.6672)	0.4685 (0.2890)	0.5169 (0.2348)	-0.4953 (0.2582)	-0.0180 (0.9694)	0.209 1 (0.6527)	0.4772 (0.2789)
BARS	0.1429 (0.7599)	-0.4325 (0.3325)	-0.1786 (0.7017)	-0.57 14 (0.1802)	0.400 1 (0.3738)	-0.2857 (0.5345)	0.0180 (0.9694)	-0.6108 (0.145 1)

Table A.2. Cluster 2. Spearman's correlation coefficient (r_s) for plot variables, with p-values in parentheses ($\alpha = 0.05$).

	PAVINC	GE	TPH	CCF	[illegible]	BAEH	[illegible]	BARS
[illegible]	[illegible] (0.6000)	-0.8000 (0.2000)	[illegible] (0.6000)	[illegible] (0.6000)	[illegible] (0.8000)	0.0000 (1.0000)	[illegible] (0.6000)	[illegible] (0.8000)
PAVINC		[illegible] (0.8000)	**-1.0000 (0.0001)**	**1.0000 (0.0001)**	[illegible] (0.2000)	[illegible] (0.2000)	**-1.0000 (0.0001)**	[illegible] (1.0000)
[illegible]			-0.2000 (0.8000)	[illegible] (0.8000)	[illegible] (0.6000)	0.4000 (0.6000)	-0.2000 (0.8000)	[illegible] (0.6000)
TPH				**-1.0000 (0.0001)**	-0.8000 (0.2000)	-0.8000 (0.2000)	[illegible] ([illegible])	[illegible] (1.0000)
[illegible]					[illegible] (0.2000)	[illegible] (0.2000)	**-1.0000 (0.0001)**	[illegible] (1.0000)
[illegible]						[illegible] (0.6000)	-0.8000 (0.2000)	-0.6000 (0.4000)
BAEH							-0.8000 (0.2000)	0.4000 (0.6000)
BABF								0.0000 (1.0000)

Table A.2. Cluster 2. Continued.

	LAC	LAD	LAE	TPHB	TPHC	TPHD	TPHE
LAB	-0.8000 (0.2000)	0.4000 (0.6000)	-0.2 108 (0.7892)	0.3162 (0.6838)	-0.4000 (0.6000)	0.8000 (0.2000)	-0.2108 (0.7892)
LAC		-0.8000 (0.2000)	-0.3 162 (0.6838)	-0.3 162 (0.6838)	0.2000 (0.8000)	-1.0000 (0.0001)	-0.3 162 (0.6838)
LAD			0.3162 (0.6838)	0.6324 (0.3675)	-0.4000 (0.6000)	0.8000 (0.2000)	0.3162 (0.6838)
LAE				-0.5000 (0.5000)	0.7378 (0.262 1)	0.3162 (0.6838)	1.0000 (0.0001)
TPHB					-0.9486 (0.05 13)	0.3162 (0.6838)	-0.5000 (0.5000)
TPHC						-0.2000 (0.8000)	0.7378 (0.262 1)
TPHD							0.3162 (0.6838)

Table A.2. Cluster 2. Continued.

	LAB	LAC	LAD	LAE	TPHB	TPHC	TPHD	TPHE
LAI	-0.4000 (0.6000)	0.8000 (0.2000)	-1.0000 (0.0001)	-0.3162 (0.6838)	-0.6324 (0.3675)	0.4000 (0.6000)	-0.8000 (0.2000)	-0.3162 (0.6838)
PAVINC	-0.6000 (0.4000)	0.8000 (0.2000)	-0.4000 (0.6000)	-0.6324 (0.3675)	0.3162 (0.6838)	-0.4000 (0.6000)	-0.8000 (0.2000)	-0.6324 (0.3675)
GE	0.2000 (0.8000)	-0.4000 (0.6000)	0.8000 (0.2000)	-0.2108 (0.7892)	0.9486 (0.0513)	-0.8000 (0.2000)	0.4000 (0.6000)	-0.2108 (0.7892)
TPH	0.6000 (0.4000)	-0.8000 (0.2000)	0.4000 (0.6000)	0.6324 (0.3675)	-0.3162 (0.6838)	0.4000 (0.6000)	0.8000 (0.2000)	0.6324 (0.3675)
CCF	-0.6000 (0.4000)	0.8000 (0.2000)	-0.4000 (0.6000)	-0.6324 (0.3675)	0.3162 (0.6838)	-0.4000 (0.6000)	-0.8000 (0.2000)	-0.6324 (0.3675)
BA	0.0000 (1.0000)	0.4000 (0.6000)	-0.2000 (0.8000)	-0.9486 (0.0513)	0.6324 (0.3675)	-0.8000 (0.2000)	-0.4000 (0.6000)	-0.9486 (0.0513)
BAEH	-0.8000 (0.2000)	0.6000 (0.4000)	0.0000 (1.0000)	-0.1054 (0.8946)	0.3162 (0.6838)	-0.2000 (0.8000)	-0.6000 (0.4000)	-0.1054 (0.8946)
BABF	0.6000 (0.4000)	-0.8000 (0.2000)	0.4000 (0.6000)	0.6324 (0.3675)	-0.3162 (0.6838)	0.4000 (0.6000)	0.8000 (0.2000)	0.6324 (0.3675)
BARS	-0.8000 (0.2000)	0.4000 (0.6000)	-0.2000 (0.8000)	0.7378 (0.2621)	-0.6324 (0.3675)	0.8000 (0.2000)	-0.4000 (0.6000)	0.7378 (0.2621)

BIOGRAPHY OF THE AUTHOR

Laura Susan Kenefic (nee Wolslegel) was born in Troy, New York on October 26, 1970, the daughter of John N. and Susan A. Wolslegel. She was raised in rural Cropseyville, N.Y., and graduated from Brittonkill Central Schools. She attended the State University of New York at Binghamton and graduated with honors in 1992, with a B.A. in Environmental Studies and a minor in Russian Language. She married Richard Kenefic, a classical musician, in 1992. Laura enrolled in the State University of New York College of Environmental Science and Forestry in Syracuse in 1992, where she studied hardwood silviculture with Ralph Nyland. She moved with her husband to Maine in 1994 to accept an appointment as Cooperative Education Graduate Student with the U.S.D.A. Forest Service, Northeastern Research Station. Laura has been stationed at the Penobscot Experimental Forest while pursuing studies at The University of Maine in Quantitative Silviculture with Robert Seymour. She graduated from SUNY-CESF in 1995 with a M.S. in Forest Resource Management; her thesis assessed structural and habitat characteristics of uneven-aged northern hardwood stands.

Laura has authored or co-authored twelve scientific publications during her tenure at University of Maine, and has given one Visiting Scholar Lecture (University of Maine, Fort Kent) and myriad professional presentations, guest lectures, and scientific tours. She has acted as a technical reviewer for the Northern Journal of Applied Forestry, Forest Science, and McGraw-Hill Publishers. Laura taught Silviculture and co-taught the Silviculture/Forest Ecology laboratory in the Department of Forest Ecosystem Science in 1997. She is a member of the Society of American Foresters, the Ecological Society of

America, the University of Maine Cooperative Forestry Research Unit Hardwood Subcommittee, and participates in the Penobscot Experimental Forest Research Operations Team and the U.S.D.A. Forest Service International Forestry Russia Program.

Laura is a recipient of the Ralph Griffin Memorial Award (1996), Charles Schomaker Memorial Scholarship (1998), a combined George F. Dow and Fred Griffee Scholarship (1998), and was featured as an outstanding graduate student in the Maine Perspective (1999). She is a member of Phi Beta Kappa and Phi Kappa Phi Honor Societies. Laura has two children - Liam Foster Kenefic (born June 24, 1996) and Evan Lukas Kenefic (born November 12, 1999), and is an active parent in the University of Maine Children's Center. She is a founding member of the College of Natural Sciences, Forestry, and Agriculture's Women in Science Club. Following completion of her degree, Laura will be employed as a Research Forester in the Northeastern Research Station and will be appointed to the faculty of the Department of Forest Ecosystem Science, University of Maine. Laura is a candidate for the Doctor of Philosophy degree in Forest Resources from The University of Maine in December, 2000.